Calhoun: The NPS Institutional Archive

DSpace Repository

Theses and Dissertations | 1. Thesis and Dissertation Collection, all items

1951

Reinforced circular holes in bending with shear.

Heller, Samuel Ries

Massachusetts Institute of Technology

http://hdl.handle.net/10945/14550

Downloaded from NPS Archive: Calhoun

http://www.nps.edu/library

Calhoun is the Naval Postgraduate School's public access digital repository for research materials and institutional publications created by the NPS community. Calhoun is named for Professor of Mathematics Guy K. Calhoun, NPS's first appointed -- and published -- scholarly author.

Dudley Knox Library / Naval Postgraduate School
411 Dyer Road / 1 University Circle
Monterey, California USA 93943

REINFORCED CIRCULAR HOLES IN BENDING WITH SHEAR

SAMUEL RIES HELLER, JR.

Library
U. S. Naval Postgraduate School
Monterey, California

Mark I 42
2854

Cambridge, Massachusetts
May 11, 1951

Professor J. S. Newell
Secretary of the Faculty
Massachusetts Institute of Technology
Cambridge, Massachusetts

Dear Sir:

In accordance with the requirements for the degree of Doctor of Science in Naval Architecture I submit herewith a thesis entitled, "Reinforced Circular Holes in Bending with Shear."

Respectfully,

REINFORCED CIRCULAR HOLES IN BENDING WITH SHEAR

by

Samuel Ries Heller, Jr.
Lieutenant, U. S. Navy

B.S.E., University of Michigan, 1941
Nav.E., Massachusetts Institute of Technology, 1950

Submitted in Partial Fulfillment of the

Requirements for the Degree of

DOCTOR OF SCIENCE

in

NAVAL ARCHITECTURE

at the

MASSACHUSETTS INSTITUTE OF TECHNOLOGY

(1951)

Thesis
H43

REINFORCED CIRCULAR HOLES IN BENDING WITH SHEAR

by

Samuel Ries Heller, Jr.

Submitted for the degree of DOCTOR OF SCIENCE in the Department of Naval Architecture and Marine Engineering on

May 11, 1951

The object of this thesis is to determine the effect of the reinforcement of circular holes on the stress distribution in the webs of beams subjected to bending with shear, and to devise a rapid means for predicting the increase in stress over that of the condition of no opening.

A theoretical solution for a bead-type reinforcement; i.e., a small radial thickness, is developed in APPENDIX D. The theory for the stress distribution in the web follows the work of Reissner and Morduchow, and is valid for any shape reinforcement; the theory for the stress distribution in the reinforcement, however, is for rectangular reinforcement only. The experimental evidence, obtained from SR-4 strain gauges, has been plotted in RESULTS. This evidence is based on tests with rectangular reinforcement (standard pipe) exclusively.

A family of specimens covering the usual structural practice, holes up to half the depth of the web, was tested. Reinforcement of twice the area of the hole was originally provided; successive machining operations reduced the amount of reinforcement in steps of half the hole area to zero reinforcement. Strain gauge observations at the hole, in the web, and on the flange of the I-beam were made and the maximum stress in each area determined.

From this investigation it is concluded that: the theoretical solution is satisfactory for design purposes when the diameter of the hole does not exceed 1/4 the depth of the beam; it is impossible to design a reinforcement that will reduce the stress level to that existing for no hole; reinforcement with an area to that of the hole causes a sharp drop in stress and appears to be about the economic limit; the shape of the bead-type reinforcement, flat bar, angle, channel, I, etc., is unimportant, but the area of reinforcement is paramount; the experimental solution is suitable for design purposes for I-beams of usual structual proportions.

21000

ACKNOWLEDGMENT

The author desires to express his appreciation to those whose help was of such great value in the preparation of this thesis: to Captain R. E. Cronin, USN, Commander F. Caracciolo, USN, Messrs. C. G. Lutts, M. Graham, D. Cuozzo, and W. Hegan, of the Boston Naval Shipyard who gave their time and effort unselfishly to make the experimental work embodied in this report a success; to Professor C. H. Norris whose friendly advice and counsel served as steady guide; to Professor R. D. Douglass for his assistance in the mathematics of the solution; to Professor J. H. Evans who proposed the study; to Mr. J. S. Brock of the staff of the David Taylor Model Basin, Washington, D. C., who introduced the author into the field of stress concentrations; and to the Bureau of Ships without whose financial aid this investigation would have been impossible.

TABLE OF CONTENTS

Section	Contents	Page
I	Introduction.....	1
II	Procedure.....	3
III	Results.....	9
IV	Discussion of Results.....	16
V	Conclusions.....	19
VI	Recommendations.....	20
VII	Appendix.....	21
	A. Details of Procedure.....	22
	B. Sample Calculations.....	45
	C. Original Data.....	49
	D. Development of Theoretical Solution	70
	E. Bibliography.....	125

TABLE OF FIGURES

Figure	Description	Page
I	Arrangement and Details of Test Specimen.....	4
II	Schematic Wiring Diagram.....	5
III	Test Arrangement for Pure Bending.....	6
IV	Test Arrangement for Bending with Shear.....	7
V	Stress Concentration Factor at Edge of Hole vs. Weight Ratio for $r_2/h = 0.125$.....	10
VI	Stress Concentration Factor at Edge of Hole vs. Weight Ratio for $r_2/h = 0.2417$.....	11
VII	Stress Concentration Factor at Edge of Hole vs. Weight Ratio for $r_2/h = 0.4206$.....	12
VIII	Stress Concentration Factor at Edge of Hole vs. Weight Ratio for $r_2/h = 0.5056$.....	13
IX	Stress Concentration Factor at Edge of Beam vs. Weight Ratio for $r_2/h = 0.125$.....	14
X	Stress Concentration Factor at Edge of Beam vs. Weight Ratio for $r_2/h = 0.2417$.....	14
XI	Stress Concentration Factor at Edge of Beam vs. Weight Ratio for $r_2/h = 0.4206$.....	14
XII	Stress Concentration Factor at Edge of Beam vs. Weight Ratio for $r_2/h = 0.5056$.....	14
XIII	Design Chart for Reinforcement.....	15
XIV	Geometry and Notation for Bending with Shear.	23
XV(a)	Schematic Test Arrangement for Bending with Shear.....	23
XV(b)	Schematic Test Arrangement for Pure Bending..	23
XVI	Geometry and Notation of Rectangular Strip Reinforcement.....	25
XVII	Basic SR-4 Gauge Locations.....	25

Figure	Description	Page
XVIII	Photograph of Gauges Mounted on Flange and Web.....	28
XIX	Photograph of Gauges Mounted on Edge of Hole	29
XX	Photograph of Instrument Center.....	30
XXI	Load vs. Strain for τ/σ =0.5; r_2/h = 0.4206; WR = 2	33
XXII	Nomographic Solution for Gauge R45; τ/σ =0.5; r_2/h = 0.4206; WR = 2	34
XXIII	Stress Concentration Factor at Edge of Hole vs. Shear-Bending Ratio for r_2/h = 0.4206; WR = 2	36
XXIV	Stress Concentration Factor at Edge of Hole vs. Angle from Vertical for r_2/h = 0.4206; WR = 2	37
XXV	Stress Concentration Factor at Edge of Hole vs. Shear-Bending Ratio for r_2/h = 0.4206...	38
XXVI	Stress Concentration Factor at Edge of Hole vs. Diameter-Depth Ratio for WR = 2	39
XXVII	Stress Concentration Factor at Edge of Beam vs. Distance from ℄ of Hole in Diameters for r_2/h = 0.4206; τ/σ =0.5	41
XXVIII	Cross-Fairing Methods for Stress Concentration Factor at Edge of Beam.....	42
XXIX	Stress Concentration Factor in Web vs. Distance from ℄ of Hole Diameters for r_2/h = 0.4206; θ = 45 ; τ/σ =0.5; WR = 2	44
XXX(a)	Positive Orientation of Stress Resultants and Displacements.....	75
XXX(b)	Positive Orientation of Stresses.....	75
XXX(c)	Equilibrium of Ring Particle.....	75
XXXI	Beam in Pure Bending.....	75
XXXII	Beam with Pure Shear at y-axis.....	75

Figure	Description	Page
XXXIII	Contribution of Curvature of Ring to Extension.....	91
XXXIV	k_{31}/K vs. α , Contours of δ	120
XXXV	k_{23}/K vs. α , Contours of δ	121
XXXVI	k_{43}/K vs. α , Contours of δ	122
XXXVII	k'_{22}/K vs. α , Contours of δ	123
XXXVIII	k'_{42}/K vs. α , Contours of δ	124

INTRODUCTION

In almost all structures openings of some sort are required, either for access or for passing piping, ventilation, or electrical systems to the various compartments. It, therefore, behooves the structural designer to make proper provision for these requirements without adversely affecting the structure as a whole.

Much time has been devoted to the analysis of the effect of such openings,[1] but a scarcity of information about the effect of reinforcement exists. Timoshenko [11][2] developed an approximate analysis for reinforcement around a circular hole in a uniform tension field; Sobrero [12] and Gurney [13] continued this work. Reissner and Nordecow [14] developed a general solution for reinforcement of a circular hole for various types of loadings - hydrostatic pressure, uniform shear, uniform tension, and pure bending. The United States Experimental Model Basin [19] published the results of an experimental study on various types of reinforcements on various types of openings subjected to uniform tension. Ballinger and Obermeyer [18] performed a similar experimental investigation on a flat ovaloid hole which had been reinforced. Quite recently Tifird and Skinner [17] tested an elliptical hole with varying reinforcement subjected to both pure bending and bending with shear.

---

1. A fairly complete list is included in BIBLIOGRAPHY.
2. Numbers in brackets refer to the BIBLIOGRAPHY.

This thesis is devoted to the effect of a reinforced circular cutout subjected to both pure bending and bending with shear. The effect of finite depth is evolved from an analysis of experimental data rather than by a rigorous mathematical treatment. It is the purpose of this thesis to correlate data from actual experiments with large models having a systematic variation in the size of opening, ratio of diameter of hole to depth of beam; a systematic variation in the degree of reinforcement; and a systematic variation in the ratio of nominal shear to nominal bending. This correlation includes a check on the mathematical solution developed in the APPENDIX.

PROCEDURE

The models were prepared from a standard rolled steel section: 12" x 6½" x 28# WF. Fig. I is a detail drawing of the model series and includes a machining schedule for the variation of reinforcement. Fig. II is a schematic wiring diagram for the use of Baldwin SR-4 Strain Gauges.

All testing was performed in a 200,000 pounds hydraulic type Baldwin-Southwark testing machine fitted with an Amery-Tatnall weighing mechanism. A 24" x 9" x 94# WF Section was used to support the test specimen and transfer the load back into the machine for measuring. Circular bars and Vee-blocks, fitted with a radius at the small end, were used for application of load and support to assure as nearly "line loading" as was feasible. Figs. III and IV show the typical arrangement for pure bending and bending with shear respectively.

After the specimen was installed in the test position and carefully aligned to ensure proper loading and support positions, all strain gauges were read for the no load or "zero" reading. Then the test load was applied. All gauges were read at several intervals, load increments, until the full test load was applied. This enabled a load versus strain plot to be made for each gauge. After the readings were made at the full load, this load was removed and a second "zero" reading made. The

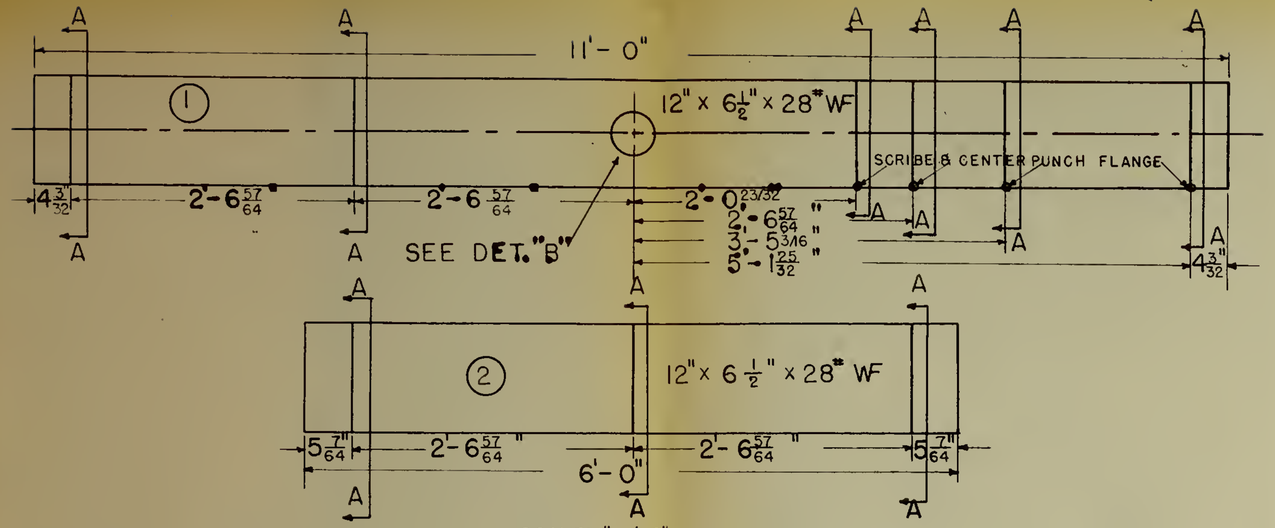

SCALE: 1" = 1'-0"

BILL OF MATERIAL

PC. NO	QUANT	SIZE	LENGTH	MAT'L
1	1	12"X6½"X28#	11'-0"	M.S.
2	1	12"X6½"X28#	6'-0"	M.S.
3	18	10.2 R.	12"X3"	M.S.
4	1	1.5" XHVY P.	1.25"	M.S.
5	1	3" XHVY P.	1.5"	M.S.
6	1	5" STD P.	2.75"	M.S.
7	1	6" STD P.	3"	M.S.

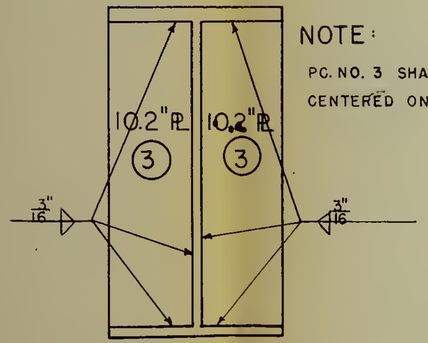

SEC. "A-A"
SCALE: 3" = 1'-0"

NOTE:
PC. NO. 3 SHALL BE CENTERED ON LOCATION.

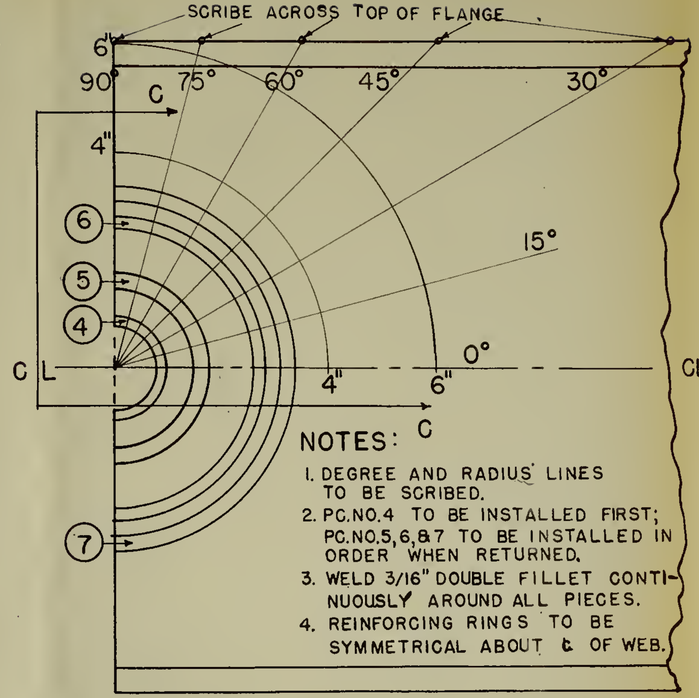

NOTES:
1. DEGREE AND RADIUS LINES TO BE SCRIBED.
2. PC. NO. 4 TO BE INSTALLED FIRST; PC. NO. 5, 6, & 7 TO BE INSTALLED IN ORDER WHEN RETURNED.
3. WELD 3/16" DOUBLE FILLET CONTINUOUSLY AROUND ALL PIECES.
4. REINFORCING RINGS TO BE SYMMETRICAL ABOUT ℄ OF WEB.

DETAIL "B"
SCALE: 6" = 1'-0"

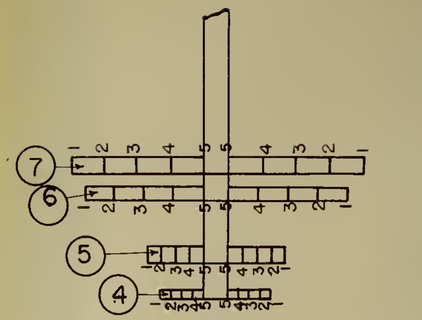

SEC. "C-C"
FULL SIZE

MACHINING SCHEDULE

CUT	WIDTHS			
	PC. 4	PC. 5	PC. 6	PC. 7
1	1.034 ± .002	1.291 ± .002	2.475 ± .003	2.725 ± .003
2	0.836 ± .002	1.028 ± .002	1.915 ± .003	2.103 ± .003
3	0.637 ± .001	0.766 ± .002	1.356 ± .002	1.482 ± .002
4	0.438 ± .001	0.503 ± .001	0.798 ± .002	0.861 ± .002
5	0.24 ± 0	0.24 ± 0	0.24 ± 0	0.24 ± 0

FIG. I
TEST SPECIMEN
ARR'G'T & DETAILS

S.R.H.
7-21-50

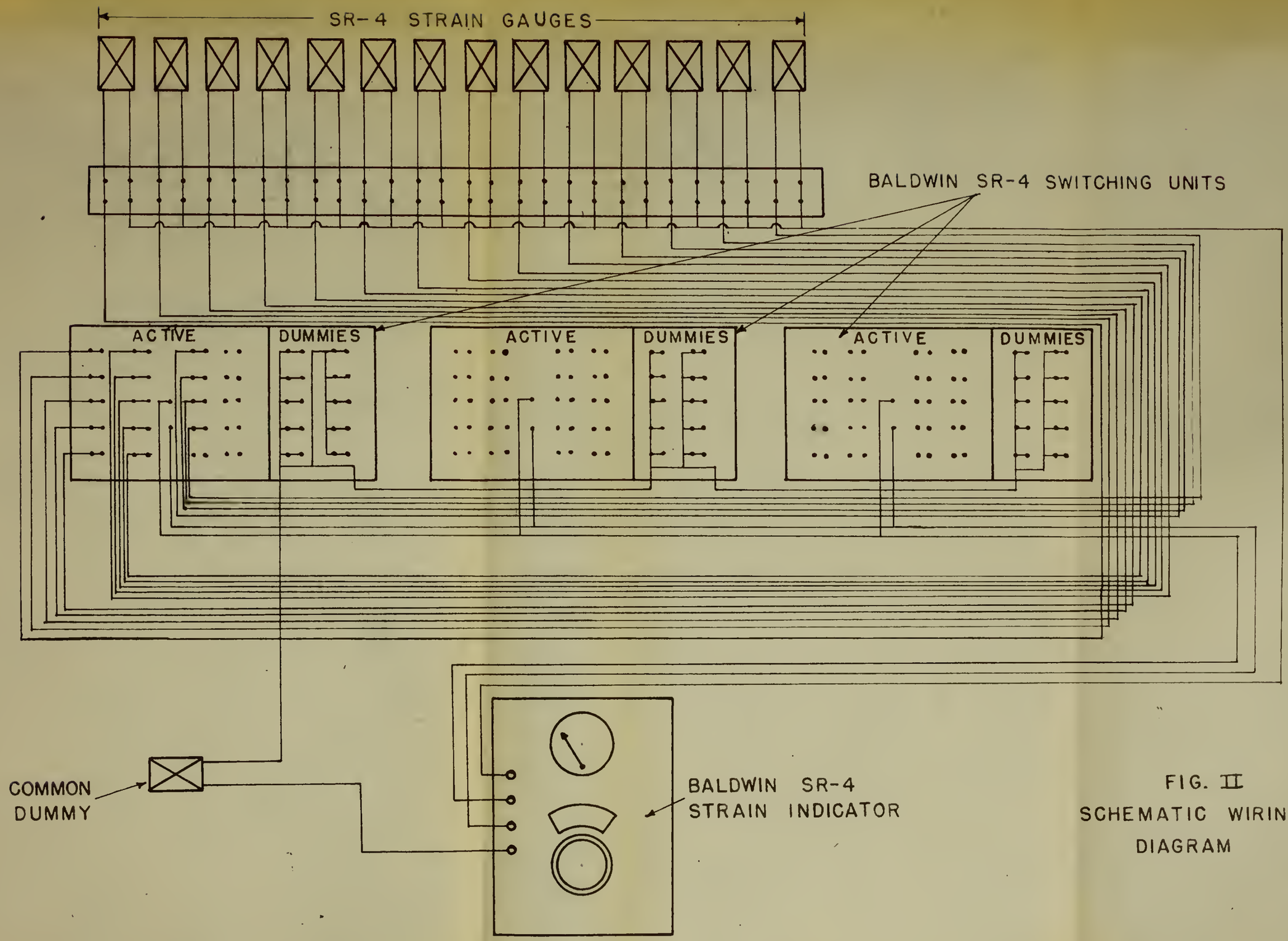

FIG. II
SCHEMATIC WIRING DIAGRAM

S.R.H.
7-7-50

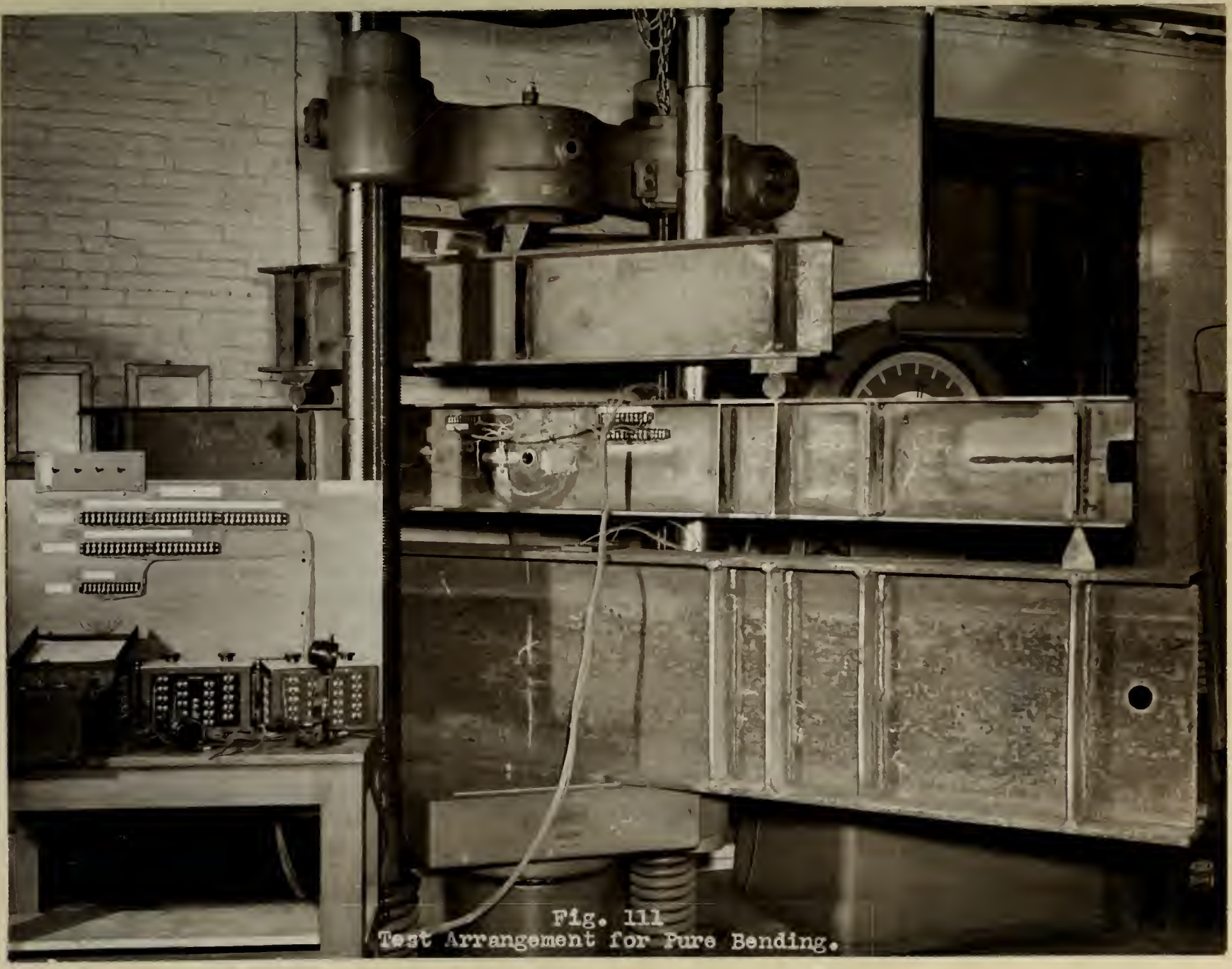

Fig. 111
Test Arrangement for Pure Bending.

Fig. IV
Test Arrangement for Bending with Shear.

average of the two "zero" readings was used as the basis for determining strain. When one such test was completed, the specimen was then realigned with different load and support positions for the next test with a different ratio of nominal shear to nominal bending.

After the completion of such a series of tests, the specimen was removed for the machining of the reinforcement. Thus the specimen was tested first with maximum reinforcement and then with successively smaller amounts of reinforcement until there was none. After this series, twenty-five (25) tests: five (5) degrees of reinforcement tested for each of five (5) ratios of shear to bending, a larger hole was machined and the process repeated.

RESULTS

The results of the experimental data are incorporated in Figures V through XII. Figures V - VIII are plots of stress concentration factor at the edge of the hole versus the ratio of the weight of the reinforcement material to the weight of the material removed in forming the hole in contours of the ratio of nominal shear to nominal bending stress, for various ratios of diameter of hole to depth of web. Figures IX - XII are similar plots with the stress concentration factor at the edge of the beam as the substituted variable. The various experimental data are shown on these plots. Theoretical solutions are superimposed in Figures V - VIII.

Figure XIII is an improved plot of the foregoing Figures incorporating all information into a single chart which is suitable for design or other engineering purposes. In this chart a new independent variable, a dimensionless area parameter, is substituted for the aforementioned weight ratio.

FIG. V
STRESS CONCENTRATION FACTOR AT EDGE OF HOLE
VS.
WEIGHT RATIO
CONTOURS OF $\frac{\tau}{\sigma}$ FOR $r_2/h = 0.125$
o MAX. EXPERIMENTAL VALUES
— — — THEORY

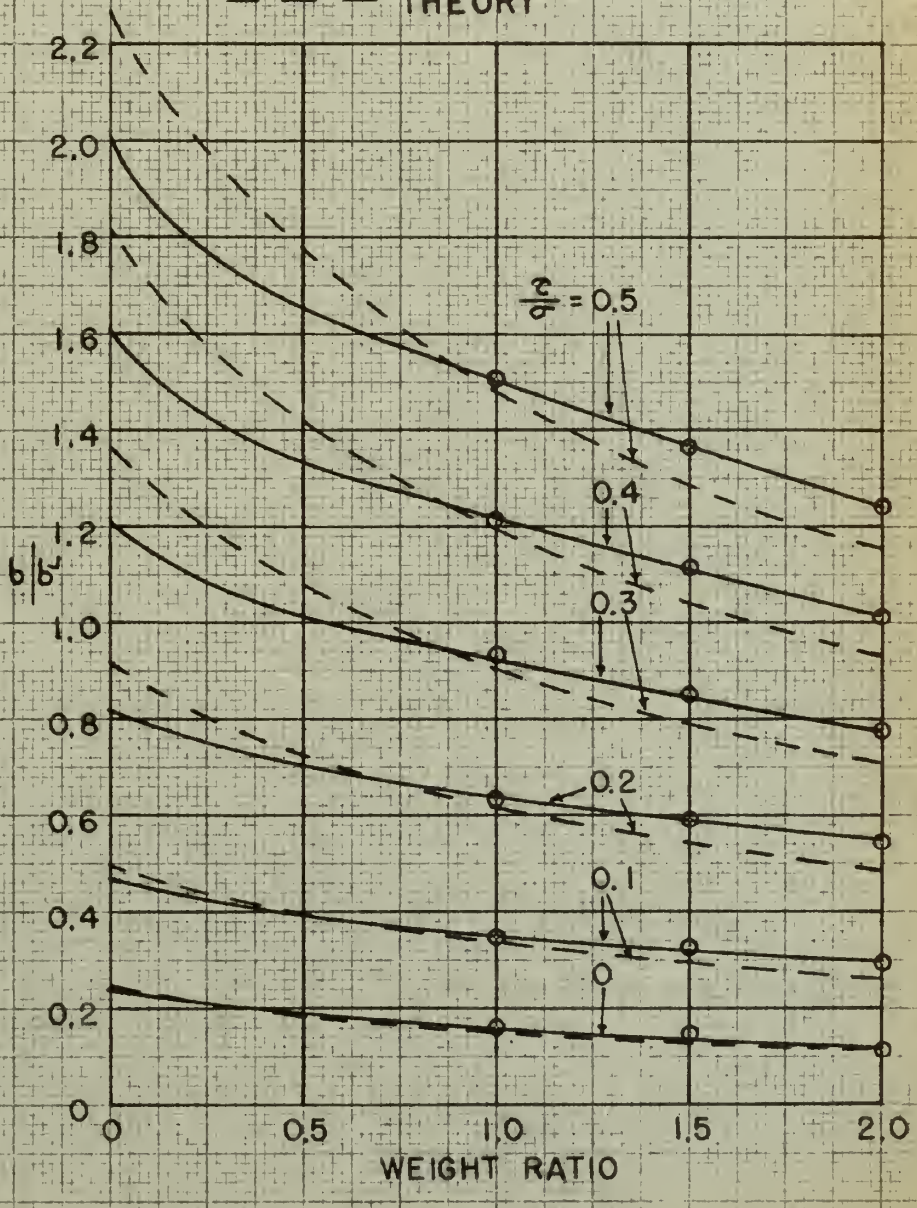

S.R.H.
3-9-51

FIG. VI

STRESS CONCENTRATION FACTOR AT EDGE OF HOLE VS. WEIGHT RATIO

CONTOURS OF $\frac{\tau}{\sigma}$ FOR $r_2/h = 0.2417$

o MAX. EXPERIMENTAL VALUES

— — — — THEORY

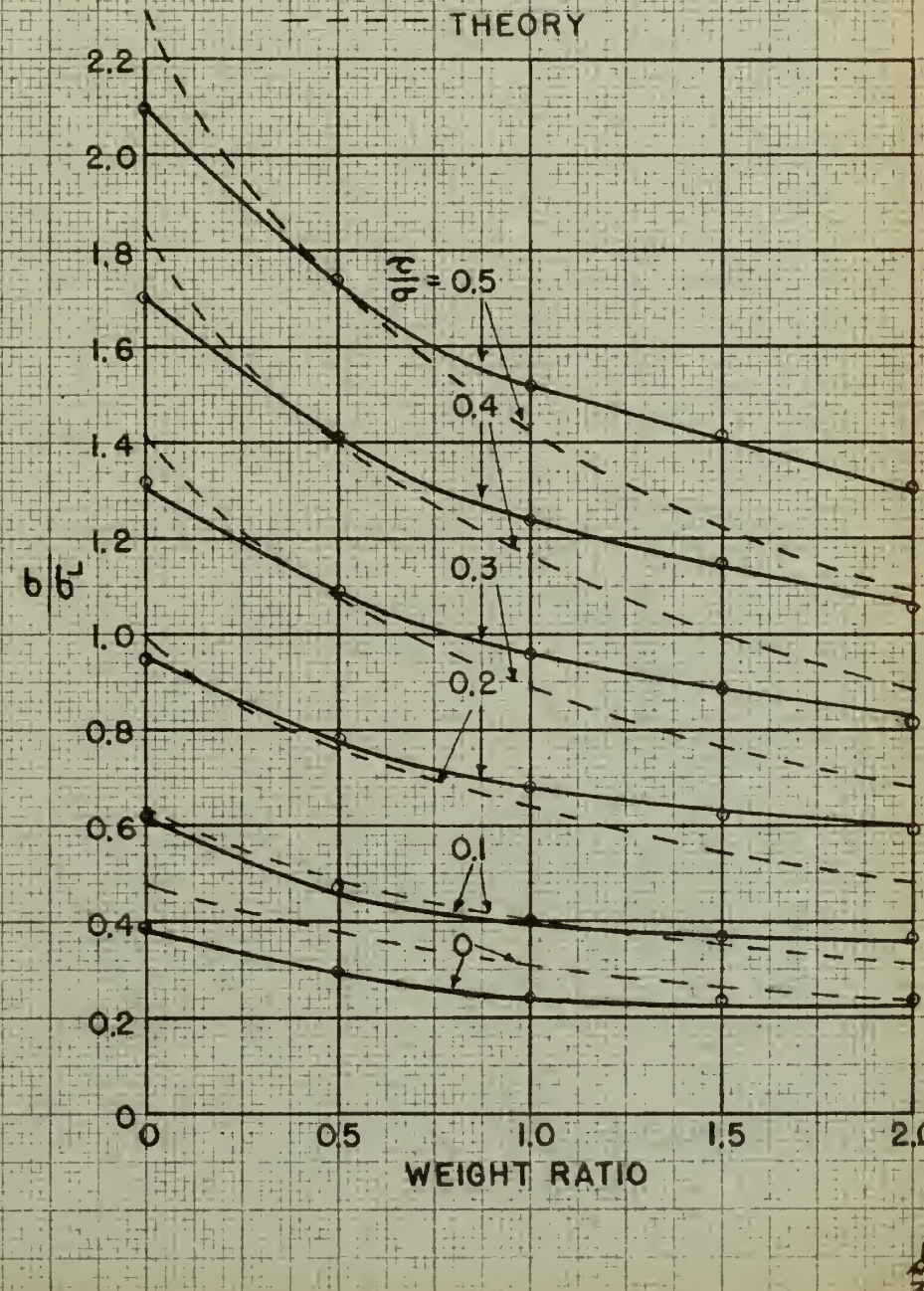

L.R.H.
3-9-51

FIG. VII

STRESS CONCENTRATION FACTOR AT EDGE OF HOLE VS. WEIGHT RATIO CONTOURS OF $\frac{\tau}{\sigma}$ FOR $r_2/h = 0.4206$

o MAX. EXP. VALUES

– – – – – THEORY

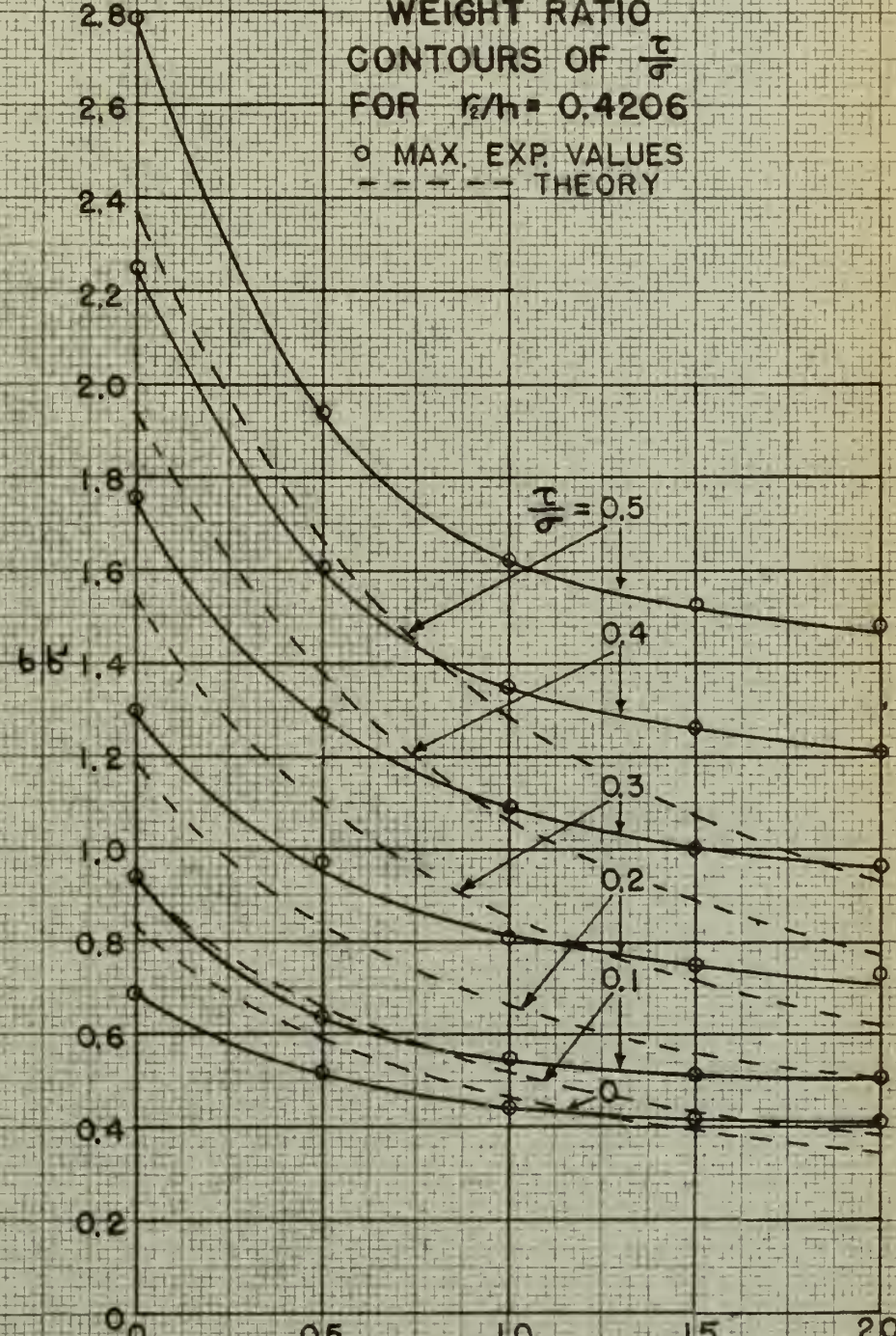

S.R.H.
3-9-51

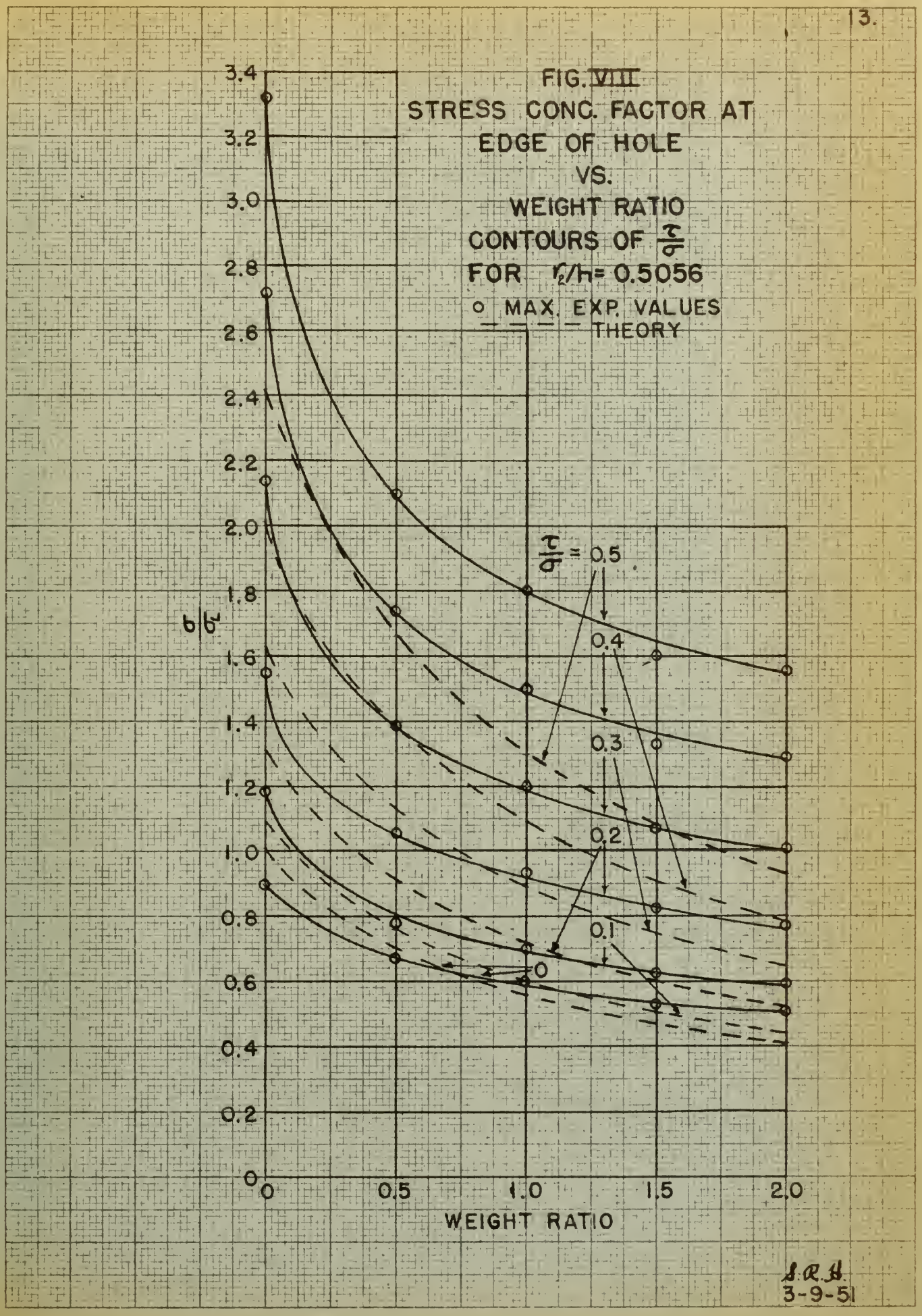
FIG. VIII
STRESS CONC. FACTOR AT EDGE OF HOLE VS. WEIGHT RATIO
CONTOURS OF $\frac{\tau}{\sigma}$
FOR $r_2/h = 0.5056$
o MAX. EXP. VALUES
THEORY
$\frac{\tau}{\sigma} = 0.5$
0.4
0.3
0.2
0.1
0
b/σ
WEIGHT RATIO
0
0.5
1.0
1.5
2.0
0.2
0.4
0.6
0.8
1.0
1.2
1.4
1.6
1.8
2.0
2.2
2.4
2.6
2.8
3.0
3.2
3.4

J.R.H.
3-9-51

STRESS CONCENTRATION FACTOR AT EDGE OF BEAM VS. WEIGHT RATIO CONTOURS OF $\frac{r}{d}$

MAX. EXPERIMENTAL VALUES

$\frac{r}{d}$ = 0 ○
0.2 ●
0.3 ◐
0.4 ◑
0.5 ●

FIG. IX FOR $r_c/h = 0.125$

FIG. X FOR $r_c/h = 0.2417$

FIG. XI FOR $r_c/h = 0.4206$

FIG. XII FOR $r_c/h = 0.5056$

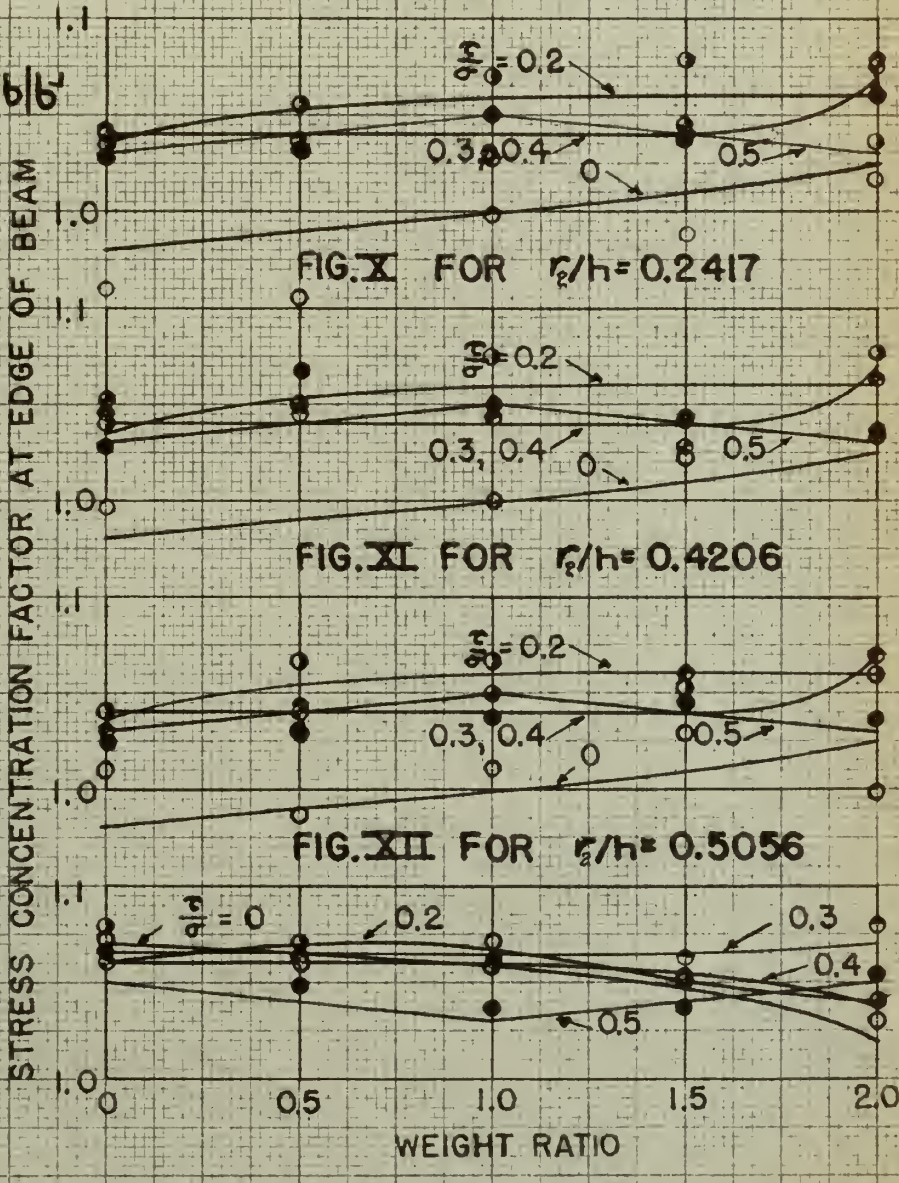

S.Q.H.
3-11-51

FIG. XIII

DESIGN CHART

FOR

RECTANGULAR REINFORCEMENT

LINEAR INTERPOLATION IS SATISFACTORY

$$\alpha' = \frac{E_r}{E_w} \cdot \frac{b}{r_o} \cdot \frac{t_r}{t_w}$$

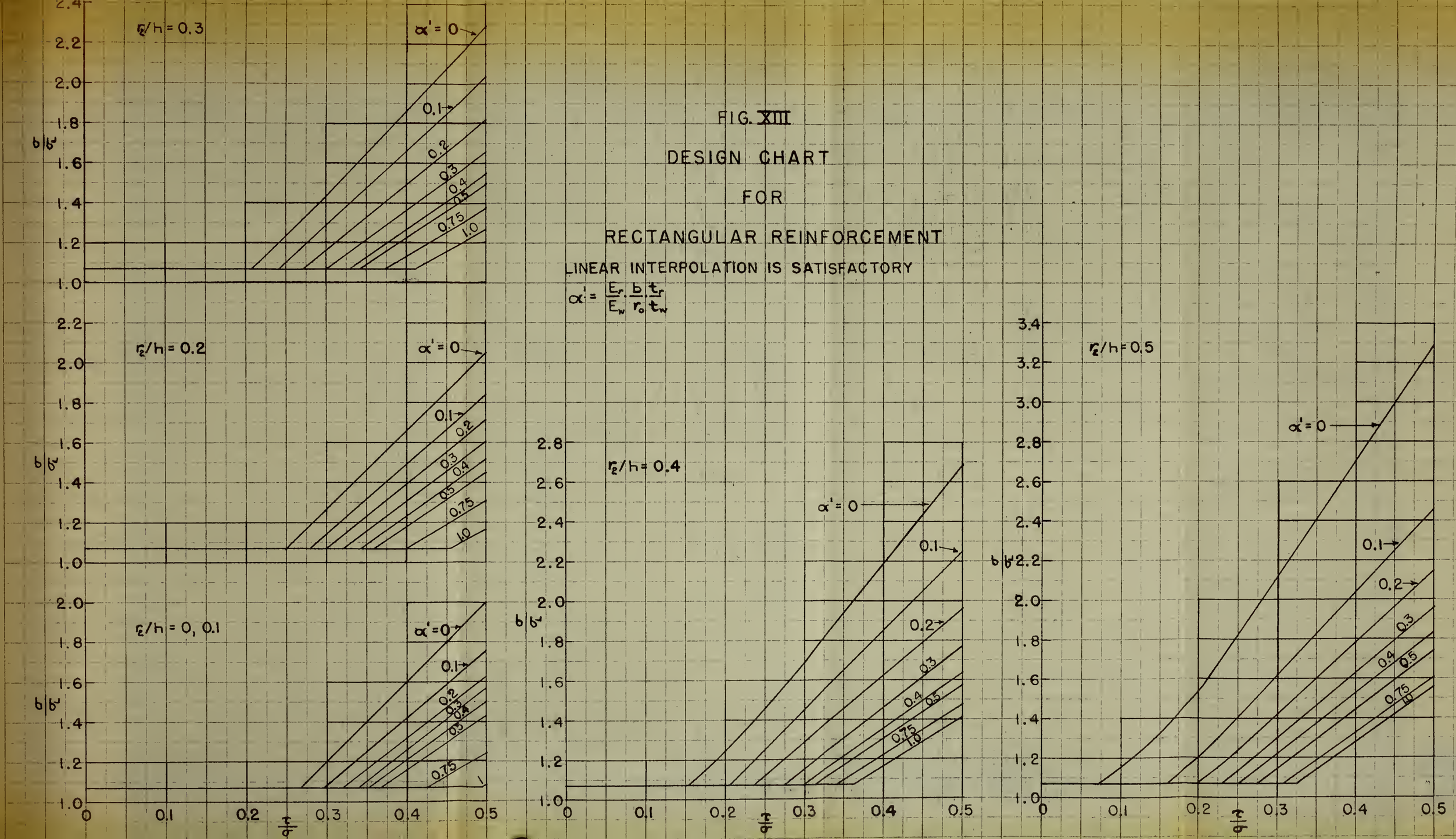

DISCUSSION OF RESULTS

Figures V - VIII show the remarkable fact that the presence of any reinforcement, no matter how small, markedly decreases the high stress concentration at the edge of the hole, but that the addition of greater amounts of reinforcement does not provide a proportionate decrement. In none of the cases actually tested did the reinforcement, which was installed, reduce the stress to that existing with no hole. This is in conformity with the theory developed in APPENDIX D which states that no practical reinforcement provides elastic equivalence of the hole. This explains the asymptotic character of the curves.

It should be noted that, as the ratio of the diameter of the hole to the depth of the web increases, the experimental points for pure bending with no reinforcement no longer agree with theory developed for the simple plate, [2] and [3] . This points out the stiffening effect of the flanges of the I-beam as the edge of the hole gets closer to these flanges. This stiffening effect is similar to a virtual increase in the depth of the web. This virtual increase in the web depth is, of course, a fictitious thing and is not the same as that depth which would provide an equivalent moment of inertia, but is merely a physical kind of reasoning. This same characteristic is not evident for the larger values of the ratio of nominal shear to nominal bending. This can partially be explained by the point of maximum stress, which is located at the vertical for pure bending

and between 30° and 45° from the vertical for the cases of bending with shear. In the latter cases the points of maximum stress are somewhat more remote from the flanges than those for pure bending and hence derive a smaller stiffening effect from them. Another contributing factor to this discrepancy between theory and experiment (for no reinforcement) is the somewhat simplified shear distribution assumed. This distribution is derived from an extension of plane elasticity into the flanges of the section without due regard for the three-dimensional effect at the junction, and, hence, is not exact. A further contributing factor is that discussed in[3] : a static check across the net section is not obtained, and the edges of the beam are not free of shear stresses when the depth is finite.

In spite of these known discrepancies for the limiting case of no reinforcement, the good agreement between theory and experiment for the entire range of reinforcement tested for low values of the ratio of diameter of hole to depth of web (the admitted region of validity of the theory), see Figures V and VI, is gratifying and lends confidence to the entire work.

Figures IX - XII follow the trend shown in[17] : for a given ratio of diameter of hole to depth of web and with a given reinforcement, the maximum stress at the edge of the beam varies but little, but does pass through a maximum - at a ratio of nominal shear to nominal bending between 0.3 and 0.4. For a given size hole at a given ratio of nominal shear to nominal

bending, the relation between the maximum stress at the edge of the beam and the amount of reinforcement is ambiguous. There appears to be no rational explanation for this seemingly haphazard relation. Fortunately, however, the variation of maximum stress at the edge of the beam with change in reinforcement is quite small. For practical purposes, the maximum stress at the beam edge may be taken as a constant.

CONCLUSIONS

1. It is impossible to design a reinforcement for a circular cutout subjected to bending with shear which will restore the stress distribution existing prior to the cut. This is predicted by the theory and verified by those experiments actually performed.

2. For the usual type of reinforcement - a bead in contrast to a doubler plate - the shape is immaterial; the area supplied is paramount. In short, the reinforcement does its work in either tension or compression; not in bending.

3. Any reinforcement reduces the stress level at the edge of the hole; however, after a certain amount, usually the same area as that of the hole, the effect of additional reinforcement is negligible.

4. The theoretical solution developed in APPENDIX D is satisfactory for engineering design purposes when the ratio of diameter of hole to depth of web is less than 0.25.

5. For the usual proportions of I-beams; i.e., the ratio of flange area to total area of about 0.5 to 0.7, Figures V - XIII are satisfactory for design purposes.

RECOMMENDATIONS

1. Further theoretical and experimental investigations for the effect of doubler plate reinforcement are desirable.

2. Further theoretical and experimental investigations for the effect of reinforcement of ellipses and flat ovaloids subjected to bending with shear are desirable.

3. Further investigations of related problems when the portions of the beam immediately adjacent to the cutout are subjected to uniformly distributed and uniformly varying loads are desirable.

4. In order to refine existing theory, such as that developed here, for stress distribution near cutouts in structural sections and to extend other such theory it is necessary that a simple analytical expression for shear distribution in I- and T-beams be developed. This expression may involve such gross parameters as the ratio of flange area to total area, ratio of flange thickness to depth, and some relation between web area and gross moment of inertia. Empirical equations based on existing soap-film analogy or other experiments appear fruitful.

APPENDIX

APPENDIX A

DETAILS OF PROCEDURE

I. Description of Models

A detailed working drawing, Fig. I, was prepared for fabrication purposes. This, along with Figs. III and IV, have already been used to illustrate the test procedure. For the sake of clarity the following amplification is made:

Fig. XIV shows the geometry of a simple case of bending with shear. From this notation the usual beam formulas give the nominal bending and shear stresses, for the uncut beam, at the location of the hole:

$$\sigma = PLh/I \qquad (A1)$$

$$\tau = \frac{P}{2ht_w} \qquad (A2)$$

From Equations (A1) and (A2) the ratio of nominal shear to nominal bending stress is derived:

$$\frac{\tau}{\sigma} = \frac{I}{2h^2Lt_w} \qquad (A3)$$

which is, as is seen, a function of the geometric properties of the beam.

The test arrangement is shown schematically in Figs. XV(a) and XV(b), for bending with shear and pure bending respectively. Using the notation of these figures, the physical dimensions shown in Fig. I were calculated. These calculations are incorporated in Table I.

FIG. XIV

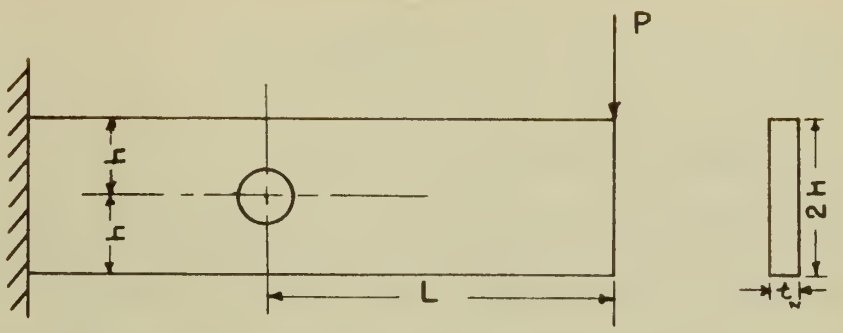

GEOMETRY AND NOTATION FOR BENDING WITH SHEAR

FIG. XV a

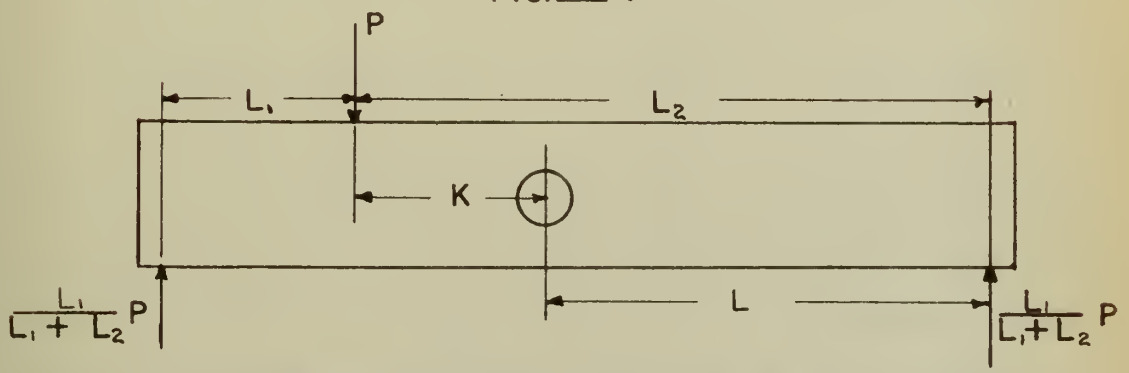

TEST ARRANGEMENT FOR BENDING WITH SHEAR

FIG. XV b

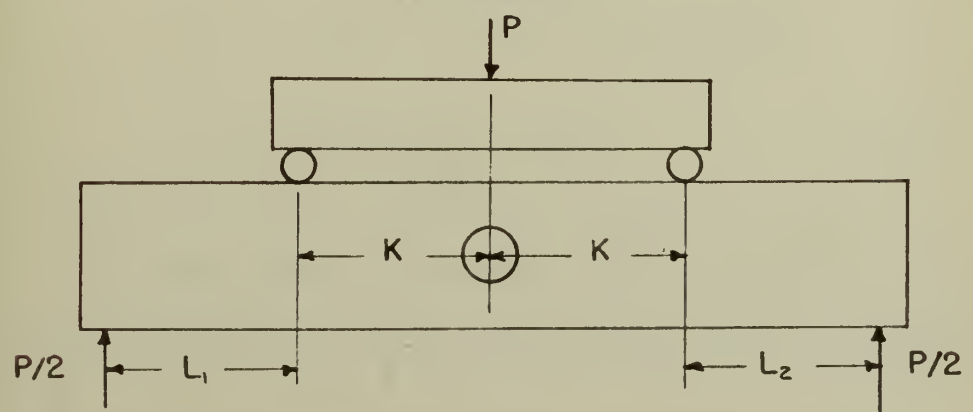

TEST ARRANGEMENT FOR PURE BENDING

S.R.N.
3-6-51

From Equation (A3) with the properties of a 12" x 6½" x 28# WF Section inserted:

$$\frac{\tau}{\sigma} = \frac{12.35}{L} \qquad (A4)$$

where L is given in inches.

Fig. XVI shows the geometry and notation for the typical rectangular or "flat-bar" type reinforcement which was used in this experimental work.

The weight of the material removed is given by:

$\pi \gamma_w r_2^2 t_w$ where γ_w is the specific weight of the web material.

The weight of the reinforcement is given by:

$2\pi \gamma_r r_o (A_r - t_r t_w)$ where γ_r is the specific weight of the reinforcement material, A_r is the area of reinforcement and adjacent web area.

Accordingly the Weight Ratio, WR, is defined as:

$$WR = \frac{\text{Weight of Reinforcement}}{\text{Weight of Material Removed}}$$

$$WR = \frac{2\gamma_r r_o (A_r - t_r t_w)}{\gamma_w r_2^2 t_w} \qquad (A5)$$

For the usual structural work the reinforcement material is the same as the web material and the Weight Ratio becomes:

FIG. XVI

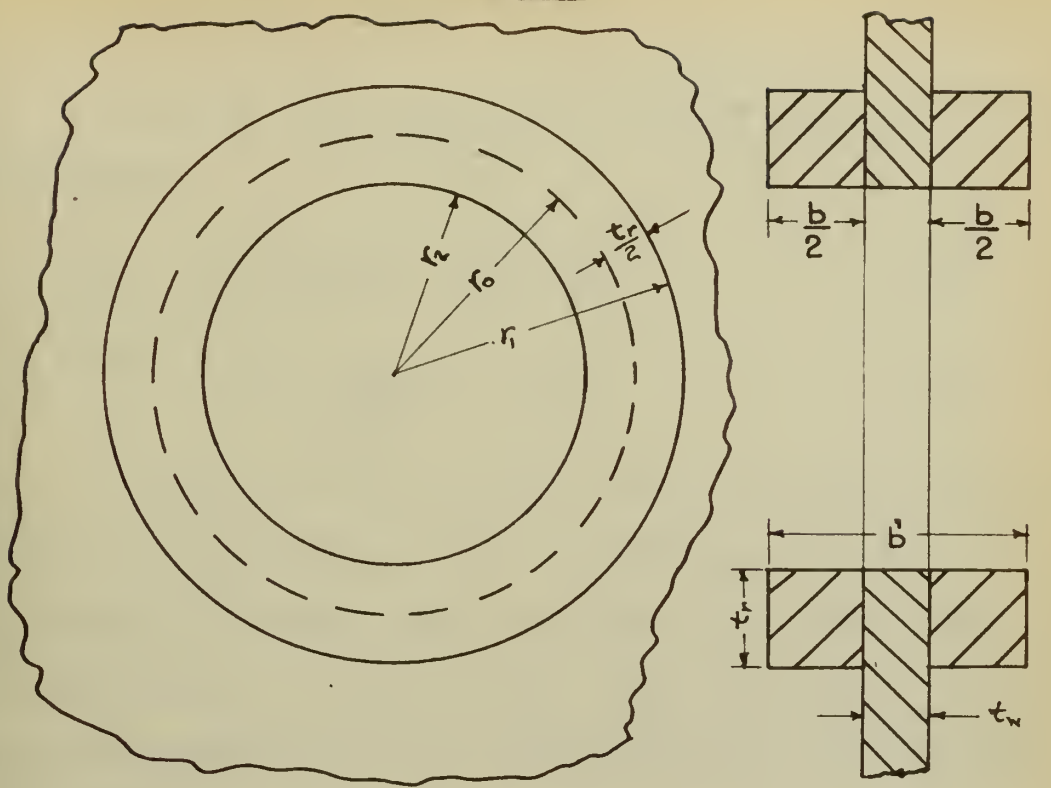

GEOMETRY AND NOTATION OF RECTANGULAR STRIP REINFORCEMENT

FIG. XVII

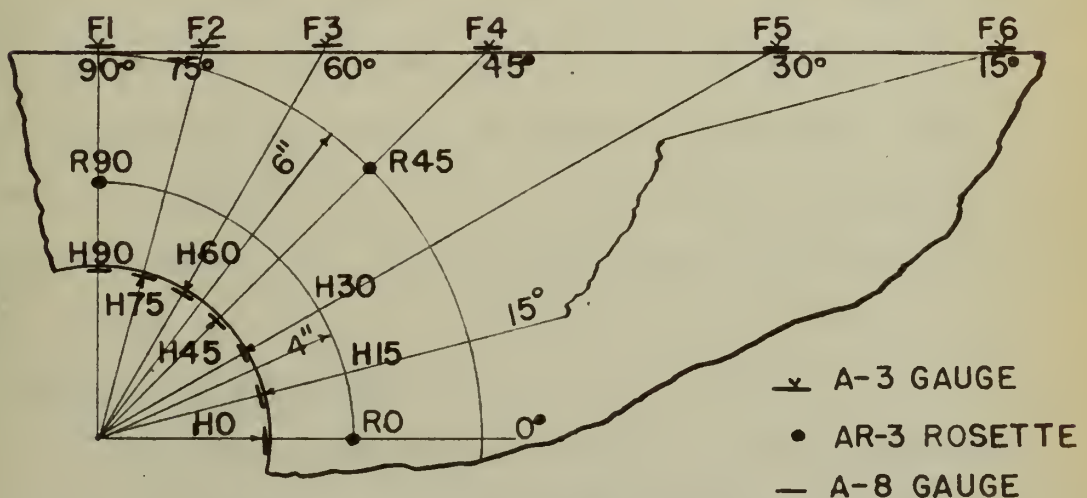

BASIC SR-4 GAUGE LOCATIONS

S.R.H.

$$WR = \frac{2r_o(A_r - t_r t_w)}{r_2^2 t_w} \qquad (A5a)$$

For the rectangular type reinforcement this further simplifies to:

$$WR = 2\frac{t_r}{r_2}\left(1 + \frac{t_r}{2r_2}\right)\left(\frac{b'}{t_w} - 1\right) \qquad (A5b)$$

or

$$WR = 2\frac{bt_r}{r_2 t_w}\left(1 + \frac{t_r}{2r_2}\right) \qquad (A5c)$$

Because of its simplicity pipe was chosen for reinforcement. A further practical consideration entered into this choice: in actual construction pipe is widely used for this same purpose. Table II shows the determination of the machining schedule in Fig. I using Equation (A5b) for this calculation.

Fig. XVII shows the basic gauge locations for all models. This choice of locations made possible plots of stress concentration factors at the edge of the hole, at the edge of the beam, and along several radial lines. Fig. XVIII shows the gauges mounted on the flange and web of the beam; Fig. XIX shows the gauges mounted at the edge of the hole. Fig. XX shows the main instrument center with a SR-4 Strain Indicator and the Baldwin Switching Units for multiple gauge readings at a single load.

II. Methods of Analysis

Standard experimental stress analysis procedures were used. Single strain gauge readings were reduced to strain

TABLE I

Determination of Model Dimensions

τ/σ	0	0.2	0.3	0.4	0.5
L(in)	---	61.776	41.184	30.888	24.711
K(in)	30.888	30.888	30.888	30.888	30.888
L_2(in)	30.888	92.664	72.072	61.776	55.599
L_1(in)	30.888	30.888	30.888	30.888	30.888
L_1+L_2(in)	61.776	123.552	102.96	92.664	86.487
$\frac{L_1}{L_1+L_2}$	0.5	0.25	0.3	0.333	0.357
$\frac{L_1L_2}{L_1+L_2}$(in)	15.444	23.166	21.622	20.592	19.857
$\frac{L_1L_2h}{(L_1+L_2)I}(\frac{1}{in^2})$	0.434	0.651	0.608	0.579	0.558
P for 32000 psi at L_2(#)	73729	49153	52663	55297	57344
P(#)	60000	48000	52000	55000	56000
$\frac{L_1L_2h}{(L_1+L_2)I}(\frac{1}{in^2})$	0.434	0.434	0.347	0.289	0.248
σ_L(psi)	-26041	-20832	-18055	-15914	-13889

TABLE II

Determination of Machining Schedule

Pipe Size	1½" X Hvy	3" X Hvy	5" Std.	6" Std.
t_r(in.)	0.2	0.3	0.258	0.28
r_2/h	0.125	0.2417	0.4206	0.5056
b'(in.)				
WR = 0	0.24	0.24	0.24	0.24
WR = 0.5	0.438	0.503	0.798	0.861
WR = 1	0.637	0.766	1.356	1.482
WR = 1.5	0.836	1.028	1.915	2.103
WR = 2	1.034	1.291	2.473	2.725

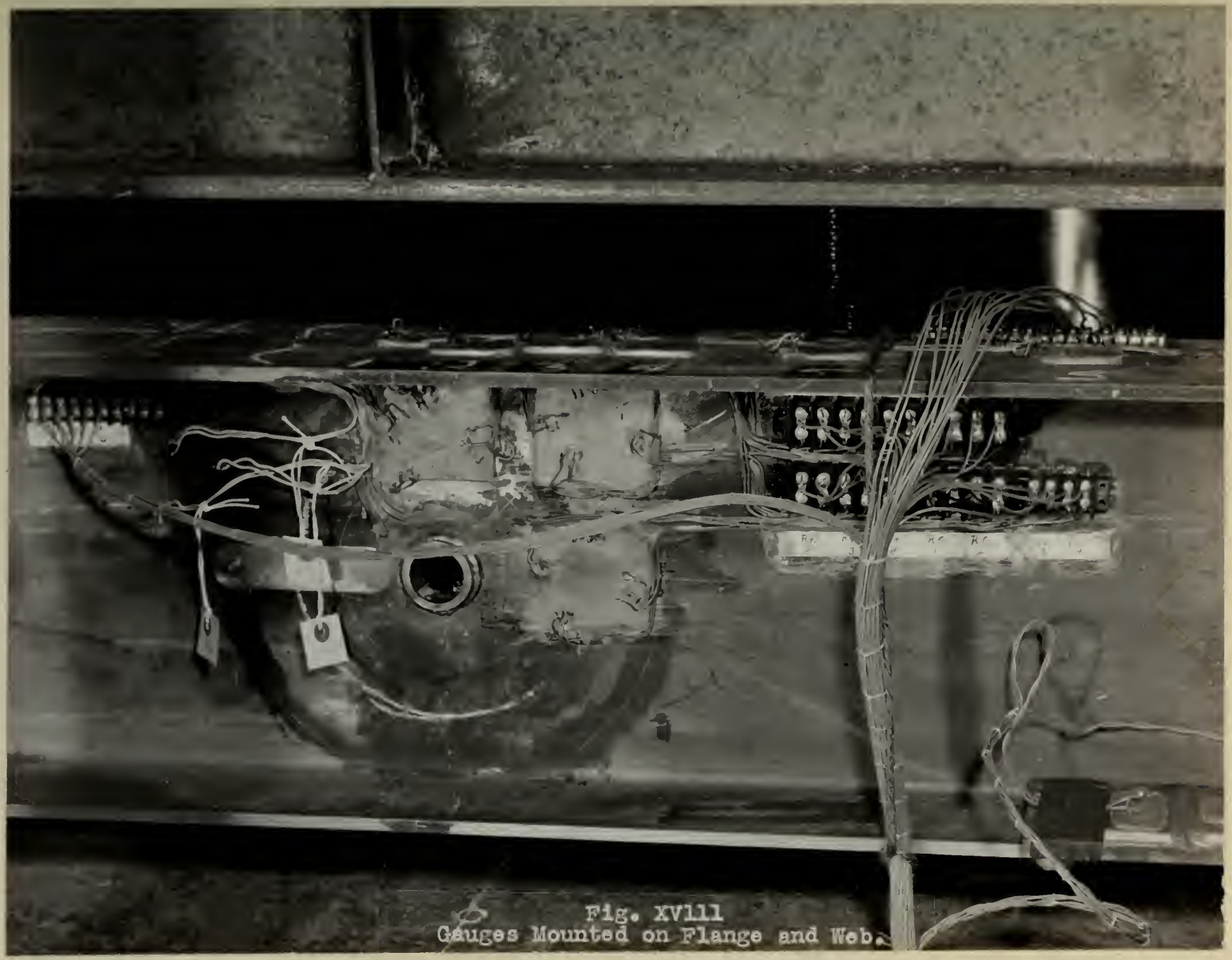

Fig. XVIII
Gauges Mounted on Flange and Web.

Fig. XX
Gauges Mounted on Edge of Hole.

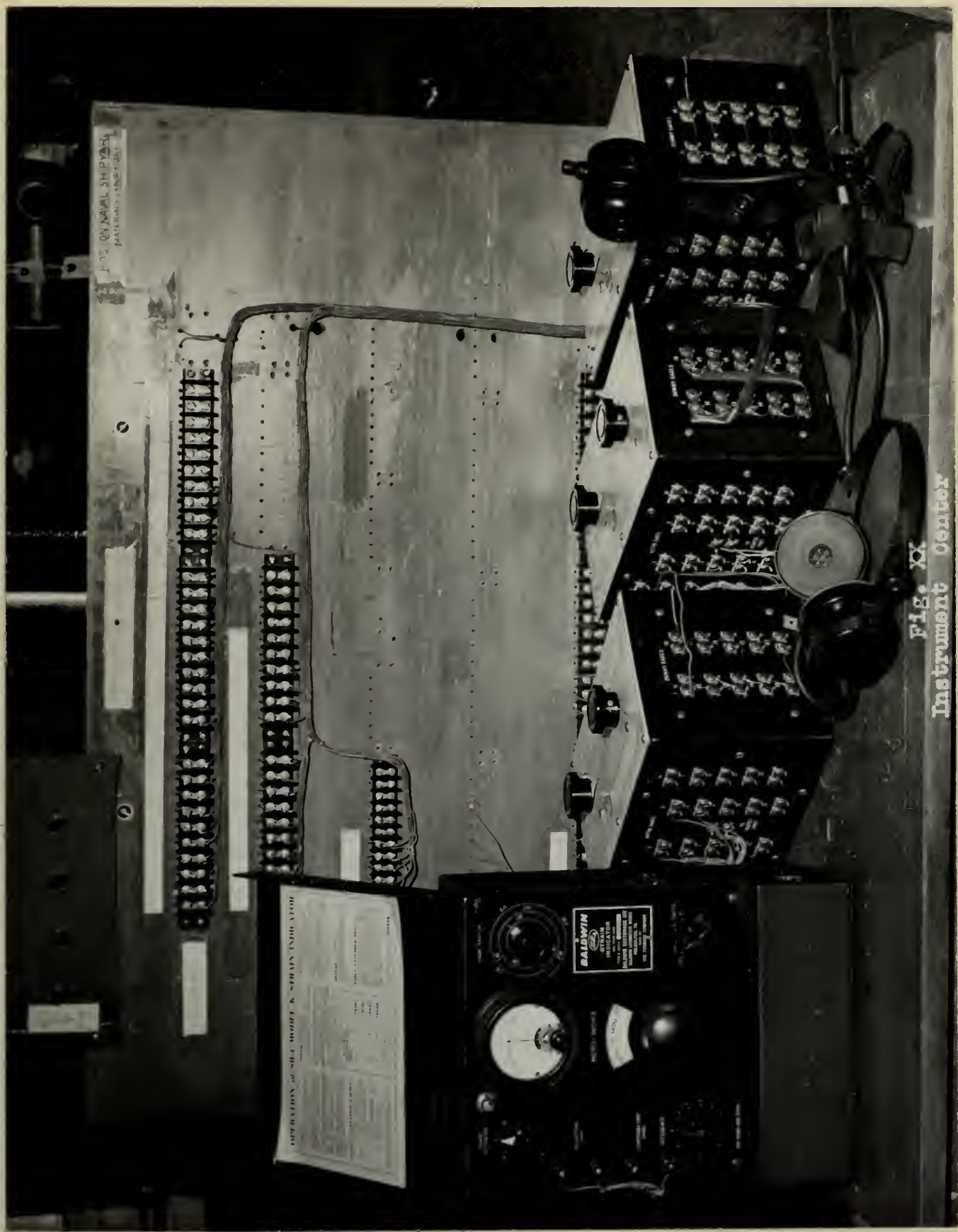

Fig. X
Instrument Counter

in microinches per inch corresponding to a given load in pounds, see Table III. These readings, corrected for an "average zero" readings, were then plotted versus the corresponding load and the best straight line passed through the experimental points, see Fig. XXI. The corrected strain corresponding to the rated test load was then determined by a parallel shifting of this best straight line to obtain zero strain at zero load; i.e., "corrected" strain was determined as the change in strain corresponding to a change in load.

Stress was determined in two different ways:

a.) For uniaxial gauges, those mounted on free boundaries where the stress is uniaxial, stress was obtained by multiplying the strain at that point by the modulus of elasticity.

b.) For strain rosettes, those mounted on the web where biaxial stress as well as shear can exist, stress was obtained using nomographs developed in [22], see Fig. XXII.

In both instances standard values of Poisson's Ratio and modulus of elasticity, 0.3 and 30 x 10^6 psi respectively, were used.

III. Correlation Procedure

Satisfactory bases for plotting were unknown at the outset; but, as sufficient data became available and after several schemes had been tried, a workable system was evolved.

Bending with shear, with stresses below the elastic limit, can be treated as the superposition of "pure shear" at

TABLE III

Load-Strain Data: $\frac{\tau}{\sigma} = 0.5$; $\frac{r_2}{h} = 0.4206$; MR = 2

Load	F1	F2	F3	F4	F5	F6	H0	H15
Zero	80869	70943	61202	60833	60952	71470	61218	81540
AVE 0	80869	70942	61195	60833	60951	71469	61216	81545
14000#	80749	70843	61116	60741	60880	71464	61222	81478
	-120	-99	-79	-92	-71	-5	+ 6	-67
AVE 0	80869	70942	61195	60833	60951	71469	61216	81545
28000#	80628	70748	61028	60650	60808	71460	61229	81413
	-241	-194	-167	-183	-143	-9	+13	-132
AVE 0	80869	70942	61195	60833	60951	71469	61216	81545
42000#	80508	70655	60940	60561	60738	71455	61238	81349
	-361	-287	-255	-272	-213	-14	+ 22	-196
AVE 0	80869	70942	61195	60833	60951	71469	61216	81545
56000#	80383	70559	60852	60473	60660	71450	61247	81285
	-486	-383	-343	-360	-291	-19	+31	-260
Zero	80869	70941	61188	60833	60950	71468	61214	81550

Load	H30	H45	H60	H75	H90	R45-1	R45-2	R45-3	R45-4
Zero	91442	80950	91672	101002	90770	71082	70780	61340	61234
AVE 0	91447	80956	91682	101010	90773	71091	70779	61344	61236
14000#	91323	80787	91511	100906	90741	71076	70670	61362	61146
	-124	-169	-171	-104	- 32	-15	-109	+18	-90
AVE 0	91447	80956	91682	101010	90773	71091	70779	61344	61236
28000#	91202	80618	91349	100804	90710	71064	70562	61382	61056
	-245	-338	-333	-206	-63	-27	-217	+38	-180
AVE 0	91447	80956	91682	101010	90773	71091	70779	61344	61236
42000#	91087	80451	91183	100704	90679	71052	70456	61401	60969
	-360	-505	-499	-306	-94	-39	-323	+57	-267
AVE 0	91447	80956	91682	101010	90773	71091	70779	61344	61236
56000#	90970	80283	91019	100603	90646	71040	70347	61420	60880
	-477	-673	-663	-407	-127	-51	-432	+76	-356
Zero	91452	80962	91692	101018	90776	71100	70778	61348	61238

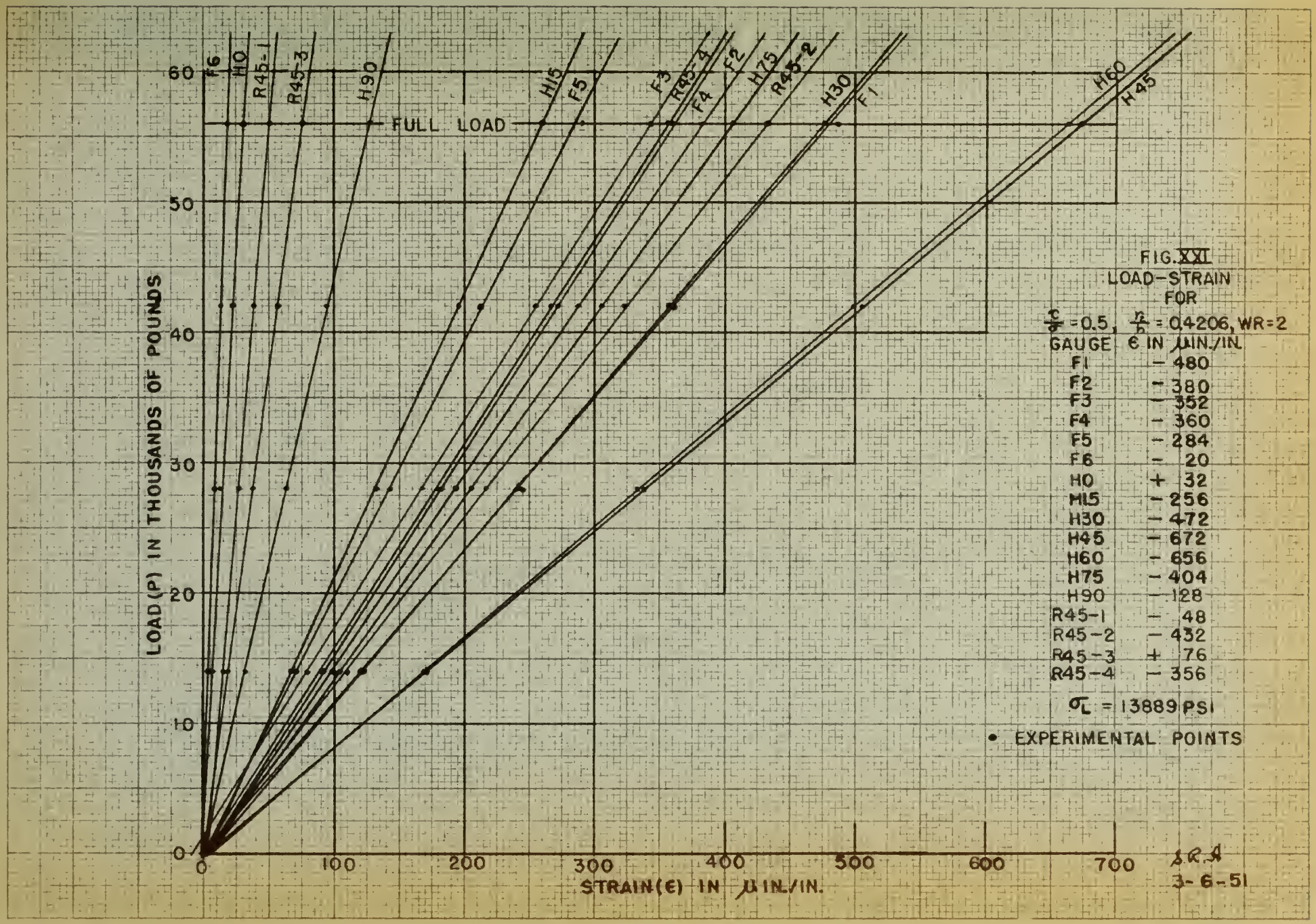

FIG. XXI
LOAD-STRAIN
FOR
$\frac{c}{a}$ = 0.5, $\frac{r_i}{b}$ = 0.4206, WR = 2

GAUGE	ϵ IN μIN./IN.
F1	− 480
F2	− 380
F3	− 352
F4	− 360
F5	− 284
F6	− 20
H0	+ 32
H15	− 256
H30	− 472
H45	− 672
H60	− 656
H75	− 404
H90	− 128
R45-1	− 48
R45-2	− 432
R45-3	+ 76
R45-4	− 356

σ_L = 13889 PSI

• EXPERIMENTAL POINTS

S.R.A
3-6-51

FIG. XXII

GAUGE R45

$\frac{\tau}{\sigma} = 0.5$; $\epsilon/h = 0.4206$; WR=2

TEE - DELTA

STRAIN ROSETTE

NOMOGRAPH

DATA

$E = 30 \times 10^6$ PSI $\quad \mu = 0.3$

$\epsilon_B = -0.000051 \quad \sigma_1 = 0$ PSI

$\epsilon_C = -0.000432 \quad \sigma_2 = -10460$ P

$\epsilon_A = +0.000076 \quad \tau_M = +5230$ P

$\epsilon_D = -0.000356 \quad \phi = 22.5$ DEG.

$\frac{\sigma}{\sigma_1} = 0.753$

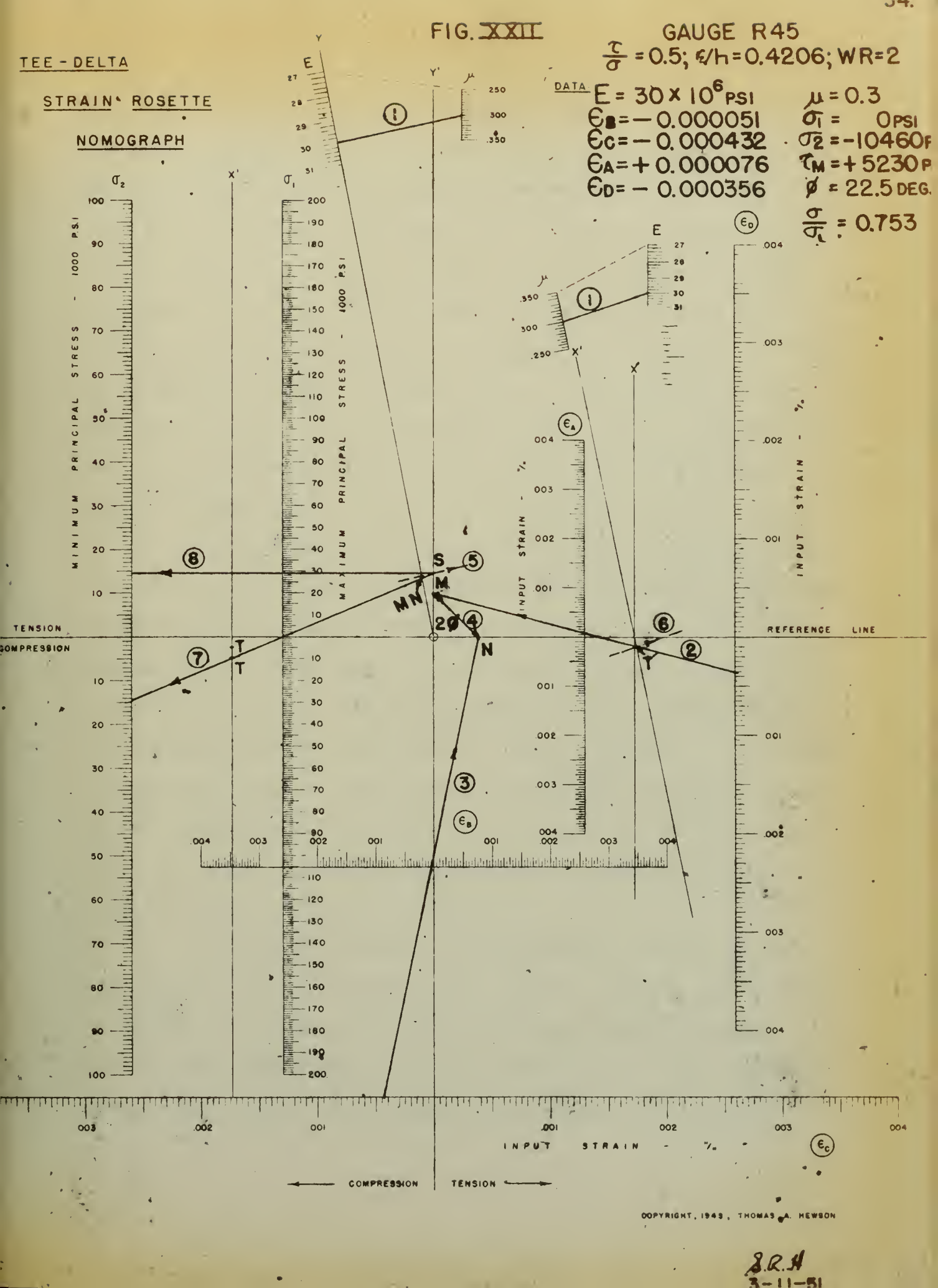

COPYRIGHT, 1943, THOMAS A. HEWSON

S.R.H
3-11-51

the vertical axis of symmetry on pure bending, see [3] and [6] and APPENDIX D. For each size hole and degree of reinforcement, the stress concentration factor at the edge of the hole and in the web was plotted, in contours of angular location, against the shear to bending ratio as a straight line, see Fig. XXIII. Faired data from this type plot were then plotted as stress concentration factor versus angular location in contours of shear to bending ratio. The maximum for each such contour was then determined, see Fig. XXIV. These maxima were then transferred back to Fig. XXIII and a smooth curve passed through them.

Plots similar to Figs. XXIII and XXIV were prepared for each size hole and each degree of reinforcement. Fig. XXV is essentially a compilation of the maximum curves from plots similar to Fig. XXIII for varying degrees of reinforcement for a single size hole. The cross-fairing of all data from this kind of plot is shown in Figs. V - VIII in RESULTS. These data were cross-faired by yet another method: stress concentration factor versus ratio of diameter to depth of web in contours of shear to bending ratio for each degree of reinforcement. A sample of such a plot is Fig. XXVI.

Similarly the stress concentration factors at the edge of the beam were correlated, but by a slightly different procedure. For each size hole and for each ratio of shear to bending, the experimental data was plotted as stress concentration factor versus the distance from the vertical diameter of the

FIG. XXIII

STRESS CONCENTRATION FACTOR AT EDGE OF HOLE VS. SHEAR-BENDING RATIO

CONTOURS OF ANGLE FROM VERTICAL

FOR $r/h = 0.4206$; WR = 2

○ EXPERIMENTAL VALUES

● MAX. FAIRED VALUES

— — LOCUS OF MAXIMA

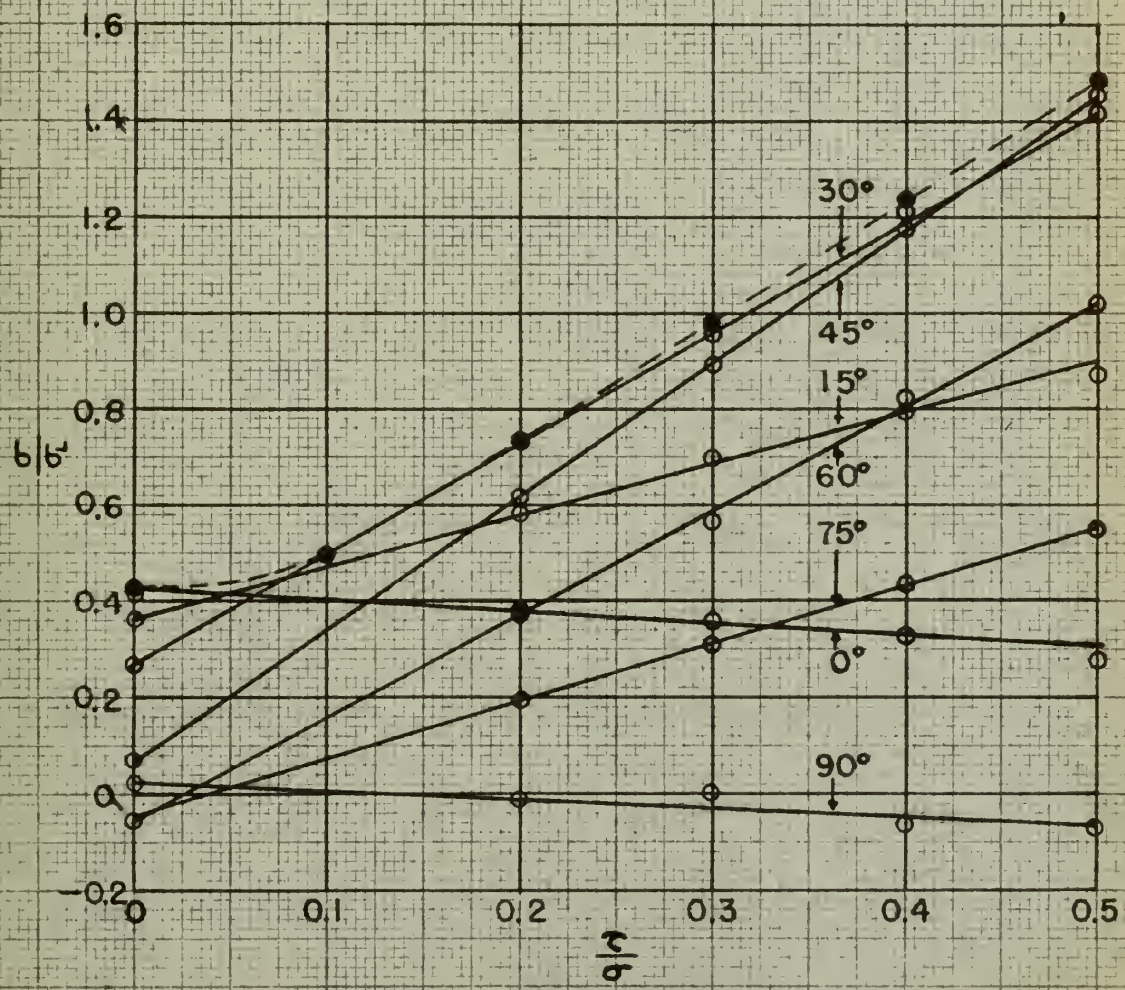

S.R.H.
3-11-51

FIG. XXIV

STRESS CONCENTRATION FACTOR AT EDGE OF HOLE VS. ANGLE FROM VERTICAL

CONTOURS OF $\frac{\tau}{\sigma}$ FOR $r/h = 0.4206$; WR=2

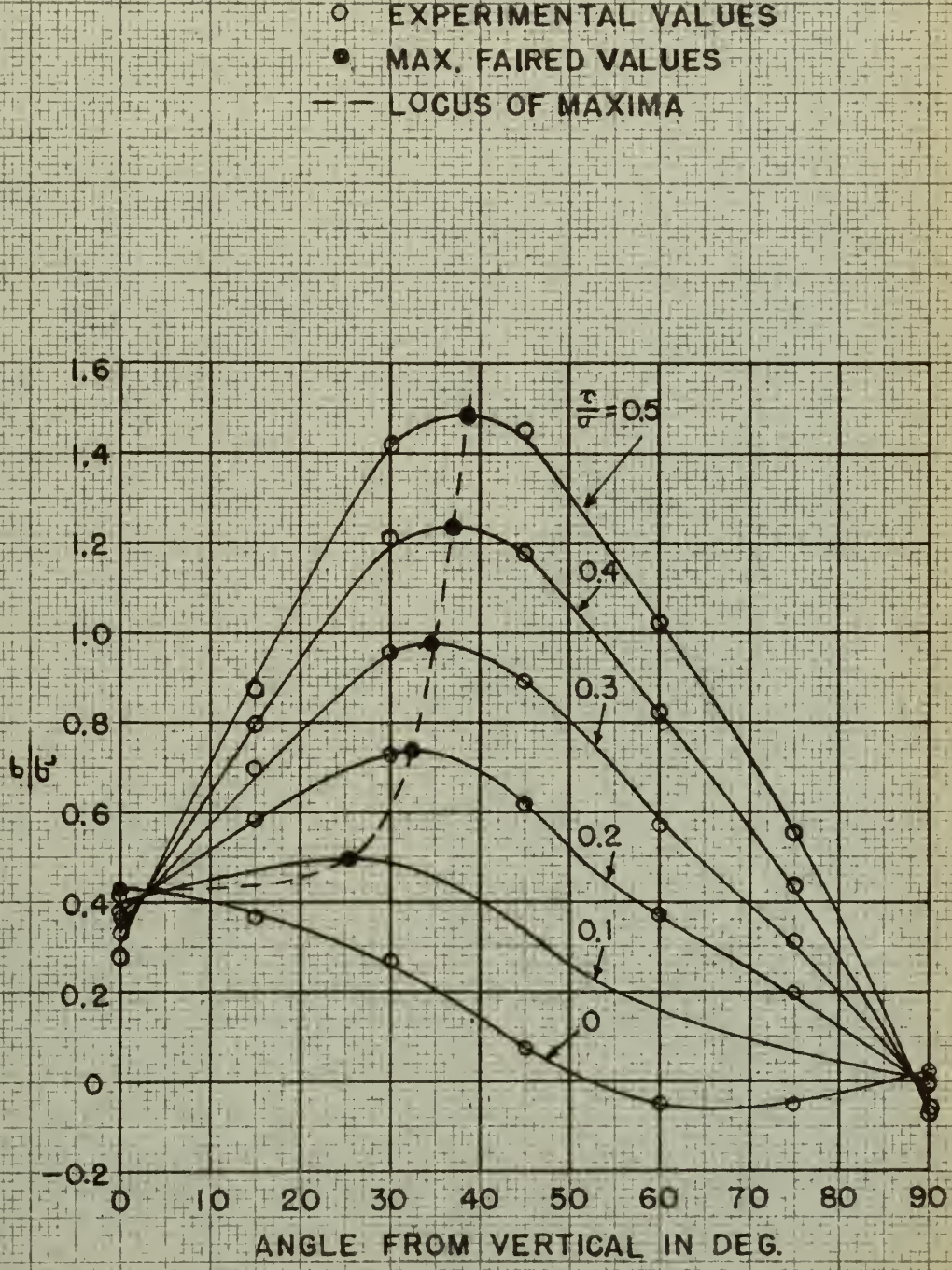

S.R.H.
3-11-51

FIG. XXV

STRESS CONCENTRATION FACTOR AT EDGE OF HOLE VS. SHEAR-BENDING RATIO CONTOURS OF WEIGHT RATIO FOR $r_2/h = 0.4206$

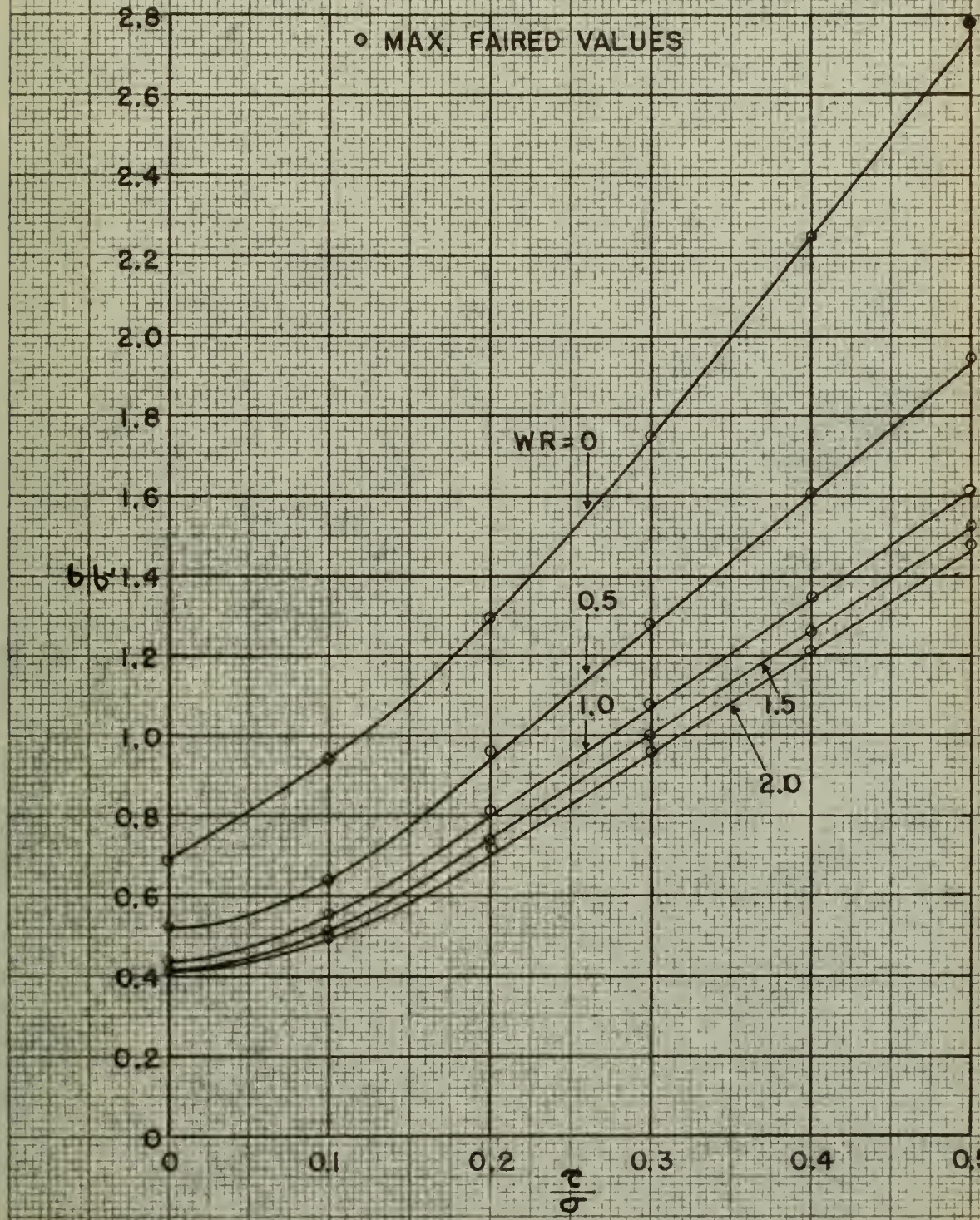

S.R.H.
3-12-51

FIG. XXVI
STRESS CONCENTRATION FACTOR AT EDGE OF HOLE
VS.
DIAMETER-DEPTH RATIO
CONTOURS OF $\frac{r}{d}$ FOR WR = 2
○ MAX. FAIRED EXP. VALUES

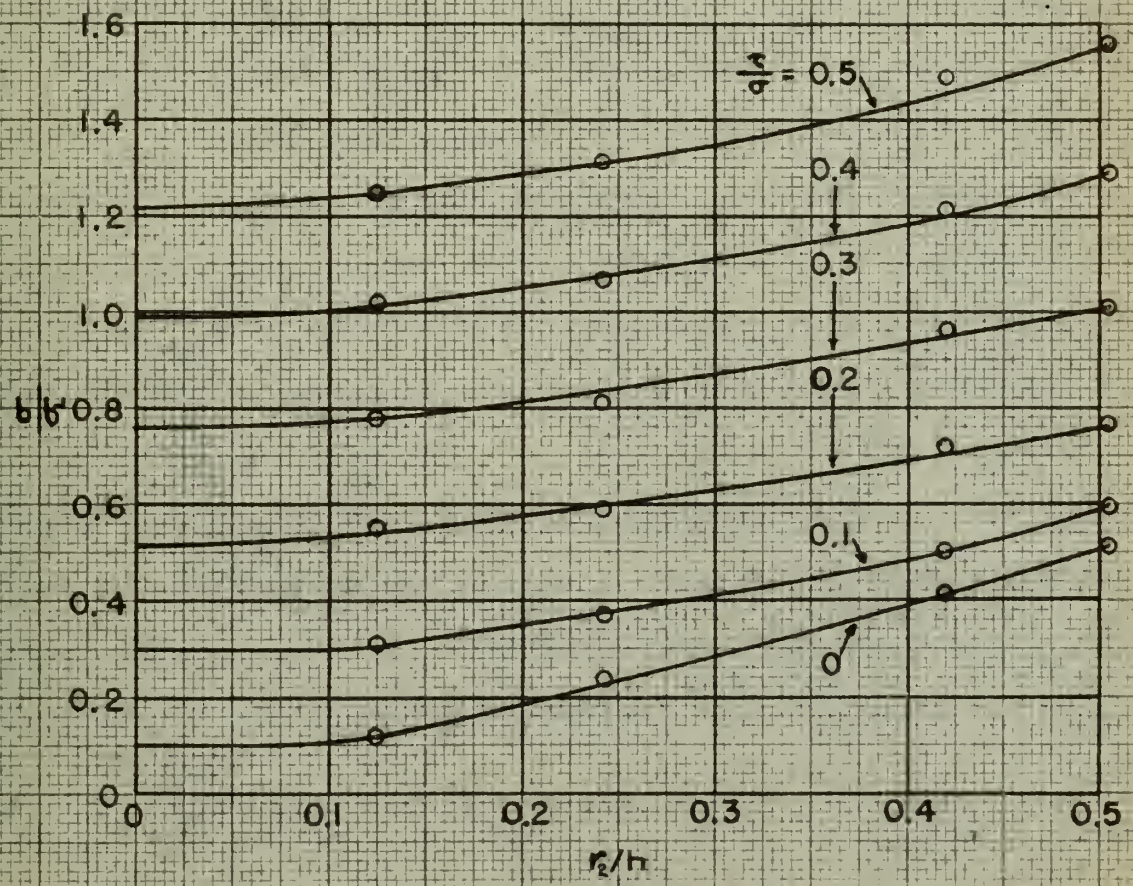

J.R.H.
3-12-51

hole in diameters of the hole, in contours of degree of reinforcement, see Fig. XXVII. The faired maxima were then plotted versus the degree of reinforcement, Weight Ratio, see also Fig. XXVII. The compilation of such plots are shown in Figs. IX - XII in RESULTS. These data were also cross-faired as stress concentration factor versus ratio of diameter of hole to depth of web in contours of Weight Ratio for each ratio of shear to bending, see Fig. XXVIII; an additional method of cross-fairing is also shown in Fig. XXVIII: stress concentration factor versus ratio of shear to bending in contours of Weight Ratio for each size hole. From the latter plot it was determined that for practical purposes the augmentation of stress at the edge of the beam was constant despite the variation of shear to bending, Weight Ratio, or size of hole and was 7%. This constant value was used in the preparation of Fig. XIII.

It was also desired to determine whether the stress in the web ever exceeded the maximum obtained either at the edge of the hole or the edge of the beam. In this connection the principal stress at each rosette determined by nomograph, see Fig. XXI, and plotted as stress concentration factor versus ratio of shear to bending for each size hole and for each Weight Ratio, similar to Fig. XXIII. These faired data were then plotted, in conjunction with faired data from plots similar to Figs. XXIII and XXVII, as stress concentration factor versus distance from the center of the hole in diameters for each

FIG. XXVII

STRESS CONCENTRATION FACTOR AT EDGE OF BEAM VS. DISTANCE FROM CENTER OF HOLE IN DIAMETERS

CONTOURS OF WEIGHT RATIO FOR $r_e/h_1 = 0.4206$

$\frac{\tau}{\sigma} = 0.5$

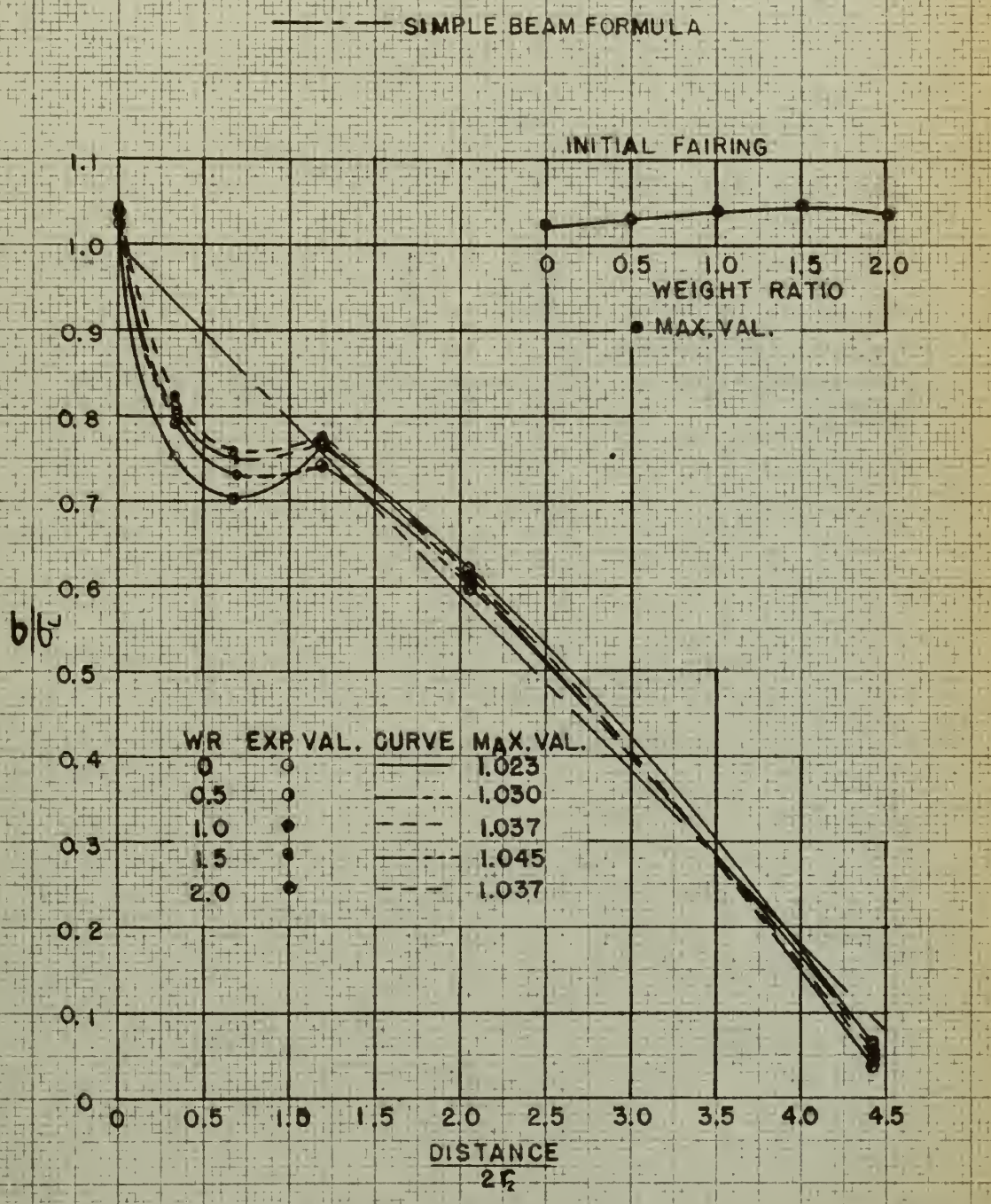

S.R.H.
3-13-51

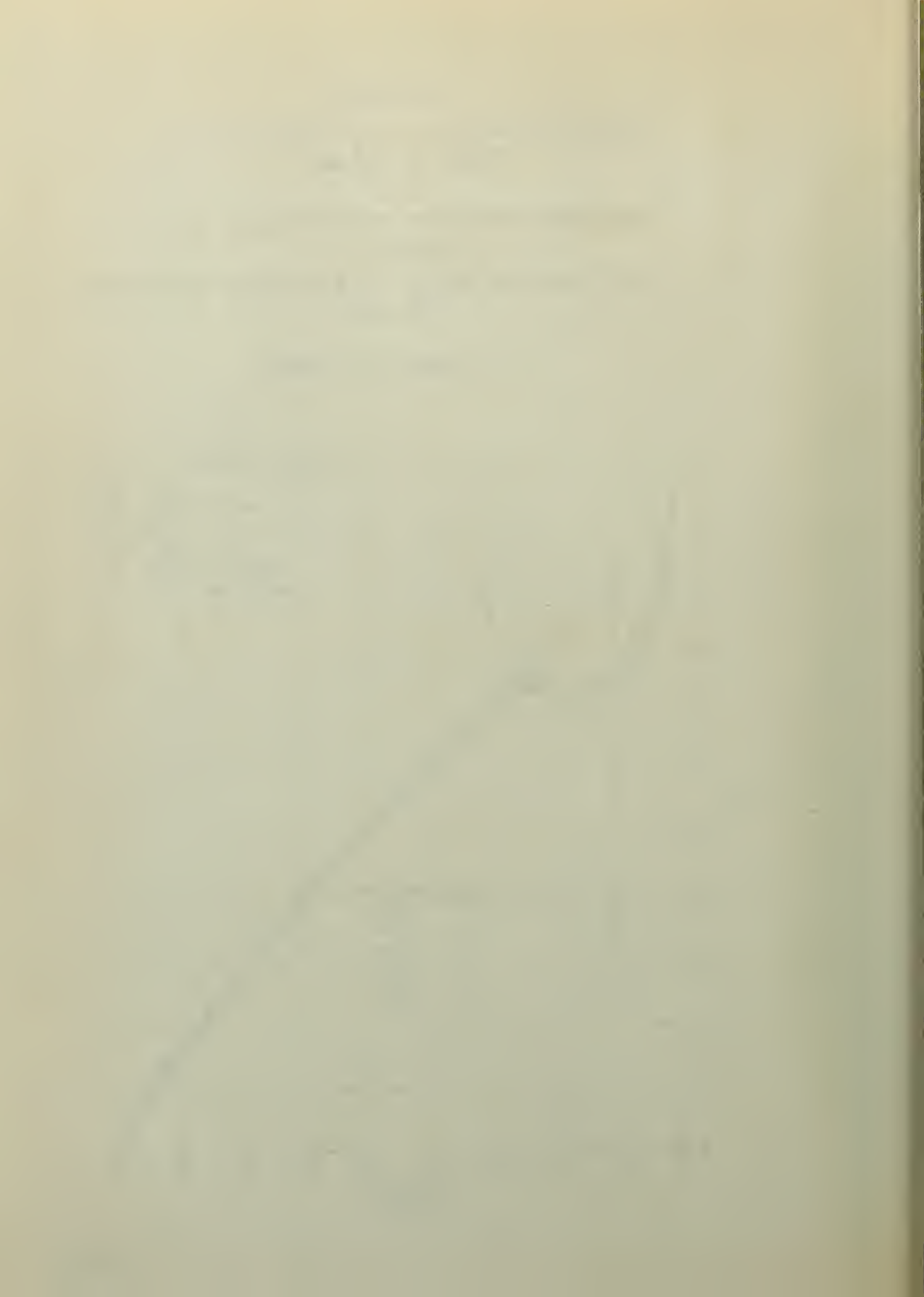

FIG. XXVIII
CROSS-FAIRING METHODS FOR STRESS CONCENTRATION FACTOR AT EDGE OF BEAM

$\frac{\sigma}{\sigma_c}$ VS r_2/h
CONTOURS OF $\frac{\tau}{\sigma}$
FOR WR=2
MAX. FAIRED VALUES

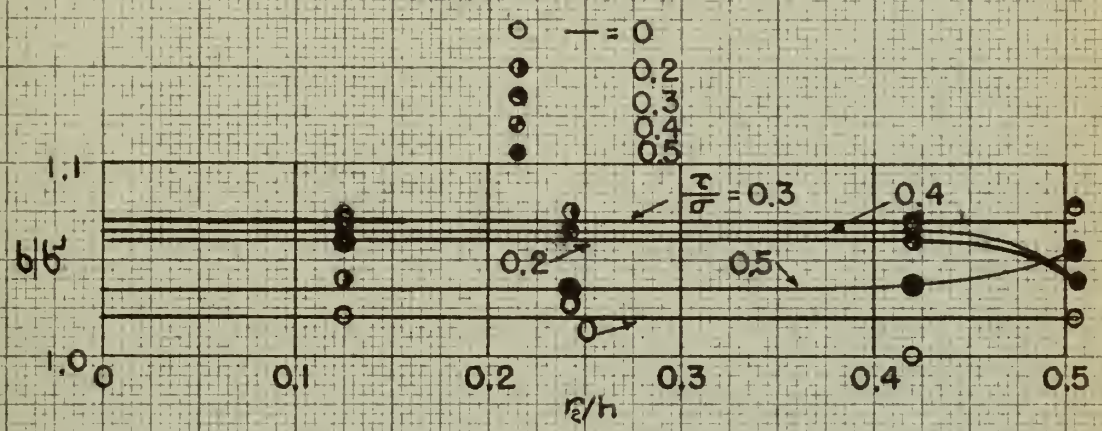

$\frac{\sigma}{\sigma_c}$ VS. $\frac{\tau}{\sigma}$
FOR $r_2/h = 0.4206$; WR=2

○ MAX. FAIRED VALUES

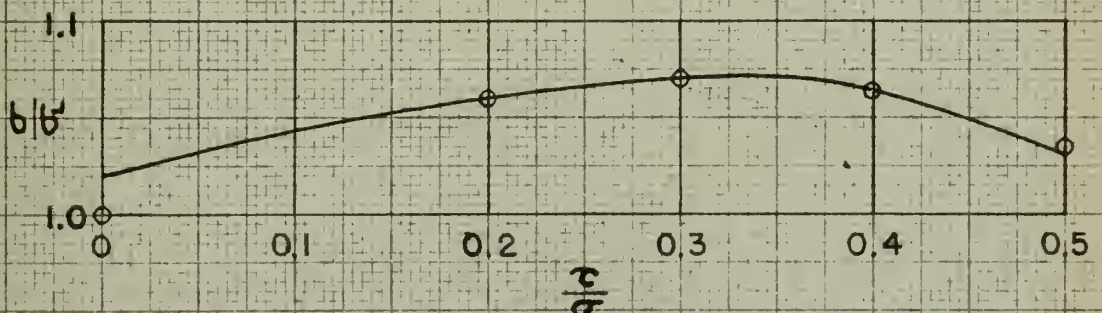

S.R.H.
3-13-51

radial line wherein a rosette was located, see Fig. XXIX. In no case was the maximum stress concentration factor at either the edge of the hole or the edge of the beam, whichever was greater, exceeded. This, of course, was predicted in the theoretical development in APPENDIX D.

FIG. XXIX

STRESS CONCENTRATION FACTOR IN WEB
VS.
DISTANCE FROM CENTER OF HOLE IN DIAMETERS
FOR $r/h = 0.4206$; $WR = 2$; $45°$; $\frac{r}{d} = 0.5$

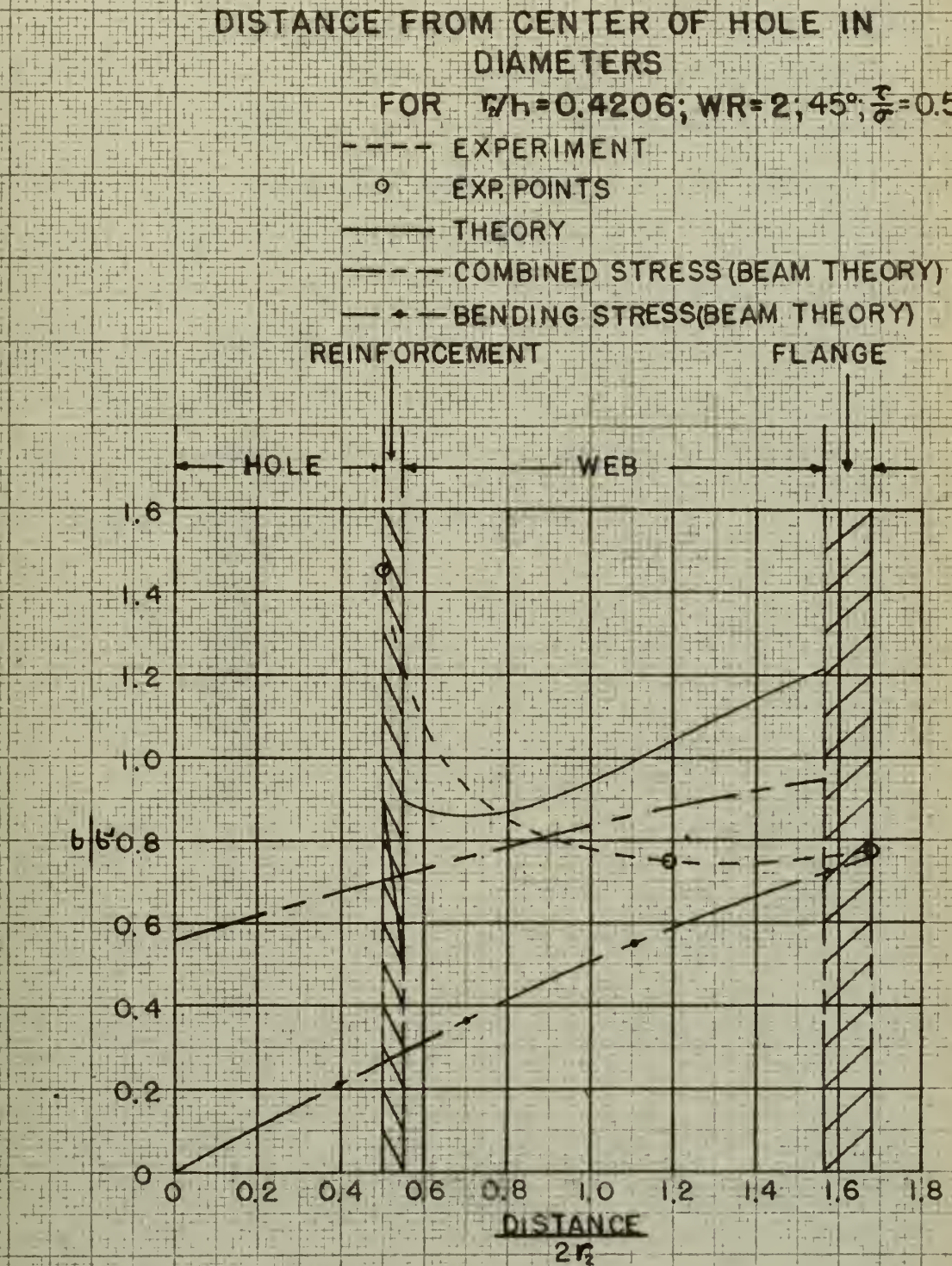

S.R.H.
3-13-51

APPENDIX B

SAMPLE CALCULATIONS

The data are summarized in Figs. V-XII of RESULTS. Table III and Figs. XXI-XXIX, referred to in APPENDIX A, are shown to illustrate the methods of analysis, correlation procedures, and typical calculations of stress concentration factors. Tables V and VI, calculations of stress concentration factors at the edge of the beam and the edge of the hole respectively, are adapted from Table III and Fig. XXI and others similar (see Table IV) to assist in the preparation of Figs. XXIII and XXVII. One sample of each type of plot made in fairing the data is included.

TABLE IV

Strain at Full Load for $r_2/h = 0.4206$; WR = 2.

$\frac{r}{a}$	0	0.2	0.3	0.4	0.5
Gage					
F1	-866	-754	-632	-550	-480
F2	-862	-677	-556	-453	-380
F3	-862	-672	-536	-440	-352
F4	-854	-668	-532	-433	-360
F5	-851	-628	-480	-367	-284
F6	-830	-456	-280	-144	-20
H0	-20	+8	0	+33	+32
H15	+45	-137	-186	-231	-256
H30	+45	-256	-340	-436	-472
H45	-60	-428	-536	-623	-672
H60	-232	-508	-576	-642	-656
H75	-316	-404	-420	-422	-404
H90	-360	-264	-216	-172	-128
R45-1					-48
R45-2					-432
R45-3					+76
R45-4					-356
σ_L	-26041	-20832	-18055	-15914	-13889

TABLE V

Calculation of Stress Concentration Factors at Edge of Beam

$r_2/h = 0.4206$; WR = 2

$\frac{\tau}{\sigma}$	Dist. from ℄ Hole in Diameter	0	0.318	0.686	1.189	2.059	4.437
0	ϵ	-866	-862	-862	-854	-851	-830
	σ	-25980	-25860	-25860	-25620	-25530	-24900
	σ/σ_c	0.998	0.993	0.993	0.984	0.980	0.956
0.2	ϵ	-754	-677	-672	-668	-628	-456
	σ	-22620	-20310	-20160	-20040	-18840	-13680
	σ/σ_c	1.086	0.975	0.968	0.962	0.904	0.657
0.3	ϵ	-632	-556	-536	-532	-480	-280
	σ	-18960	-16680	-16080	-15960	-14400	-8400
	σ/σ_c	1.050	0.924	0.891	0.884	0.798	0.465
0.4	ϵ	-550	-453	-440	-433	-367	-144
	σ	-16500	-13590	-13200	-12990	-11010	-4320
	σ/σ_c	1.037	0.854	0.829	0.816	0.692	0.271
0.5	ϵ	-480	-380	-352	-360	-284	- 20
	σ	-1400	-11400	-10560	-10800	-8520	-600
	σ/σ_c	1.037	0.821	0.760	0.778	0.613	0.043

TABLE VI

Calculation of Stress Concentration Factor at Edge of Hole

$r_2/h=0.4206$; MR = 2

$\frac{\tau}{\sigma}$	Angle from Vertical	0	15	30	45	60	75	90
0	ϵ	-360	-316	-232	-60	+45	+45	-20
	σ	-10800	-9480	-6960	-1800	+1350	+1350	-600
	σ/σ_c	0.415	0.364	0.267	0.069	-0.052	-0.052	0.023
0.2	ϵ	-264	-404	-508	-428	-256	-137	+8
	σ	-7920	-12120	-15240	-12840	-7680	-4110	+240
	σ/σ_c	0.380	0.582	0.732	0.616	0.369	0.197	-0.012
0.3	ϵ	-216	-420	-576	-536	-340	-186	0
	σ	-6480	-12600	-17280	-16080	-10200	-5580	0
	σ/σ_c	0.359	0.698	0.957	0.891	0.565	0.309	0
0.4	ϵ	-172	-422	-642	-623	-436	-231	+33
	σ	-5160	-12660	-19260	-18690	-13080	-6930	+990
	σ/σ_c	0.324	0.796	1.210	1.174	0.822	0.435	-0.062
0.5	ϵ	-128	-404	-656	-672	-472	-256	+32
	σ	-3840	-12120	-19680	-20160	-14160	-7680	+960
	σ/σ_c	0.276	0.873	1.417	1.452	1.020	0.553	-0.069

APPENDIX C

ORIGINAL DATA

The original data are presented in Table VII as strain in microinches per inch for each gauge for each ratio of shear to bending. These data are tabulated separately for each Weight Ratio and each ratio of diameter of hole to depth of beam.

TABLE VII

Strain in Microinches per inch at Full Load

WR = 0; r_2/h = 0.125

Gage	$\frac{r}{b}$ =0	$\frac{r}{b}$ =0.2	$\frac{r}{b}$ =0.3	$\frac{r}{b}$ =0.4	$\frac{r}{b}$ =0.5
F1	-793	-714	-629	-552	-476
F2	-824	-697	-598	-499	-419
F3	-812	-686	-576	-484	-392
F4	-832	-654	-544	-448	-347
F5	-814	-594	-470	-366	-259
F6	-785	-438	-274	-146	-4
1	+97	+198	+239	+269	+297
2_{R0}	-85	-223	-277	-332	-331
3	+9	-20	+20	+7	+29
4	0	-10	-32	-46	-24
1	-275	-170	-90	-31	+44
2_{R45}	-498	-488	-465	-451	-433
3	+158	+136	+106	+83	+74
4	-593	-493	-428	-355	-297
1	-210	-123	-42	+26	+88
2_{R90}	-523	-536	-544	-533	-514
3	+175	+122	+113	+85	+80
4	-558	-484	-428	-357	-318
H0					
H45		I N A C T I V E			
H90					

WR = 0.5; r_2/h = 0.125

Cage	$\frac{\tau}{\sigma}$ =0	$\frac{\tau}{\sigma}$ =0.2	$\frac{\tau}{\sigma}$ =0.3	$\frac{\tau}{\sigma}$ =0.4	$\frac{\tau}{\sigma}$ =0.5
F1	-805	-719	-624	-543	-478
F2	-794	-710	-600	-526	-446
F3	-829	-685	-576	-482	-405
F4	-800	-652	-527	-427	-359
F5	-800	-595	-463	-368	-278
F6	-768	-420	-269	-139	-24
1	+38	+198	+231	+231	+262
2_{R0}	-27	-217	-266	-300	-340
3	+36	0	+30	+17	+8
4	+17	-24	-27	+24	-31
1	-347	-152	-77	-5	+56
2_{R45}	-434	-463	-471	-437	-435
3	+196	+120	+99	+84	+66
4	-588	-474	-418	-354	-300
1	-323	-120	-42	+26	+78
2_{R90}	-410	-500	-511	-517	-502
3	+165	+123	+114	+85	+77
4	-54	-465	-416	-371	-321
H0	0				
H45	-13		INACTIVE		INACTIVE
H90	Inactive				
σ_L	-26041	-20832	-18055	-15914	-13889

WR = 1.0; r_2/h = 0.125

Gage	$\frac{r}{b}$=0	$\frac{r}{b}$=0.2	$\frac{r}{b}$=0.3	$\frac{r}{b}$=0.4	$\frac{r}{b}$=0.5
F1	-844	-739	-630	-532	-489
F2	-863	-726	-576	-513	-465
F3	-852	-695	-555	-475	-422
F4	-860	-669	-517	-426	-365
F5	-840	-591	-445	-338	-278
F6	-822	-451	-246	-112	-029
1	+79	+192	+255	+273	+272
2_{R0}	-90	-260	-275	-279	-326
3	+13	-21	+37	+26	-19
4	-15	-20	-24	-9	-30
1	-338	-150	-52	+20	+66
2_{R45}	-498	-500	-458	-447	-440
3	+158	+134	+134	+106	+65
4	-625	-477	-391	-342	-307
1	-310	-121	-23	+33	+77
2_{R90}	-515	-520	-505	-485	-503
3	+145	+139	+129	+103	+74
4	-574	-497	-398	-370	-319
H0	+18	+158	+191	+188	+252
H45	-30	-440	-550	-642	-697
H90	-145	-116	-120	-130	-92
σ_t	-26041	-20832	-18055	-15914	-13889

VR = 1.5; r_2/h = 0.125

$\frac{r}{a}$	0	0.2	0.3	0.4	0.5
Gage					
F1	-807	-758	-626	-564	-480
F2	-850	-723	-590	-531	-427
F3	-856	-700	-550	-500	-415
F4	-854	-675	-532	-454	-364
F5	-841	-610	-462	-370	-263
F6	-820	-455	-276	-144	-026
1	+70	+215	+248	+262	+273
2_{R0}	-60	-284	-257	-357	-347
3	-12	-40	-12	-42	+12
4	0	-40	-21	-52	-28
1	-406	-120	-34	-38	61
2_{R45}	-492	-560	-501	-500	-462
3	+139	+138	+93	+108	+78
4	-605	-510	-406	-355	-273
1	-342	-95	-40	+30	+55
2_{R90}	-460	-569	-530	-530	-505
3	+132	+118	+90	+98	+85
4	-578	-500	-423	-382	-344
H0	0	+140	+182	+193	+218
H45	-16	-415	-511	-578	-630
H90	-118	-114	-106	-85	-80
σ_t	-26041	-20832	-18055	-15914	-13889

WR = 2; r2/h = 1.25

$\frac{\tau}{\sigma}$	0	0.2	0.3	0.4	0.5
Gage					
F1	-853	-720	-649	-570	-491
F2	-880	-698	-642	-542	-450
F3	-880	-674	-600	-511	-413
F4	-880	-643	-568	-460	-362
F5	-873	-588	-507	-372	-272
F6	-843	-460	-321	-144	-022
1	+52	+200	+196	+246	+252
2_{R0}	-48	-190	-284	-310	-320
3	0	+28	-30	-10	0
4	0	+7	-63	-44	-40
1	-368	-148	-130	-7	+40
2_{R45}	-471	-475	-517	-463	-433
3	+178	+159	+60	+80	+60
4	-624	-474	-450	-355	-302
1	-340	-123	-100	0	+42
2_{R90}	-450	-500	-562	-520	-490
3	+156	+151	+60	+79	+66
4	-582	-468	-457	-376	-328
H0	0	-100	-110	-130	-140
H45	10	-457	-422	-494	-539
H90	-105	-287	-110	-112	-102
σ_t	-26041	-20832	-18055	-15914	-13889

WR = 0; r_2/h = .2417

Gage \ σ_{θ}	0	0.2	0.3	0.4	0.5
F1	-860	-700	-598	-558	-480
F2	-868	-703	-583	-504	-424
F3	-864	-680	-570	-469	-382
F4	-860	-652	-525	-443	-364
F5	-840	-617	-480	-365	-280
F6	-800	-453	-268	-143	-26
1	+80	+218	+260	+305	+332
2_{R0}	-35	-263	-322	-386	-410
3	-9	-34	-38	-55	-52
4	0	-18	-26	-36	-32
1	-347	-200	-132	-35	+14
2_{R45}	-460	-502	-472	-456	-436
3	+180	+112	+86	+66	+54
4	-608	-520	-444	-385	-332
1	-310	-102	0	+73	+134
2_{R90}	-430	-582	-580	-593	-586
3	+156	+106	+100	+84	+75
4	-554	-486	-432	-376	-329
H0	-31	+120	+181	+234	+242
H45	+32	-385	-532	-617	-689
H90	-313	-257	-249	-181	-168
σ_L	-26041	-20832	-18055	-15914	-13889

$R = 0.5$; $r_2/h = 0.2417$

Gage \ σ_θ	0	0.2	0.3	0.4	0.5
F1		-703	-624	-562	-490
F2		-710	-601	-575	-436
F3		-702	-577	-485	-396
F4		-676	-543	-455	-356
F5		-627	-485	-373	-273
F6		-463	-280	-138	-25
1		+210	+260	+294	+322
2_{R0}		-250	-316	-373	-400
3		-26	-28	-40	-38
4		-22	-28	-39	-40
1		-210	-100	-45	+18
2_{R45}	NOT OBSERVED	-505	-472	-460	-434
3		+119	+98	+73	+62
4		-524	-434	-379	-322
1		-105	0	+65	+126
2_{R90}		-566	-560	-562	-562
3		+115	+97	+80	+70
4		-494	-430	-377	-328
H0		+120	+158	+192	+227
H45		-396	-533	-630	-678
H90		-233	-233	-181	-160
σ_L	-26041	-20832	-18055	-15914	-13889

VR = 1; $r_2/h = 0.2417$

$\frac{q}{q_b}$ Gage	0	0.2	0.3	0.4	0.5
F1	-864	-760	-651	-573	-500
F2	-837	-724	-605	-520	-440
F3	-865	-705	-577	-484	-409
F4	-854	-680	-560	-459	-369
F5	-838	-627	-480	-376	-280
F6	-810	-458	-280	-143	-36
1	+44			+287	+313
2_{R0}	-40			-370	-400
3	-10			-29	-32
4	-3			-42	-44
1	-368	NOT OBSERVED	NOT OBSERVED	-38	+25
2_{R45}	-454			-469	-444
3	+180			+73	+58
4	-600			-372	-320
1	-306			+51	+110
2_{R90}	-412			-566	-557
3	+160			+75	+64
4	-540			-373	-328
H0	-23	+86	+125	+162	+178
H45	+16	-344	-457	-532	-600
H90	-278	-238	-194	-172	-144
σ_L	-26041	-20832	-18055	-15914	-13889

WR = 1.5; r_2/h = .2417

$\frac{\tau}{\sigma}$ Gage	0	0.2	0.3	0.4	0.5
F1	-850	-721	-628	-545	-506
F2	-874	-707	-595	-502	-462
F3	-889	-675	-563	-451	-427
F4	-893	-690	-550	-470	-400
F5	-859	-607	-463	-376	-290
F6	-847	-471	-263	-165	-30
1	+57	+199	+249	+268	+300
2_{R0}	-215	-261	-305	-340	-400
3	-34	-15	-22	-28	-12
4	-41	-33	-41	-38	-40
1	-417	-210	-98	-53	+20
2_{R45}	-480	-498	-464	-470	-480
3	+158	+119	+106	+55	+71
4	-585	-542	-432	-364	-320
1	-377	-102	0	+59	+106
2_{R90}	-539	-542	-544	-560	-509
3	+149	+111	+97	+65	+63
4	-595	-496	-430	-391	-326
H0	+15	+70	+105	+121	+127
H45	-32	-345	-418	-475	-548
H90	-214	-178	-165	-150	-112
σ_L	-26041	-20832	-18055	-15914	-13889

WR = 2; r_2/h = .2417

$\frac{r}{q}$ Gage	0	0.2	0.3	0.4	0.5
F1	-728	-748	-640	-564	-476
F2	-847	-735	-606	-530	-440
F3	-880	-698	-577	-505	-401
F4	-876	-682	-549	-464	-360
F5	-872	-628	-480	-380	-272
F6	-853	-460	-280	-155	-28
1	+31	+183	+240	+264	+300
2_{R0}	-27	-236	-292	-338	-375
3	-20	0	0	-26	0
4	12	-32	-37	-35	-29
1	-403	-208	-116	-51	+46
2_{R45}	-458	-495	-465	-443	-416
3	+153	+120	+95	+56	+65
4	-625	-523	-436	-374	-319
1	-370	-152	0	+46	+100
2_{R90}	-351	-538	-518	-550	-510
3	+219	+111	+97	+75	+65
4	-553	-495	-433	-390	-334
H0	NOT OBSERVED	0	+36	0	0
H45		-300	-396	-470	-504
H90		-184	-176	-150	-66
σ_t	-26041	-20832	-18055	-15914	-13889

WR = 0; r_2/h = .4206

$\frac{\tau}{\sigma}$ Gage	0	0.2	0.3	0.4	0.5
FL	-1004	-848	-593	-465	-388
F1	-856	-723	-524	-412	-339
FR	-787	-720	-525	-405	-343
F2	-876	-640	-441	-320	-248
F3	-877	-624	-432	-300	-232
F4	-868	-648	-449	-324	-252
F5	-857	-612	-405	-280	-205
F6	-821	-448	-233	-96	-21
H0	-32	+84	+120	+125	+137
H15	+117	-120	-175	-179	-212
H30	+180	-453	-560	-600	-667
H45	4	-720	-836	-832	-896
H60	-255	-860	-893	-856	-913
H75	-540	-872	-811	-724	-735
H90	-596	-476	-328	-248	-212
1	-345				
2_{R45}	-540				
3	+187				
4	-667				
σ_t	-26041	-20832	-15268	-11560	-9920

WR = 0.5; r_2/h = .4206

$\frac{\tau}{\sigma}$ Gage	0	0.2	0.3	0.4	0.5
F1	-817	-740	-632	-550	-481
F2	-856	-681	-560	-443	-372
F3	-853	-657	-532	-436	-347
F4	-840	-669	-536	-440	-356
F5	-849	-632	-477	-366	-280
F6	-812	-461	-280	-135	-24
H0	-9	+8	+19	+33	+40
H15	+45	-180	-252	-307	-352
H30	+68	-348	-480	-579	-640
H45	-68	-556	-700	-807	-871
H60	-283	-680	-768	-839	-893
H75	-383	-529	-536	-545	-551
H90	-436	-328	-256	-208	-156
1			-180		
2_{R45}			-472		
3			+124		
4			-480		
σ_t	-26041	-20832	-18055	-15914	-13889

WR = 1; r_2/h = .4206

$\frac{\tau}{\sigma}$ Gage	0	0.2	0.3	0.4	0.5
F1	-839	-741	-628	-557	-480
F2	-857	-685	-568	-462	-380
F3	-875	-660	-539	-439	-352
F4	-871	-648	-535	-424	-360
F5	-859	-612	-480	-367	-276
F6	-835	-444	-280	-137	-27
H0	-35	+8	+28	+45	+36
H15	+53	-144	-200	-238	-280
H30	+56	-284	-400	-469	-528
H45	-56	-464	-587	-672	-720
H60	-240	-564	-643	-708	-732
H75	-336	-456	-472	-461	-464
H90	-375	-280	-240	-183	-148
1		-247			
2_{R45}		-488			
3		+168			
4		-560			
σ_t	-26041	-20832	-18055	-15914	-13889

WR = 1.5; r_2/h = 0.4206

$\frac{\tau}{\sigma}$ Gage	0	0.2	0.3	0.4	0.5
F1	-888	-760	-628	-564	-484
F2	-868	-692	-548	-451	-368
F3	-915	-688	-548	-436	-339
F4	-860	-648	-540	-409	-343
F5	-824	-624	-480	-371	-277
F6	-828	-468	-276	-121	-17
H0	-16	+24	+36	+24	+41
H15	+56	-124	-180	-245	-255
H30	+56	-260	-360	-440	-485
H45	-56	-432	-556	-631	-683
H60	-224	-520	-596	-646	-680
H75	-316	-424	-436	-418	-437
H90	-360	-260	-212	-160	-133
1				-113	
2_{R45}				-437	
3				+114	
4				-400	
σ_L	-26041	-20832	-18055	-15914	-13889

VR = 2; r_2/h = .4206

$\frac{\tau}{\sigma}$ Gage	0	0.2	0.3	0.4	0.5
F1	-866	-754	-632	-550	-480
F2	-862	-677	-556	-453	-380
F3	-862	-672	-536	-440	-352
F4	-854	-668	-532	-433	-360
F5	-851	-628	-480	-367	-284
F6	-830	-456	-280	-144	-20
H0	-20	+8	0	+33	+32
H15	+45	-137	-186	-231	-256
H30	+45	-256	-340	-436	-472
H45	-60	-428	-536	-623	-672
H60	-232	-508	-576	-642	-656
H75	-316	-404	-420	-422	-404
H90	-360	-264	-216	-172	-128
1					-48
2_{R45}	NOT				-432
3	OBSERVED				+76
4					-356
σ_r	-26041	-20832	-18055	-15914	-13889

WR = 0; r_2/h = .5056

$\frac{\tau}{\sigma}$ Gage	0	0.2	0.3	0.4	0.5
F1	-756	-628	-453	-368	-352
F2	-720	-512	-332	-240	-189
F3	-760	-520	-332	-232	-187
F4	-740	-548	-372	-280	-240
F5	-724	-523	-341	-252	-204
F6	-693	-384	-200	-96	-21
H0	-40	+60	+71	+95	+115
H15	+98	-156	-204	-241	-297
H30	+124	-428	-500	-580	-705
H45	-20	-544	-588	-652	-775
H60	-249	-892	-888	-944	-1079
H75	-416	-716	-612	-616	-640
H90	-525	-588	-484	-460	-496
1					-120
2_{R45}					-303
3					+64
4					-320
σ_L	-20832	-17360	-12494	-10412	-9920

WR = 0.5; r_2/h = .5056

$\frac{r}{\sigma}$ Gage	0	0.2	0.3	0.4	0.5
F1	-720	-744	-640	-492	-416
F2	-733	-660	-532	-369	-288
F3	-737	-644	-508	-349	-260
F4	-729	-672	-544	-384	-300
F5	-717	-628	-488	-336	-248
F6	-688	-464	-284	-125	-24
H0	-12	+28	+41	+48	+48
H15	+80	-188	-283	-297	-332
H30	+52	-420	-569	-607	-640
H45	-100	-656	-800	-804	-844
H60	-256	-688	-768	-731	-748
H75	-388	-720	-736	-664	-648
H90	-465	-468	-391	-300	-256
1	-321				
2_{R45}	-428				
3	+176				
4	-560				
σ_L	-20832	-20832	-18055	-13882	-11904

WR = 1; r_2/h = .5056

$\frac{\tau}{q}$ Gage	0	0.2	0.3	0.4	0.5
F1	-720	-757	-640	-524	-480
F2	-728	-656	-520	-400	-336
F3	-744	-648	-512	-380	-316
F4	-744	-676	-536	-416	-352
F5	-736	-632	-488	-360	-288
F6	-696	-468	-280	-136	-28
H0	0	+20	+32	+36	+43
H15	+67	-152	-227	-264	-320
H30	+40	-347	-468	-528	-616
H45	-85	-528	-664	-716	-804
H60	-229	-564	-652	-656	-704
H75	-371	-597	-612	-588	-612
H90	-416	-393	-340	-280	-252
1			-216		
2_{R45}			-476		
3			+120		
4			-512		
σ_t	-20832	-20832	-18055	-15035	-13889

$R = 1.5$; $r_o/h = .5056$

$\frac{\tau}{\sigma}$ Gage	0	0.2	0.3	0.4	0.5
FL	-877	-869	-751	-615	-579
F1	-693	-736	-640	-516	-480
FR	-648	-735	-689	-512	-476
F2	-720	-664	-532	-404	-344
F3	-713	-647	-571	-384	-320
F4	-704	-672	-540	-427	-352
F5	-709	-632	-488	-352	-284
F6	-656	-464	-284	-132	-30
H0	-4	+13	+23	+36	+40
H15	+56	-149	-213	-248	-304
H30	+45	-328	-439	-516	-587
H45	-76	-509	-620	-672	-760
H60	-197	-528	-596	-612	-665
H75	-323	-543	-572	-556	-577
H90	-352	-372	-320	-272	-245
1		-285			
2_{R45}		-505			
3		+152			
4		-589			
σ_t	-20832	-20832	-18055	-15035	-13889

VR = 2; r_a/h = .5056

$\frac{\tau}{\sigma}$ Gage	0	0.2	0.3	0.4	0.5
FL	-900	-884	-732	-639	-560
F1	-672	-724	-621	-551	-488
FR	-615	-693	-637	-557	-500
F2	-717	-653	-529	-396	-339
F3	-708	-652	-513	-394	-320
F4	-716	-664	-537	-420	-360
F5	-704	-600	-491	-371	-285
F6	-667	-440	-288	-128	-29
H0	-8	+11	+17	+36	+35
H15	+48	-144	-188	-239	-287
H30	+28	-305	-400	-490	-539
H45	-84	-472	-573	-660	-708
H60	-197	-484	-507	-566	-597
H75	-317	-523	-532	-543	-533
H90	-332	-341	-300	-254	-215
1				-149	
2_{R45}				-440	
3				+88	
4				-446	
σ_t	-20832	-20832	-18055	-15914	-13889

APPENDIX D

DEVELOPMENT OF THEORETICAL SOLUTION

I. Nomenclature

a_{mn}	Arbitrary constants in stress function ψ
A_r	Cross-sectional area of reinforcement ring plus adjacent web area.
A	Area; with subscripts f and w, area of flange (gross) and web respectively.
b	Width (net) of rectangular reinforcement.
b'	Width (gross) of rectangular reinforcement.
C_{mn}	Arbitrary constants in stress function φ
d_{mn}	Abbreviations for products of a_{mn} and powers of r_2.
e	Distance from edge to neutral fiber of reinforcement.
E_r	Modulus of elasticity of ring.
E_w	Modulus of elasticity of web.
f_n	Factor to allow for three-dimensional effect at junction of ring and web.
h	Half-height of web.
I	Moment of inertia; with subscripts e and r, the effective moment of inertia and the moment of inertia about the centroid of the ring respectively.
k_{mn}	Abbreviations for products of C_{mn} and powers of r_1.
L	Distance.
M	Bending moment.
m	Subscript.
n	Order of terms of stress function.

N	Radial shear force on cross-section of reinforcement.
p	Ratio of radii of reinforcement: $\frac{r_1}{r_2}$.
P	Load.
$P_n(r), \epsilon_n(r)$	Coefficients in stress function.
r	Radial distance from center of cutout.
r_o	Radial distance from center of cutout to center-line of reinforcement.
r_1	Radial distance from center of cutout to outer edge of reinforcement.
r_2	Radial distance from center of cutout to inner edge of reinforcement.
r_n	Radial distance from center of cutout to neutral fiber of reinforcement.
s	Arc length.
t	Thickness; with subscripts f, r, and w, thickness of flange, reinforcement, and web respectively.
T	Normal stress resultant.
u	Displacement in radial direction.
v	Displacement in tangential direction.
WR	Weight Ratio.
x, y, z	Cartesian coordinates with origin at center of cutout.
Y	Tangential load on ring per unit of circumference.
Z	Radial load on ring per unit of circumference.
α	Dimensionless parameter of area of ring: $\frac{E_r}{E_w} \cdot \frac{A_r}{r_o t_w} 2(1+\nu)$.

α' Dimensionless parameter of area of rectangular ring: $\frac{E_r}{E_w} \cdot \frac{bt_r}{r_o t_w}$.

β Dimensionless parameter of moment of inertia of ring: $\frac{E_r}{E_w} \cdot \frac{I_r}{r_o^3 t_w} 24(1 + \nu)$.

γ Specific weight; with subscripts r and w, specific weight of reinforcement and web respectively.

δ Dimensionless parameter of thickness of ring: $\frac{t_r}{2r_o}$.

ϵ_r, ϵ_θ Strain in radial and tangential directions respectively.

Γ Dimensionless parameter of shear: $\frac{3}{2(1-\eta)} - \frac{A_w h^2}{2I} \cdot \frac{\mu}{1-\mu}$

η Dimensionless parameter of flange thickness: $\frac{t_f}{h}$.

θ Angular polar coordinate.

κ_r Change of curvature of ring.

λ Ratio of width of reinforcement to web thickness: $\frac{b'}{t_w}$.

μ Dimensionless parameter of flange area (gross): $\frac{A_f}{A}$.

ν Poisson's ratio.

σ_L Nominal bending stress at extreme fiber.

σ_x, σ_y Normal stresses in x and y directions respectively.

σ_r, σ_θ Radial and tangential stresses respectively.

Σ	Summation.
τ	Average shear: $\frac{P}{A_w}$.
τ_{xy}	Shear stress (Cartesian coordinates).
$\tau_{r\theta}$	Shear stress (Polar coordinates).
φ	Stress function (Airy) for web.
Ψ	Stress function (Airy) for reinforcement.

Sub-Scripts

o	Original.
1	Constraint.
T	Total.

II. General Equations and Solutions[3]

In order to analyze the effect of a circular cutout in a plane sheet, the stresses, displacements, and strains in such a sheet are most conveniently represented by a polar-coordinate system, Fig. XXX. The original stresses and displacements, before being disturbed by the cutout, will appear in the form:

$$\left.\begin{aligned} &\sigma_{r_o} \\ &\sigma_{\theta_o} \\ &\tau_{r\theta_o} \\ &u_o \\ &v_o \end{aligned}\right\} \qquad (1)$$

The cutout edges are assumed to carry reinforcement. It is the purpose of this analysis to determine the elastic properties of such an edge reinforcement so that the increments of stress, σ_{r_1}, σ_{θ_1}, and $\tau_{r\theta_1}$, to the original stresses become as small as possible.

Throughout this analysis it is assumed that the hole is "small" compared to the size of the sheet. Such an analysis will be reasonably accurate for $\frac{r_2}{h} < 0.25$.[4]

---

3. Follows [14] .
4. See [13] , p. 3 and [3] , p. 217.

FIG. XXX

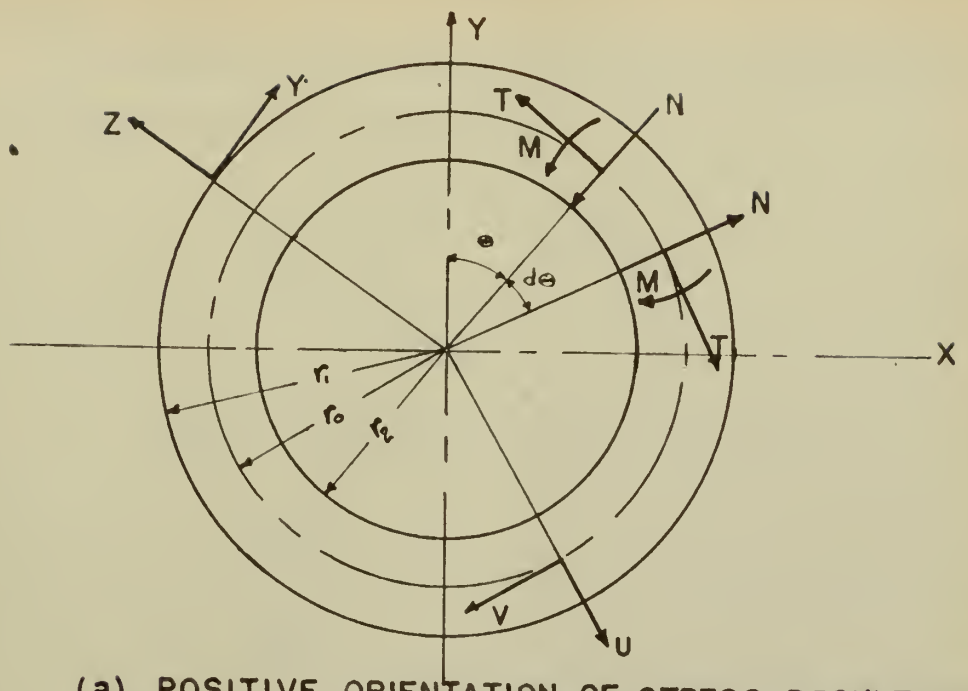

(a). POSITIVE ORIENTATION OF STRESS RESULTANTS & DISPLACEMENTS

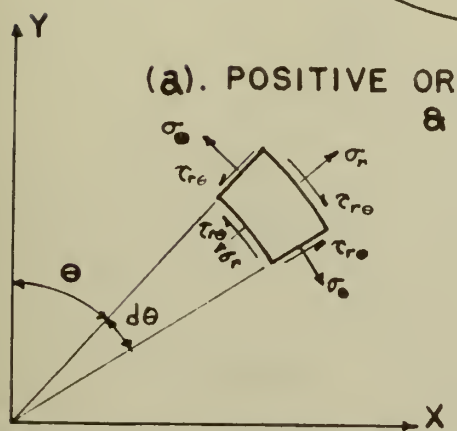

(b). POSITIVE ORIENTATION OF STRESSES

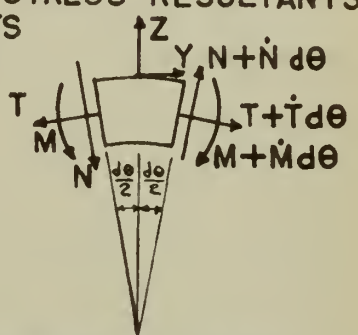

(c). EQUILIBRIUM OF RING PARTICLE

FIG. XXXI

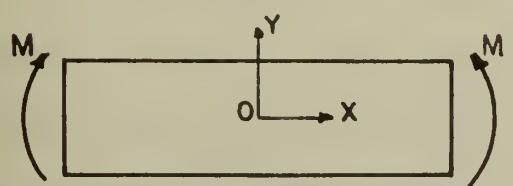

BEAM IN PURE BENDING

FIG. XXXII

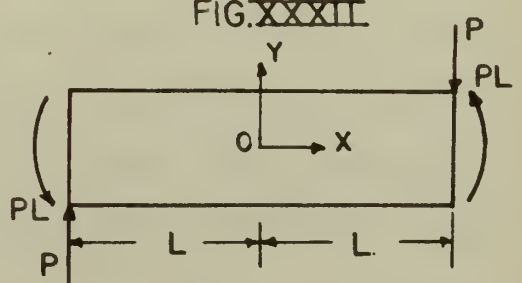

BEAM WITH PURE SHEAR AT Y-AXIS

S.R.N.
3-19-51

A. Stresses

The stresses in a plane sheet can be expressed by a stress function $\varphi(r,\theta)$ such that:

$$\left.\begin{aligned} \sigma_r &= r^{-2}\ddot{\varphi} + r^{-1}\varphi' \\ \sigma_\theta &= \varphi'' \\ \tau_{r\theta} &= -(r^{-1}\dot{\varphi})' \end{aligned}\right\}^5 \qquad (2)$$

where primes and dots are defined by:

$$\frac{\partial}{\partial r} \equiv {}'$$

$$\frac{\partial}{\partial \theta} \equiv \cdot$$

The function φ, moreover, must be such that it satisfies the biharmonic equation:

$$\Delta^2 \varphi = 0 \qquad (3)$$

where:

$$\Delta\varphi \equiv \frac{\partial^2\varphi}{\partial x^2} + \frac{\partial^2\varphi}{\partial y^2}$$

$$\equiv r^{-1}(r\varphi')' + r^{-2}\ddot{\varphi}\,.^6$$

The complete solution of Equation (3) for the case considered here, in which the edge stresses taken around the circumference of the circular cutout have zero resultant (i.e., the cutout has no external loading), may be written in the form:

---

5. Eq. (34), p. 53 of [21].
6. Eq. (35), p. 55 of [21].

$$\varphi = \sum_{o} P_n \cos n\theta + \sum_{1} Q_n \sin n\theta \qquad (3a)$$

where:
$$\left.\begin{aligned} P_o &= C_{10} + C_{20}r^2 + C_{30}\log_e r + C_{40}r^2\log_e r \\ P_1 &= C_{11}r + C_{21}r^3 + C_{31}r^{-1} + C_{41}r\log_e r \\ P_{n\geq 2} &= C_{1n}r^n + C_{2n}r^{-n} + C_{3n}r^{n+2} + C_{4n}r^{-(n-2)} \end{aligned}\right\} \qquad (3b)$$

The expressions for the functions Q_n are the same, with the possible exception of different numerical values for the constants C.

From Equations (2) and (3a) it follows that:

$$\left.\begin{aligned} \sigma_r &= \sum_{o} (-n^2 r^{-2} P_n + r^{-1} P_n') \cos n\theta \,. \\ \sigma_\theta &= \sum_{o} P_n'' \cos n\theta \,. \\ \tau_{r\theta} &= \sum_{o} (r^{-1} P_n)' n \sin n\theta \,. \end{aligned}\right\} \qquad (4)$$

The terms involving Q_n may be obtained from Equations (4) by exchanging sine for cosine and vice versa, Q_n for P_n, and making the right-hand side negative in the equation for $\tau_{r\theta}$.

B. Displacements

The radial and tangential strains follow from Hooke's Law:

---

7. See [12] or [14].

$$\left.\begin{aligned} E_w \epsilon_r &= E_w u' = \sigma_r - \nu\sigma_\theta \\ E_w \epsilon_\theta &= E_w r^{-1}(u + \dot{v}) = \sigma_\theta - \nu\sigma_r \end{aligned}\right\}^{8} \qquad (5)$$

The stress-strain relations of the reinforcement ring can be expressed by:[9]

$$\epsilon_\theta r_o = \frac{T r_o}{E_r A_r} = (u + \dot{v} + \delta\ddot{u})_{r=r_1} \qquad (6a)$$

$$\kappa_r r_o^2 = + \frac{M r_o^2}{E_r I_r} = (u + \ddot{u})_{r=r_1} \qquad (6b)$$

Now the displacements of the ring must be the same as those of the sheet at the point of attachment. Therefore, the displacements in Equations (6a) and (6b) can be obtained by putting $r = r_1$ in Equations (5) for the displacements of the sheet.

The stress and moment resultants, T and M, in the ring can be derived from the equations of equilibrium of the ring with the use of the fact that the unit loads acting on the ring are due to the stresses in the sheet acting along the circumference of the ring.[10]

---

8. Eq. (46), (47), and (48), p. 63 of [21].
9. See Section F.
10. See Section G.

C. Cross-sectional Properties in Terms of the Stress Function

The substitution of Equation (3a) into Equations (C4) and (C5) gives:

$$T = r_1 t_w \Big[\sum_0 r_1^{-1} P_n' \cos n\theta + \sum_1 r_1^{-1} Q_n' \sin n\theta \Big]_{\substack{r=r_1 \\ n\neq 1}} + C_2 \sin\theta + C_3 \cos\theta \qquad (7a)$$

$$M = r_o t_w \Big\{ \sum_0 r_o^{-1} \cos n\theta \big[r_1 P_n' - r_o P_n' - P_n \big]_{r=r_1} + \sum_1 r_o^{-1} \sin n\theta \big[r_1 Q_n' - r_o Q_n' - Q_n \big]_{r=r_1} + \frac{C_1}{r_o t_w} - \frac{C_2}{t_w} \sin\theta - \frac{C_3}{t_w} \cos\theta \Big\}_{n\neq 1} \qquad (7b)$$

The substitution of Equations (7a) and (C7b) into Equation (6a) and of Equations (7b) and (C6b) into Equation (6b) gives:

$$A_r = r_o t_w \frac{E_w}{E_r} \frac{\Big[\sum_0 P_n' \cos n\theta + \sum_1 Q_n' \sin n\theta \Big]_{r=r_1}^{n\neq 1} + \frac{C_2}{t_w} \sin\theta + \frac{C_3}{t_w} \cos\theta}{\sum_0 \cos n\theta \Big\{ n^2 \nu r_1^{-1} P_n - \nu P_n' + P_n'' r_1 + n^2 \delta \big[\nu P_n' - r_1^{-1} P_n + (n^2-1) \int P_n r^{-2} dr \big] \Big\}_{r=r_1} + \sum_1 \sin n\theta \Big\{ n^2 \nu r_1^{-1} Q_n - \nu Q_n' + Q_n'' r_1 \quad n^2 \delta \big[\nu Q_n'' - r_1^{-1} Q_n + (n^2-1) \int Q_n r^{-2} dr \big] \Big\}_{r=r_1}} \qquad (8)$$

And,

$$I = \frac{r_o^3 t_w}{r} \frac{E_w}{E_r} \frac{\left\{\sum_o r_o^{-1} \cos n\theta\left[r_1 P_n' - (r_o P_n')_{n\neq 1} - P_n\right] + \sum_1 r_o^{-1} \sin n\theta\left[r_1 Q_n' - (r_o Q_n')_{n\neq 1} - Q_n\right]\right\}_{r=r_1} + \frac{C_1}{E_w t_w} - \frac{C_2}{t_w} \sin\theta - \frac{C_3}{t_w}\cos\theta}{\sum_o (n^2-1)\cos n\theta\left[r_1^{-1} P_n - \nu P_n' - (n^2-1)\int P_n r^{-2} dr\right]_{r=r_1} + \sum_1 (n^2-1)\sin n\theta\left[r_1^{-1} Q_n - \nu Q_n' - (n^2-1)\int Q_n r^{-2} dr\right]_{r=r_1}}$$

(9)

Equations (8) and (9) are extremely important. Assume that an arbitrary original stress distribution , produced by loading at the external boundaries of the sheet, is given. P_n and Q_n are, therefore, given for equivalent reinforcement. Thus the substitution of the given P_n and Q_n into Equations (8) and (9) gives the distribution of cross-sectional area and moment of inertia of the reinforcement ring required to replace with elastic equivalence that portion of the sheet that has been cut out.

D. Pure Bending

If an I-beam, composed of a rectangular web and flanges, is subjected to a pure bending moment M about an axis perpendicular to the plane of the web, Fig. XXXI, the stress distribution will be:

$$\sigma_{x_o} = -\frac{M_y}{I}$$

$$\sigma_{y_o} = \tau_{xy_o} = 0$$

In polarcoordinates this state of stress is:

$$\left.\begin{aligned} \sigma_{r_o} &= \frac{Mr}{4I}(\cos 3\theta - \cos\theta) \\ \sigma_{\theta_o} &= -\frac{Mr}{4I}(3\cos\theta + \cos 3\theta) \\ \tau_{r\theta_o} &= -\frac{Mr}{4I}(\sin\theta + \sin 3\theta) \end{aligned}\right\} \qquad (10)$$

for which the Airy stress function is:

$$\varphi_o = -\frac{Mr^3}{8I}(\cos\theta + \frac{1}{3}\cos 3\theta) \qquad (10a)$$

By substitution into Equations (8) and (9) it is found[11] that the required proportions are:

$$\left.\begin{aligned} A_r &= \frac{E_w}{E_r} \cdot \frac{r_o t_w}{(1+\nu)(2+9\delta)} \\ I_r &= \frac{E_w}{E_r} \cdot \frac{r_o^3 t_w}{24(1+\nu)}(1 - 2\delta). \\ \delta &= 0.00693 \text{ for } \nu = 0.3 \end{aligned}\right\} \qquad (11)$$

---

11. See Section H.

In general it will not be possible to design a practical reinforcement that is the elastic equivalent of the cutout. For example, if a rectangular strip is considered:

$$\frac{I_r}{A_r} = \frac{t^2_r}{12} = \frac{r_a^2(1-2\delta)(2+9\delta)}{24}$$

$$\frac{t^2_r}{4r_a^2} = \frac{(1-2\delta)(2+9\delta)}{8} = \delta^2.$$

$$\delta = 0.3897.$$

This is not compatible with the last of Equations (11).

To determine the approximate additional stresses (in this case, practically unavoidable) due to a cutout reinforced by a given ring, there must be added to the stress function the additional terms in Equations (36) corresponding to the same trigonometric orders that appear in φ_o and which give constraint stresses which diminish with increasing r from the cutout. Thus, for stresses in the web under pure bending with a reinforced cutout:

$$\left.\begin{aligned} \varphi &= P_1\cos\theta + P_3\cos 3\theta \\ P_1 &= C_{21}r^3 + C_{31}r^{-1} \\ P_3 &= C_{13}r^3 + C_{23}r^{-3} + C_{43}r^{-1} \end{aligned}\right\} \qquad (12)$$

C_{11} has been omitted since it makes no contribution to stress.

The subsitution of Equations (12) into Equations (4) with the notation of Equations (E3) gives:

$$\left.\begin{aligned}
\sigma_r &= -\frac{Mr}{4I}(\cos\theta-\cos3\theta)-2k_{31}\left(\frac{r_1}{r}\right)^3\cos\theta-\left[12k_{23}\left(\frac{r_1}{r}\right)^5+10k_{43}\left(\frac{r_1}{r}\right)^3\right]\cos3\theta \\
\sigma_\theta &= -\frac{Mr}{4I}(3\cos\theta+\cos3\theta)+2k_{31}\left(\frac{r_1}{r}\right)^3\cos\theta+\left[12k_{23}\left(\frac{r_1}{r}\right)^5+2k_{43}\left(\frac{r_1}{r}\right)^3\right]\cos3\theta \\
\tau_{r\theta} &= -\frac{Mr}{4I}(\sin\theta+\sin3\theta)-2k_{31}\left(\frac{r_1}{r}\right)^3\sin\theta-\left[12k_{23}\left(\frac{r_1}{r}\right)^5+6k_{43}\left(\frac{r_1}{r}\right)^3\right]\sin3\theta
\end{aligned}\right\} \qquad (13)$$

where k_{31}, k_{23}, and k_{43} are evaluated from Equations (E5).

In many cases in practice the reinforcing rings are quite narrow; i.e., β and δ are quite small. The constraint stresses, then, are, with negligible error, functions of the cross-sectional area of the reinforcement alone. Equations (E5a) become:

$$\left.\begin{aligned}
\frac{2k_{31}}{K} &= -6\cdot\frac{2-2.077\alpha}{2+\alpha} \\
\frac{k_{23}}{K} &= -\frac{1.333-.359\alpha}{0.667+1.359\alpha} \\
\frac{k_{43}}{K} &= \frac{2+\alpha}{0.667+1.359\alpha}
\end{aligned}\right\} \qquad (14)$$

For $\alpha = 0$; i.e., no reinforcement; hole of radius r_1.

At $r = r_1$; Equations (13) become:

$$\left.\begin{aligned} (\sigma_r)_{r=r_1} &= 0 \\ (\sigma_\theta)_{r=r_1} &= -\frac{Mr_1}{I}(\cos\theta + \cos 3\theta) \\ (\tau_{r\theta})_{r=r_1} &= 0 \end{aligned}\right\} \qquad (14a)$$

which agrees with the solution given in [2].

E. Bending with Shear

If an I-beam is subjected to bending with shear about an axis perpendicular to the plane of the web, see Fig. XIV, the stress distribution can be approximated to a satisfactory degree[12] by:

$$\begin{aligned} \sigma_{x_o} &= \frac{P}{I}(L - x)y \\ \sigma_{y_o} &= 0 \\ \tau_{xy_o} &= -\tau\left\{\frac{3}{2(1-\eta)} - \frac{A_w h^2}{2I}\left[\left(\frac{y}{h}\right)^2 + \frac{\mu}{1-\mu}\right]\right\} \qquad |y| \le h - t_F \\ xy_o &= -\tau\frac{A_w h2}{2I}\left[1 - \left(\frac{y}{h}\right)^2\right] \qquad |y| \ge h - t_F \end{aligned} \qquad (15)$$

The stress function corresponding to Equations (15) for the web alone is:

$$\varphi_o = -\frac{P}{6I}xy^3 + \frac{PL}{6I}y^3 + \tau\Gamma xy \qquad (15a)$$

---

12. This is based on approximate theory that the web of an I-beam takes most of the shearing force and that the shearing stresses are constant across the web thickness. Cf. p. 305,[21] .

This is equivalent to the sum of two stress functions:

$\varphi_1 = \frac{PL}{6I}y$, corresponding to pure bending with M = - PL

and

$\varphi_2 = -\frac{P}{6I}xy^3 + \tau\Gamma xy$, corresponding to the loading of Fig. XXXII.

In polar coordinates:

$$\varphi_2 = -\left(\frac{Pr^4}{24I} - \frac{\tau\Gamma}{2}r^2\right)\sin 2\theta - \frac{Pr^4}{48I}\sin 4\theta \qquad (16)$$

and the corresponding stress distribution is:

$$\left.\begin{aligned} \sigma_r &= -\tau\Gamma\sin 2\theta + \frac{Pr^2}{4I}\sin 4\theta \\ \sigma_\theta &= -\frac{Pr^2}{2I}\sin 2\theta + \tau\Gamma\sin 2\theta - \frac{Pr^2}{4I}\sin 4\theta \\ \tau_{r\theta} &= +\frac{Pr^2}{4I}\cos 2\theta - \tau\Gamma\cos 2\theta + \frac{Pr^2}{4I}\cos 4\theta \end{aligned}\right\} \qquad (16a)$$

By substitution into Equations (8) and (9) it is found[13] that it is impossible to provide reinforcement that is the elastic equivalent of the cutout.

To determine the approximate additional stresses, there must be added to the stress function additional terms from Equations (3b) just as in the pure bending case. Thus, for stresses in the web under bending with shear with a reinforced cutout:

---

13. See Section K.

$$\left.\begin{aligned} \varphi &= Q_2 \sin 2\theta + Q_4 \sin 4\theta \\ Q_2 &= C_{32} r^4 + C_{12} r^2 + C_{22} r^{-2} + C_{42} \\ Q_4 &= C_{14} r^4 + C_{24} r^{-4} + C_{44} r^{-2} \end{aligned}\right\} \qquad (17)$$

The substitution of Equations (17) into Equations (4) with the notation of Equations (G3) gives:

$$\left.\begin{aligned} \sigma_r &= -\tau r \sin 2\theta + \frac{Pr^2}{4I}\sin 4\theta - [6k_{22}(\frac{r_1}{r})^4 + 4k_{42}(\frac{r_1}{r})^2]\sin 2\theta - \\ &\quad - [\,20k_{24}(\frac{r_1}{r})^6 + 18k_{44}(\frac{r_1}{r})^4]\sin 4\theta \\ \sigma_\theta &= -(\frac{Pr^2}{2I} - \tau r)\sin 2\theta - \frac{Pr^2}{4I}\sin 4\theta + 6k_{22}(\frac{r_1}{r})^4 \sin 2\theta + \\ &\quad + [20k_{24}(\frac{r_1}{r})^6 + 6k_{44}(\frac{r_1}{r})^4]\sin 4\theta \\ \tau_{r\theta} &= (\frac{Pr^2}{4I} - \tau r)\cos 2\theta + \frac{Pr^2}{4I}\cos 4\theta + [6k_{22}(\frac{r_1}{r})^4 + 2k_{42}(\frac{r_1}{r})^2]\cos 2\theta \\ &\quad + [\,20k_{24}(\frac{r_1}{r})^6 + 12k_{44}(\frac{r_1}{r})^4]\cos 4\theta \end{aligned}\right\} \qquad (18)$$

where k_{22}, k_{42}, k_{24}, and k_{44} are evaluated from Equations (G5).

When β and δ are negligibly small (see Pure Bending above), the constraint stresses are functions of α alone. Equations (G5a) become:

$$\left.\begin{aligned}
\frac{k_{22}}{K} &= \frac{\frac{r_1}{L}(4 - 4.153\alpha) + \frac{\tau r}{K}(1 - 0.269\alpha)}{2 + 2.538\alpha} \\
\frac{k_{42}}{K} &= -\frac{\frac{r_1}{L}(6 - 1.615\alpha) + \frac{\tau r}{K}(2 - \alpha)}{2 + 2.538\alpha} \\
\frac{k_{44}}{K} &= -\frac{r_1}{2L} \cdot \frac{8 - 0.923\alpha}{2 + 2.538\alpha} \\
\frac{k_{24}}{K} &= \frac{r_1}{2L} \cdot \frac{6 - 1.615\alpha}{2 + 2.538\alpha}
\end{aligned}\right\} \quad (19)$$

For $\alpha = 0$; i.e., no reinforcement; hole of radius r_1. At $r = r_1$; Equations (18) become:

$$\left.\begin{aligned}
(\sigma_r)_{r=r_1} &= 0 \\
(\sigma_\theta)_{r=r_1} &= (4\tau r - \frac{Pr_1^2}{I})\sin 2\theta - \frac{Pr_1^2}{I}\sin 4\theta \\
(\tau_{r\theta})_{r=r_1} &= 0
\end{aligned}\right\} \quad (18a)$$

which agrees with the solution given in [10].

Furthermore:

For $\eta = \mu = 0$; i.e., a rectangular plate (no flanges): $\Gamma = \frac{3}{2}$, Equations (18a) become:

$$\left.\begin{aligned} (\sigma_r)_{r=r_1} &= 0 \\ (\sigma_\theta)_{r=r_1} &= (6C - \frac{Pr_1^2}{I})\sin 2\theta - \frac{Pr_1^2}{I}\sin 4\theta \\ (\tau_{r\theta})_{r=r_1} &= 0 \end{aligned}\right\} \quad (18b)$$

which agrees with the solution given in [3] .

For the complete solution to the problem of bending with shear, Equations (13) and (18) are added.

F. Stress-Strain Relations of Reinforcement Ring

The theory of curved beams[14] states that the change of curvature κ_r of a ring due to a bending moment M[15] is:

$$\kappa_r = + \frac{M}{E_r I_e} \quad (B1)$$

where $$I_e = r_n \int_{r_1 - t_r}^{r_1} wr\,dr - Ar_n^2 \quad (B2)$$

and where w is the width perpendicular to the plane of bending of a cross-section.

Now r_n is given by:[16] $r_n \equiv r_1 - e$

$$= \frac{A}{\int_{r_1 - t_r}^{r_1} \frac{w\,dr}{r}} \quad (B3)$$

---

14. [21] , p. 58 et seq. and [20] , p. 101 et seq.
15. Positive orientation of M in Fig. XXX is opposite to that assumed in [20] .
16. [20] , p. 69 et seq.

In particular, for a rectangular cross-section:

$$r_n = \frac{t_r}{\log_e \frac{r_1}{r_1 - t_r}} \qquad (B3a)$$

But $$I_r = \frac{A t_r^2}{12} \qquad (B4)$$

Then: $$\frac{I_e}{I_r} = \frac{12}{\log_e\left(1 + \frac{t_r}{r_2}\right)} \left[\frac{r_2}{t_t} + \frac{1}{2} - \frac{1}{\log_e\left(1 + \frac{t_r}{r_2}\right)} \right] \qquad (B5)$$

From which:

$\frac{t_r}{r_2}$	$\frac{I_e}{I_r}$	$\frac{r_n}{r_o}$
.1	.99717	.99925
.2	.99649	.99725
.3	.99619	.99432

TABLE VIII

Comparison of Exact and Approximate
Moments of Inertia and Location of Neutral Fiber

Table VIII[17] shows that for a rectangular cross-section with values of $\frac{t_r}{r_2} \leq 0.3$, those usually encountered in practice, a ring may be treated as a straight beam, so that it is permissible to put:

---

17. Cf. Table on p. 34, [14] , for I-shaped reinforcement.

$$r_n = r_1 - \frac{t_r}{2} \equiv r_o$$

$$e = \frac{t_r}{2}$$

$$I_e = I_r$$

Then:

$$\kappa_r = + \frac{M}{E_r I_r} \tag{B6}$$

and

$$\left.\begin{aligned} \epsilon_\theta r_o &= u_o + \dot{v}_o \quad [18] \\ \kappa_r r_o^2 &= (u_o + \ddot{u}_o) \quad [19] \end{aligned}\right\} \tag{B7}$$

where the subscript o indicates the neutral fiber $r = r_o$.

Assuming, as is customary in curved bar theory, that no radial pressure between fibers exists, then, for any given θ, u is constant over the thickness of the bar. Therefore,

$$\kappa_r r_o^2 = .(u_o + \ddot{u}_o) = .(u + \ddot{u})_{r=r_1} \tag{B7a}$$

The tangential strain, however, will vary along the thickness of the bar, see Fig. XXXIII.

---

18. Eq. (46), p. 63, [21] .
19. Eq. (95), p. 107, [20] .

FIG. XXXIII

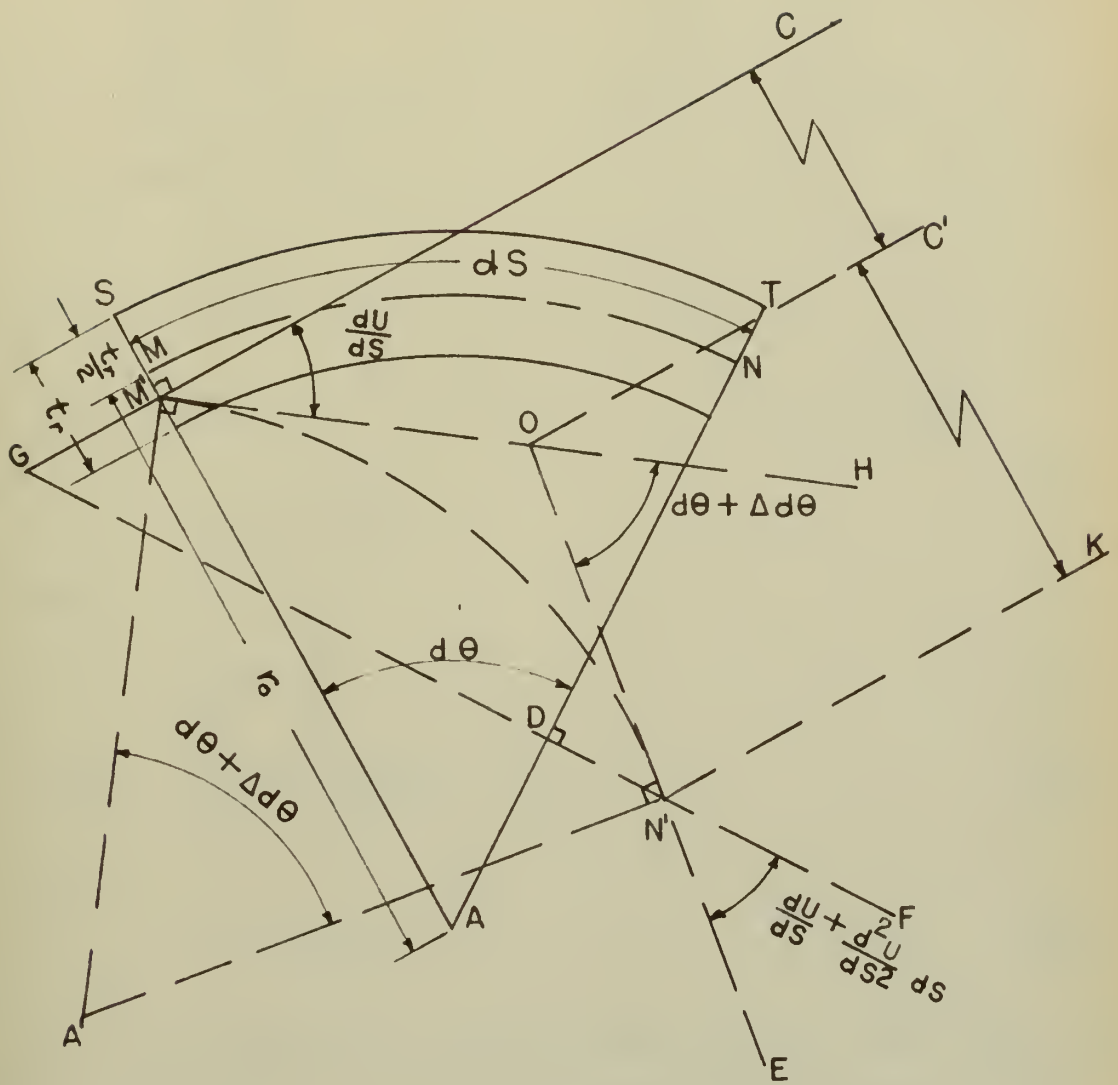

CONTRIBUTION OF CURVATURE OF RING TO EXTENSION AT OUTER BOUNDARY OF RING

S.R.H.
3-21-51

$\angle MAN = d\theta$ $\qquad$ $\angle M'A'N' = d\theta + \Delta\, d\theta$

$\widehat{MN} = ds$ $\qquad$ $ON' \perp A'N'$

$FN' \perp AN$ $\qquad$ $OM' \perp A'M'$

$KN' \parallel CM' \perp AM$ $\qquad$ $\angle HON' = \angle M'A'N'$

$\angle KN'F = \angle MAN$ $\qquad$ $KN' \parallel ON$

$\angle C'ON' = \angle KN'E$

But $\angle C'ON' = \angle C'OH + \angle HON' = \frac{du}{ds} + d\theta + \Delta\, d\theta$

And $\angle KN'E = \angle KN'F + \angle FN'E = d\theta + \frac{du}{ds} + \frac{d^2u}{ds^2}ds.$

$$\Delta\, d\theta = \frac{d^2u}{ds^2}ds. \tag{B8}$$

But $ds = r_o d\theta$

$$\frac{d\theta}{ds} = \frac{1}{r_o}$$

Then: $$\frac{d^2u}{ds^2} = \frac{d^2u}{d\theta^2}\left(\frac{d\theta}{ds}\right)^2 = \frac{\ddot{u}}{r_o^2} \tag{B8a}$$

or

$$\Delta\, d\theta = \frac{\ddot{u}}{r_o}d\theta. \tag{B8a}$$

In considering displacements of the right end relative to the left, we note that there is no rotation of the tangent at M.

Rel. Tan. Disp. of T with respect to M $= \Delta\ v_1 = \frac{\partial v_1}{\partial \theta}d\theta$

Rel. Tan. Disp. of N with respect to M $= \Delta\ v_o = \frac{\partial v_o}{\partial \theta}d\theta$

But $\Delta v_1 = \Delta v_o - \frac{t_r}{2}\Delta\, d\theta$

$$\dot{v}_1 = \dot{v}_o - \frac{t_r}{2r_o}\ddot{u}_o \tag{B9}$$

Therefore: $\epsilon_\theta r_o = (u + \dot{v} + \delta\ddot{u})_{r=r_1}$ (B7b)

C. Stress Resultants and Strains in the Reinforcement Ring

From Fig. XXXc, the three equations for static equilibrium of the ring are:

$$\left.\begin{aligned} \dot{N} - T &= -(\sigma_r)_{r=r_1} r_1 t_w \\ \dot{T} + N &= -(\tau_{r\theta})_{r=r_1} r_1 t_w \\ \dot{M} - Nr_o &= -(\tau_{r\theta})_{r=r_1} \frac{r_1 t_w t_r}{2} \end{aligned}\right\} \qquad (C1)$$

Equations (C1) may be solved for T and M:

$$\ddot{T} + T = r_1 t_w (\sigma_r - \dot{\tau}_{r\theta})_{r=r_1} \qquad (C2)$$

$$M = -Tr_o - r_1^2 t_w \int (\tau_{r\theta})_{r=r_1} d\theta + C_1 \qquad (C3)$$

The substitution of Equations (2) into Equations (C2) and (C3) gives:

$$T = r_1 t_w (r^{-1}\varphi')_{r=r_1} + C_2 \sin\theta + C_3 \cos\theta \qquad \text{for } n \neq 1 \qquad (C4)$$

$$M = \frac{r_1 t_w t_r}{2} (r^{-1}\varphi')_{r=r_1} - r_1^2 t_w (r^{-2}\varphi)_{r=r_1}$$

$$+ C_1 - C_2 r_o \sin\theta - C_3 r_o \cos\theta \qquad (C5)$$

$$\text{for } n \neq 1$$

and

$$T_1 = C_2 \sin\theta + C_3 \cos\theta \qquad \text{for } n = 1 \qquad (C4a)$$

$$M_1 = C_1 - C_2 r_o \sin\theta - C_3 r_o \cos\theta + r_1^2 t_w (r^{-1}\varphi' - r^{-2}\varphi)_{r=r_1} \qquad (C5a)$$

T and M may be obtained in terms of P_n, Q_n, and θ by substituting Equations (3a) and (3b) into Equations (C4), (C4a), (C5), and (C5a).

Similarly the extension strain may be found in terms of P_n, Q_n, and θ by a similar substitution into Equations (5) followed by integration for u and v.[20]

From the first of Equations (5):

$$E_w u = \int \frac{\ddot{\varphi} + \varphi}{r^2} dr + r^{-1}\varphi - \nu\varphi' \qquad (C6a)$$

$$E_w(u + \ddot{u}) = \int \frac{\dddot{\varphi} + 2\ddot{\varphi} + \varphi}{r^2} dr + r^{-1}(\ddot{\varphi} + \varphi) - \nu(\ddot{\varphi} + \varphi)' \qquad (C6b)$$

From the second of Equations (5):

$$E_w(u + \dot{v}) = r\varphi'' - \nu r^{-1}\ddot{\varphi} - \nu\varphi' \qquad (C7a)$$

$$E_w(u + \dot{v} + \delta\ddot{u}) = \delta \int \frac{\ddddot{\varphi} + \ddot{\varphi}}{r^2} dr - r^{-1}\ddot{\varphi}(\nu - \delta) + r\varphi'' - \nu\delta\ddot{\varphi}' - \nu\varphi' \qquad (C7b)$$

Substituting Equations (3a) and (6b) into Equation (C6b) and noting that $\delta = \frac{r_1}{r_o} - 1$ yields:

---

20. Two arbitrary functions $f_1(r)$ and $f_2(\theta)$ will appear as a result of this integration, but these are already included in Equations (3a) and (3b)--cf. p. 37, [14] and p. 5, [13].

$$E_v(u+\ddot{u})_{r=r_1} = -\sum_{o}(n^2-1)\cos n\theta\,[P_n r_1^{-1} - \nu P_n' - (n^2-1)\int P_n r^{-2}dr]_{r=r_1}$$

$$-\sum_{1}(n^2-1)\sin n\theta\,[Q_n r_1^{-1} - \nu Q_n' - (n^2-1)\int Q_n r^{-2}dr]_{r=r_1}$$

(C8)

Similar treatment of Equation (C7b) gives:

$$E_w(u+\dot{v}+\delta\ddot{u})_{r=r_1} = \sum_{o}\cos n\theta\left\{n^2\nu P_n r_1^{-1} - \nu P_n' + P_n''\,r_1 + n^2\delta\,[\nu P_n' - P_n r_1^{-1} + (n^2-1)\int P_n r^{-2}dr]\right\}_{r=r_1}$$

$$+\sum_{1}\sin n\theta\left\{n^2 Q_n \nu r_1^{-1} - \nu Q_n' + Q_n''\,r_1 + n^2\delta\,[\nu Q_n' - Q_n r_1^{-1} + (n^2-1)\int Q_n r^{-2}dr]\right\}_{r=r_1}$$

(C9)

H. Practical Impossibility of Perfect Equivalent for Pure Bending

From Equation (10a):

$$\left.\begin{aligned} P_1 &= -\frac{Mr^3}{8I} \\ P_3 &= -\frac{Mr^3}{24I} \end{aligned}\right\} \qquad (D1)$$

Because of anti-symmetry about the x-axis and symmetry about the y-axis:

$$C_1 = C_2 = 0 \qquad (D2)$$

Substitution of Equations (D1) and (D2) into Equations (8) and (9) yields:

$$A_r = \frac{r_o t_w}{(1+\nu)(2+9\delta)} \cdot \frac{E_w}{E_r} \cdot \frac{\cos 3\theta - \frac{8I C_3}{M r_1^2 t_w}\cos\theta}{\frac{6-2\nu+\delta(3\nu-1)}{(1+\nu)(2+9\delta)}\cos\theta + \cos 3\theta} \qquad (D3)$$

$$I_r = \frac{r_o^3 t_w}{24(1+\nu)} \cdot \frac{E_w}{E_r}(1-2\delta) \cdot \frac{-\frac{6}{1-2\delta}(1+\delta+\frac{4I C_3}{M r_1^2 t_w})\cos\theta + \cos 3\theta}{\cos 3\theta} \qquad (D4)$$

From Equation (D4), in order that I_r be everywhere positive, it is necessary that:

$$C_3 = -\frac{M r_1^2 t_w}{4I}(1+\delta) \qquad (D5)$$

The substitution of Equation (D5) into Equation (D3) gives:

$$A_r = \frac{r_o t_w}{(1+\nu)(2+9\delta)} \cdot \frac{E_w}{E_r} \cdot \frac{2(1+\delta)\cos\theta + \cos 3\theta}{\frac{6-2\nu+\delta(3\nu-1)}{(1+\nu)(2+9\delta)}\cos\theta + \cos 3\theta} \qquad (D6)$$

A_r will be everywhere positive if and only if:

$$\delta = \frac{-11 + \frac{3\nu-1}{2(1+\nu)} \pm \left[49 + \frac{36(3-\nu)}{1+\nu} - \frac{11(3\nu-1)}{1+\nu} + \frac{(3\nu-1)^2}{4(1+\nu)^2}\right]^{\frac{1}{2}}}{18} \qquad (D7)$$

For $\nu = 0.3$; $\delta = 0.00693$. (D7a)

For practical design work, this low value of δ is incompatible with the large required moment of inertia:

$$I_r = \frac{r_o^3 t_w}{24(1+\nu)} \cdot \frac{E_w}{E_r}(1 - 2\delta) \qquad (D4a)$$

J. Derivation of Constraint Constants for Pure Bending

The substitution of Equations (12) into Equations (8) and (9) gives:

$$\alpha = \frac{k_3\cos\theta - (3K + 3k_{23} + k_{43})\cos 3\theta}{\left\{K\left[-\frac{3(3-\nu)}{1+\nu} + \frac{3(1-3\nu)}{2(1+\nu)}\delta\right] + k_{31}\left(1 - \frac{\delta}{2}\right)\right\}\cos\theta + \left[-K\left(3 + \frac{27}{2}\delta\right) + k_{23}\left(6 - \frac{27}{2}\delta\right) + k_{43}\frac{2+10\nu-9\delta(5+\nu)}{2(1+\nu)}\right]\cos 3\theta} \qquad (E1)$$

$$\beta = \frac{\left[-k_3 - (1+\delta)(6K+2k_{31})\right]\cos\theta + \left[K(1-2\delta) - k_{23}(1+4\delta) - k_{43}(1+2\delta)\right]\cos 3\theta}{\left[K + k_{23} + \frac{5+\nu}{3(1+\nu)}k_{43}\right]\cos 3\theta} \qquad (E2)$$

where:

$$K = \frac{Mr_1}{24I} \qquad k_{23} = C_{23}r_1^{-5}$$

$$C_{13}r_1 = -K \qquad k_{43} = C_{43}r_1^{-3}$$

$$C_{21}r_1 = -3K \qquad k_{31} = C_{31}r_1^{-3}$$

$$k_3 = \frac{C_3}{r_1 t_s} \qquad (E3)$$

Clearing Equations (E1) and (E2) of fractions and equating coefficients of like trigonometric terms:

$$\left.\begin{aligned}
k_3 &= \alpha\left\{K\left[-\frac{3(3-\nu)}{1+\nu}+\frac{3(1-3\nu)}{2(1+\nu)}\delta\right]+k_{31}\left(1-\frac{\delta}{2}\right)\right\}\\
-(3K+3k_{23}+k_{43}) &= \alpha\left[-K\left(3+\frac{27}{2}\delta\right)+k_{23}\left(6-\frac{27}{2}\delta\right)+k_{43}\cdot\frac{2^{*}10\nu-9\delta(5+\nu)}{2(1+\nu)}\right.\\
-k_3-(1+\delta)(6K+2k_{31}) &= 0\\
K(1-2\delta)-k_{23}(1+4\delta)-k_{43}(1+2\delta) &= \beta\left[K+k_{23}+\frac{5+\nu}{3(1+\nu)}k_{43}\right]
\end{aligned}\right\} \qquad (E4)$$

From which:

$$\left.\begin{aligned}
k_3 &= -6K\cdot\frac{\frac{4}{1+\nu}-\delta}{\left(1-\frac{\delta}{2}\right)+2(1+\delta)}\alpha(1+\delta)\\
k_{31} &= -3K\cdot\frac{2(1+\delta)-\alpha\left[\frac{3-\nu}{1+\nu}-\frac{1-3\nu}{2(1+\nu)}\delta\right]}{\left(1-\frac{\delta}{2}\right)+2(1+\delta)}
\end{aligned}\right\} \qquad (E5)$$

(E5)

$$k_{23} = -K \cdot \frac{1-\alpha(1+\frac{9}{2}\delta)\left[1+\beta\cdot\frac{5+\nu}{3(1+\nu)}+2\delta\right]+(1-\beta-2\delta)\left[\frac{1}{3}+\alpha\cdot\frac{2+10\nu-9\delta(5+\nu)}{6(1+\nu)}\right]}{1+\alpha(2-\frac{9}{2}\delta)\left[1+\beta\cdot\frac{5+\nu}{3(1+\nu)}+2\delta\right]-(1+\beta+4\delta)\left[\frac{1}{3}+\alpha\cdot\frac{2+10\nu-9\delta(5+\nu)}{6(1+\nu)}\right]}$$

$$k_{43} = \frac{\left[1-\alpha(1+\frac{9}{2}\delta)\right]\left[1+\beta+4\delta\right)+(1-\beta-2\delta)\left[1+\alpha(2-\frac{9}{2}\delta)\right]}{\left[1+\alpha(2-\frac{9}{2}\delta)\right]\left[1+\beta\cdot\frac{5+\nu}{3(1+\nu)}+2\delta\right]-(1+\beta+4\delta)\left[\frac{1}{3}+\alpha\cdot\frac{2+10\nu-9\delta(5+\nu)}{6(1+\nu)}\right]}$$

For $\nu = 0.3$:

(E5a)

$$k_3 = -\frac{Mr_1}{4I}\cdot\frac{\alpha(1+\delta)(3.077-\delta)}{\alpha(1-0.5\delta)+2(1+\delta)}$$

$$k_{31} = -\frac{Mr_1}{8I}\cdot\frac{2(1+\delta)-\alpha(2.077-0.038\delta)}{(1-0.5\delta)+2(1+\delta)}$$

$$k_{23} = -\frac{Mr_1}{24I}\cdot\frac{(\beta-1+2\delta)[\alpha(0.641-6.115\delta)+0.333]+(1.359\beta+1+2\delta)[\alpha(1+4.5\delta)-1]}{(\beta+1+4\delta)[\alpha(0.641-6.115\delta)+0.333]-(1.359\beta+1+2\delta)[\alpha(2-4.5\delta)+1]}$$

$$k_{43} = \frac{Mr_1}{24I}\cdot\frac{(\beta-1+2\delta)[\alpha(2-4.5\delta)+1]+(\beta+1+4\delta)[\alpha(1+4.5\delta)-1]}{(\beta+1+4\delta)[\alpha(0.641-6.115\delta)+0.333]-(1.359\beta+1+2\delta)[\alpha(2-4.5\delta)+1]}$$

K. Impossibility of Perfect Equivalence for Bending with Shear

From Equations (16a):

$$\left.\begin{aligned} Q_2 &= -\frac{Pr^4}{24I} + \frac{\tau r}{2} r^2 \\ Q_4 &= -\frac{Pr^4}{48I} \end{aligned}\right\} \qquad (F1)$$

Because of anti-symmetry about both x- and y-axes and polar symmetry:

$$C_1 = C_2 = C_3 = 0 \qquad (F2)$$

Substitution of Equations (F1) and (F2) into Equations (8) and (9) yields:

$$\alpha = \frac{(-\frac{4r_1}{3L} + \frac{8I\tau r}{PLr_1})\sin 2\theta - \frac{2r_1}{3L}\sin 4\theta}{[-\frac{2r_1}{3L}\cdot\frac{3+4\delta}{1+\nu} + \frac{4I\tau r}{PLr_1}(1+4\delta)]\sin 2\theta - \frac{r_1}{3L}(3+16\delta)\sin 4\theta} \qquad (F3)$$

$$\beta = \frac{[-\frac{r_1}{L}(1-3\delta) + \frac{12I\tau r}{PLr_1}(1-\delta)]\sin 2\theta - \frac{r_1}{2L}(1-3\delta)\sin 4\theta}{(-\frac{r_1}{2L}\cdot\frac{\nu}{1+\nu} + \frac{3I\tau r}{PLr_1})\sin 2\theta - \frac{5r_1}{6L}\sin 4\theta} \qquad (F4)$$

From Equation (F4), in order that β be everywhere positive, it is necessary that:

$$\left.\begin{aligned} \frac{r_1}{L}(1-3\delta) - \frac{12I\tau r}{PLr_1}(1-\delta) &= \frac{r_1}{2L}\cdot\frac{\nu}{1+\nu} - \frac{3I\tau r}{PLr_1} \\ \frac{r_1}{2L}(1-3\delta) &= \frac{5r_1}{6L} \end{aligned}\right\} \qquad (F5)$$

From the second of Equations (F5),

$$\delta = -\frac{2}{9} . \qquad (F5a)$$

This is physically impossible. Hence perfect elastic equivalence for bending with shear is impossible.

L. Derivation of Constraint Constants for Bending with Shear

The substitution of Equations (17) into Equations (8) and (9) gives:

$$\alpha = \frac{(4\frac{r_1}{L}K+\tau r-2k_{22})\sin 2\theta + (2\frac{r_1}{L}K-4k_{24}-2k_{44})\sin 4\theta}{\left[2\frac{r_1}{L}K\cdot\frac{3+4\delta\nu}{1+\nu}+\frac{\tau r}{2}(1+4\delta)+k_{22}(3-4\delta)+k_{42}\cdot\frac{2(\nu-4\delta)}{1+\nu}\right]\sin 2\theta + \left[\frac{r_1}{L}K(3+16\delta)+2k_{24}\left(\frac{3+5\nu}{1+\nu}-16\delta\right)+\right.}$$

$$\left. + k_{44}\cdot\frac{3+9\nu-16\delta(3-\nu)}{1+\nu}\right]\sin 4\theta \qquad (G1)$$

$$= \frac{\left[\frac{r_1K}{L}(1-3\delta)+\frac{\tau r}{2}(1-\delta)+k_{22}(1+3\delta)\ k_{42}(1+\delta)\right]\sin 2\theta+\left[\frac{r_1K}{L}(1-3\delta)+k_{24}(1+5\delta)+k_{44}(1+3\delta)\right]\sin 4\theta}{\left[\frac{r_1K}{L}\cdot\frac{\nu}{2(1+\nu)}+\frac{\tau r}{8}-\frac{k_{22}}{4}-k_{42}\cdot\frac{1}{2(1+\nu)}\right]\sin 2\theta+\left[\frac{5r_1K}{4L}-\frac{5}{2}k_{24}-\frac{5(3+\nu)}{4(1+\nu)}k_{44}\right]\sin 4\theta} \qquad (G2)$$

where:

$$K = -\frac{PLr_1}{24I} \qquad k_{22} = C_{22}r_1^{-4}$$

$$\frac{\tau r}{2} = C_{12} \qquad k_{24} = C_{24}r_1^{-6}$$

$$C_{14}r_1 = \frac{K}{2L} \qquad k_{42} = C_{42}r_1^{-2}$$

$$C_{32}r_1 = \frac{K}{L} \qquad k_{44} = C_{44}r_1^{-4} \qquad (G3)$$

Clearing Equations (G1) and (G2) of fractions and equating coefficients of like trigonometric terms:

$$4\frac{r_1K}{L}+\tau r-2k_{22} = \alpha\left[\frac{2r_1K}{L}\cdot\frac{3+4\delta\nu}{1+\nu}+\frac{\tau r}{2}(1+4\delta)+k_{22}(3-4\delta)+k_{42}\frac{2(\nu-4\delta)}{1+\nu}\right]$$

$$2\frac{r_1K}{L}-4k_{24}-2k_{44} = \alpha\left[\frac{r_1K}{L}(3+16\delta)+2k_{24}\left(\frac{3+5\nu}{1+\nu}-16\delta\right)+k_{44}\frac{3+9\nu-16\delta(3-\nu)}{1+\nu}\right] \qquad (G4)$$

$$k_{42}(1+\delta)+\frac{r_1K}{L}(1-3\delta)+\frac{\tau r}{2}(1-\delta)+k_{22}(1+3\delta)=\beta\left[\frac{r_1K}{L}\cdot\frac{\nu}{2(1+\nu)}+\frac{\tau r}{8}-\frac{k_{22}}{4}-k_{42}\cdot\frac{1}{2(1+\nu)}\right.$$

$$\left.\frac{r_1K}{2L}(1-3\delta)+k_{24}(1+5\delta)+k_{44}(1+3\delta)=\beta\left[\frac{5r_1K}{4L}\cdot\frac{5k_{24}}{2}-\frac{5(3+\nu)}{4(1+\nu)}k_{44}\right]\right\} \quad (G4)$$

From which:

$$\frac{k_{22}}{K}=\frac{\left\{\frac{r_1}{L}[4-2\alpha\cdot\frac{3+4\nu\delta}{1+\nu}]+\frac{\tau r}{2K}[2-\alpha(1+4\delta)]\right\}[1+\delta+\frac{\beta}{2(1+\nu)}]+\left\{\frac{r_1}{L}[1-3\delta-\frac{\beta\nu}{2(1+\nu)}]+\frac{\tau r}{2K}[1-\delta-\frac{\beta}{4}]\right\}\frac{2\alpha(\nu-4\delta)}{1+\nu}}{[2+\alpha(3-4\delta)][1+\delta+\frac{\beta}{2(1+\nu)}]-(1+3\delta+\frac{\beta}{4})\cdot\frac{2\alpha(\nu-4\delta)}{1+\nu}}$$

$$\frac{k_{42}}{K}=\frac{\left\{\frac{r_1}{L}[4-2\alpha\cdot\frac{3+4\nu\delta}{1+\nu}]+\frac{\tau r}{2K}[2-\alpha(1+4\delta)]\right\}[(1+3\delta+\frac{\beta}{4})+\left\{\frac{r_1}{L}[1-3\delta-\frac{\beta\nu}{2(1+\nu)}]+\frac{\tau r}{2K}(1-\delta-\frac{\beta}{4})\right\}[2+\alpha(3-4\delta)]}{[2+\alpha(3-4\delta)][1+\delta+\frac{\beta}{2(1+\nu)}]-(1+3\delta+\frac{\beta}{4})\cdot\frac{2\alpha(\nu-4\delta)}{1+\nu}} \quad (G5)$$

$$\frac{k_{24}}{K}=\frac{r_1}{2L}\frac{[4-2\alpha(3+16\delta)][1+3\delta+\beta\cdot\frac{5(3+\nu)}{4(1+\nu)}]+(1-3\delta-\frac{5}{2}\beta)[2+\alpha\cdot\frac{3+9\nu-16\delta(3-\nu)}{1+\nu}]}{[4+2\alpha(\frac{3+5\nu}{1+\nu}-16\delta)][1+3\delta+\beta\frac{5(3+\nu)}{4(1+\nu)}]-(1+5\delta+\frac{5}{2}\beta)[2+\alpha\cdot\frac{3+9\nu-16\delta(3-\nu)}{1+\nu}]}$$

$$\frac{k_{44}}{K} = -\frac{r_1}{2L}\cdot\frac{[4-2\alpha(3+16\delta)](1+5\delta+\frac{5}{2}\beta)+(1-3\delta-\frac{5}{2}\beta)[4+2\alpha(\frac{3+5\nu}{1+\nu}-16\delta)]}{[4+2\alpha(\frac{3+5\nu}{1+\nu}-16\delta)][1+3\delta+\beta\cdot\frac{5(3+\nu)}{4(1+\nu)}]-(1+5\delta+\frac{5}{2}\beta)[2+\alpha\cdot\frac{3+9\nu-16\delta(3-\nu)}{1+\nu}]} \qquad (G5)$$

For $\nu = 0.3$

$$\left.\begin{aligned}
\frac{k_{22}}{K} &= \frac{\left\{\frac{r_1}{L}[4-\alpha(4.615+1.846\delta)]+\frac{r_2}{2K}[2-\alpha(1+4\delta)]\right\}(1+\delta+.385\beta)+[\frac{r_1}{L}(1-3\delta-.115\beta)+\frac{r_2}{2K}(1-\delta-.25\beta)]\alpha(.462-6.154\delta)}{[2+\alpha(3-4\delta)](1+\delta+.385\beta)-(1+3\delta+.25\beta)\alpha(.462-6.154\delta)} \\
\frac{k_{42}}{K} &= -\frac{\left\{\frac{r_1}{L}[4-\alpha(4.615+1.846\delta)]+\frac{r_2}{2K}[2-\alpha(1+4\delta)]\right\}(1+3\delta+.25\beta)+[\frac{r_1}{L}(1-3\delta-.115\beta)+\frac{r_2}{2K}(1-\delta-.25\beta)][2+\alpha(3-4\delta)]}{[2+\alpha(3-4\delta)](1+\delta+.385\beta)-(1+3\delta+.25\beta)\alpha(.462-6.154\delta)} \qquad (G5a) \\
\frac{k_{44}}{K} &= -\frac{r_1}{2L}\cdot\frac{[4-\alpha(6+32\delta)](1+5\delta+2.5\beta)+(1-3\delta-2.5\beta)[4+\alpha(6.923-32\delta)]}{[4+\alpha(6.923-32\delta)](1+3\delta+3.173\beta)-(1+5\delta+2.5\beta)[2+\alpha(4.385-33.231\delta)]} \\
\frac{k_{24}}{K} &= \frac{r_1}{2L}\cdot\frac{[4-\beta(6+32\delta)](1+3\delta+3.173\beta)+(1-3\delta-2.5\beta)[2+\alpha(4.385-33.231\delta)]}{[4+\alpha(6.923-32\delta)](1+3\delta+3.173\beta)-(1+5\delta+2.5\beta)[2+\alpha(4.385-33.231\delta)]}
\end{aligned}\right\}$$

III. Particular Case of Rectangular Reinforcement[21]

This solution, although basically the same as in the preceding Section, is presented from a slightly different point of view. Two separate stress functions, one for the web and the other for the reinforcement are derived. The boundary conditions to be satisfied are:

1.) At great distances from the hole, $r >> r_2$, the stress distribution tends to conform to that existing in the uncut web.

2.) No external forces are applied at the inner edge of the ring, $r = r_2$.

3.) At the junction of the ring and the web, $r = r_1$, the radial and tangential displacements of the ring must be equal to those of the plate.

4.) At the junction of the ring and the web, $r = r_1$, the forces acting on the outer edge of the ring must be equal and opposite to the corresponding forces acting on the inner edge of the web.

In Figs. XVI and XXX the ring has been shown to be abruptly joined to the web. If this is the case, there will be a local stress concentration at this junction. This has not been taken into consideration since, in practice, a small fillet, probably a weld, would be present to relieve this con-

---

21. Follows [13] .

centration. Strictly speaking, the stress distribution at the junction is three-dimensional. This has not been considered. Otherwise this solution conforms to the usual elasticity procedure and assumptions--Hooke's Law; homogeneous and isotropic material; "small" displacements.

A. Pure Bending

Boundary Conditions (1) and (3) have been used in Section II to determine φ for the web:

$$\varphi = \left[-\frac{M}{8I}r^3 + k_{31}r_i^2\left(\frac{r}{r_1}\right)^{-1}\right]\cos\theta + \left[-\frac{Mr^3}{24I} + k_{23}r_i^2\left(\frac{r}{r_1}\right)^{-3} + k_{43}r_i^2\left(\frac{r}{r_1}\right)^{-1}\right]\cos 3\theta \tag{20}$$

The stress function ψ for the ring will have the same general form as φ for the web but with possibly different constants:

$$\begin{aligned}
\psi &= (a_{21}r^3 + a_{31}r^{-1})\cos\theta + (a_{13}r^3 + a_{23}r^{-3} + a_{33}r^5 + a_{43}r^{-1})\cos 3\theta \\
\sigma_r &= (2a_{21}r - 2a_{31}r^{-3})\cos\theta - (6a_{13}r + 12a_{23}r^{-5} + 4a_{33}r^3 + 10a_{43}r^{-3})\cos 3\theta \\
\sigma_\theta &= (6a_{21}r + 2a_{31}r^{-3})\cos\theta + (6a_{13}r + 12a_{23}r^{-5} + 20a_{33}r^3 + 2a_{43}r^{-3})\cos 3\theta \\
\tau_{r\theta} &= (2a_{21}r - 2a_{31}r^{-3})\sin\theta + (6a_{13}r - 12a_{23}r^{-5} + 12a_{33}r^3 - 6a_{43}r^{-3})\sin 3\theta
\end{aligned} \tag{21}$$

From Boundary Condition (2): $(\sigma_r)_{r=r_2} = (\tau_{r\theta})_{r=r_2} = 0$

$$\left.\begin{aligned}
d_{21} - d_{31} &= 0 \\
3d_{13} + 6d_{23} + 2d_{33} + 5d_{43} &= 0 \\
d_{13} - 2d_{23} + 2d_{33} - d_{43} &= 0
\end{aligned}\right\} \tag{22}$$

where:

$$\left.\begin{aligned}
d_{21} &= a_{21}r_2 & d_{23} &= a_{23}r_2^{-5} \\
d_{31} &= d_{31}r_2^{-3} & d_{33} &= a_{33}r_2^3 \\
d_{13} &= a_{13}r_2 & d_{43} &= a_{43}r_2^{-3}
\end{aligned}\right\} \tag{23}$$

From Boundary Condition (4): Force Equilibrium at $r = r_1$

$$\left.\begin{aligned} f_1\lambda\,(d_{21}p - d_{31}p^{-3}) &= -3K - k_{31} \\ f_3\lambda\,(3d_{13}p + 6d_{23}p^{-5} + 2d_{33}p^{3} + 5d_{43}p^{-3}) &= -3K + 6k_{23} + 5k_{43} \\ f_3\lambda\,(d_{13}p - 2d_{23}p^{-5} + 2d_{33}p^{3} - d_{43}p^{-3}) &= -K - 2k_{23} - k_{43} \end{aligned}\right\} \qquad (24)$$

where: $\lambda = \dfrac{b'}{tw}$

$$p = \frac{r_1}{r_2}$$

f_1, f_3 = factors to allow for three-dimensional effect at junction of ring and web.

From Equations (22) and (24):

$$\left.\begin{aligned} \frac{d_{21}}{K} &= \frac{d_{31}}{K} = -\frac{(3+\frac{k_{31}}{K})}{f_1\lambda\,(p-p^{-3})} \\ \frac{d_{13}}{K} &= \frac{-(p^3+8p^{-3}-9p^{-5}) + \frac{4k_{23}}{K}(p^3-p^{-3}) + \frac{3k_{43}}{K}(p^3-p^{-5})}{f_3\lambda D} \\ \frac{d_{23}}{K} &= \frac{-2(p^3-p^{-3}) + \frac{k_{23}}{K}(8p^3-9p\,p^{-3}) + \frac{6k_{43}}{K}(p^3-p)}{f_3\lambda D} \\ \frac{d_{33}}{K} &= \frac{6(p^{-3}-p^{-5}) - \frac{3k_{23}}{K}(p-p^{-3}) - \frac{2k_{43}}{K}(p-p^{-5})}{f_3\lambda D} \\ \frac{d_{43}}{K} &= \frac{3(p^3-p^{-5}) - \frac{12k_{23}}{K}(p^3-p) - \frac{k_{43}}{K}(9p^3-8p-p^{-3})}{f_3\lambda D} \\ D &= p^4 - 9 + 16p^{-2} - 9p^{-4} + p^{-8}. \end{aligned}\right\} \qquad (25)$$

When $\lambda = 1$; i.e., no reinforcement for a hole whose radius = r_2,

$$\left.\begin{aligned} \frac{3d_{21}}{K} + \frac{d_{31}}{K} &= -\frac{12}{p} \\ \frac{3d_{13}}{K} + \frac{6d_{23}}{K} + \frac{10d_{33}}{K} + \frac{d_{43}}{K} &= -\frac{12}{p} \end{aligned}\right\}^{22} \qquad (26)$$

Therefore:

$$\left.\begin{aligned} f_1 &= \frac{3 + (\frac{k_{31}}{K})_{\lambda=1}}{3(1 - p^{-4})} \\ f_3 &= \frac{(p^3 - 4p^{-3} + 3p^{-5}) - (4p^3 - 6p + 2p^{-3})(\frac{k_{23}}{K})_{\lambda=1} - (3p^3 - 4p + p^{-5})(\frac{k_{43}}{K})_{\lambda=1}}{Dp^{-1}} \end{aligned}\right\} \qquad (26a)$$

and:

$$\left.\begin{aligned} \frac{d_{21}}{K} &= \frac{d_{31}}{K} = -\frac{3}{p\lambda} \cdot \frac{3 + \frac{k_{31}}{K}}{3 + (\frac{k_{31}}{K})_{\lambda=1}} \\ \frac{d_{13}}{K} &= -\frac{(p^3 - 8p^{-3} - 9p^{-5}) - \frac{4k_{23}}{K}(p^3 - p^{-3}) - \frac{3k_{43}}{K}(p^3 - p^{-5})}{p\lambda D'} \\ \frac{d_{23}}{K} &= -\frac{2(p^3 - p^{-3}) - \frac{k_{23}}{K}(8p^3 - 9p + p^{-3}) - \frac{6k_{43}}{K}(p^3 - p)}{p\lambda D'} \\ \frac{d_{33}}{K} &= \frac{6(p^3 - p^{-5}) - \frac{3k_{23}}{K}(p - p^{-3}) - \frac{2k_{43}}{K}(p - p^{-5})}{p\lambda D'} \\ \frac{d_{43}}{K} &= \frac{3(p^3 - p^{-5}) - \frac{12k_{23}}{K}(p^3 - p) - \frac{k_{43}}{K}(9p^3 - 8p - p^{-5})}{p\lambda D'} \\ D' &= (p^3 - 4p^{-3} + 3p^{-5}) - (4p^3 - 6p + 2p^{-3})(\frac{k_{23}}{K})_{\lambda=1} - (3p^3 - 4p + p^{-5})(\frac{k_{43}}{K})_{\lambda=1} \end{aligned}\right\} \qquad (27)$$

It is interesting to note that as $p \longrightarrow 1$ (i.e., no reinforcement for a hole of radius = r_1), $\frac{k_{31}}{K} \longrightarrow -3$, $\frac{k_{23}}{K} \longrightarrow -2$, and and $\frac{k_{43}}{K} \longrightarrow 3$.

---

22. See Eq. (13a).

and $$\frac{d_{21}}{K} = \frac{d_{31}}{K} = \frac{d_{13}}{K} = \frac{d_{23}}{K} = \frac{d_{33}}{K} = \frac{d_{43}}{K} \longrightarrow 0 \qquad (27a)$$

which certainly agrees with the fact that with no reinforcement present there can be no stress in the reinforcement.

If Equations (23) and (27) are substituted into Equations (21) at $r = r_2$:

$$\left.\begin{aligned}
(\sigma_r)_{r=r_2} &= 0 \\
(\sigma_\theta)_{r=r_2} &= -\frac{24K}{p\lambda}\left[\frac{3+\frac{k_{31}}{K}}{3+(\frac{k_{31}}{K})_{\lambda=1}}\cos\theta\ \frac{(p^3-4p^{-3}+3p^{-5})-(4p^3-6p+2p^{-3})\frac{k_{23}}{K}-(3p^3-4p+p^{-5})\frac{k_{43}}{K}}{(p^3-4p^{-3}+3p^{-5})-(4p^3-6p+2p^{-3})(\frac{k_{23}}{K})_{\lambda=1}-(3p^3-4p+p^{-5})(\frac{k_{43}}{K})_{\lambda=1}}\cos 3\theta\right] \\
(\tau_{r\theta})_{r=r_2} &= 0
\end{aligned}\right\} \qquad (28)$$

To obtain greater utility from Equation (28), it is made dimensionless (i.e., a stress concentration factor is determined) by dividing by the nominal bending stress at the extreme fiber: $\sigma_L = -\frac{Mh}{I}$

$$\frac{(\sigma_\theta)_{r=r_2}}{\sigma_L} = \frac{r_2}{h\lambda}\left[\frac{3+\frac{k_{31}}{K}}{3+(\frac{k_{31}}{K})_{\lambda=1}}\cos\theta+\frac{(p^3-4p^{-3}+3p^{-5})-(4p^3-6p+2p^{-3})\frac{k_{23}}{K}-(3p^3-4p+p^{-5})\frac{k_{43}}{K}}{(p^3-4p^{-3}+3p^{-5})-(4p^3-6p+2p^{-3})(\frac{k_{23}}{K})_{\lambda=1}-(3p^3-4p+p^{-5})(\frac{k_{43}}{K})_{\lambda=1}}\cos 3\theta\right] \qquad (28a)$$

B. Bending with Shear

Boundary Conditions (1) and (3) have been used in Section II to determine φ for the web:

$$\varphi = \left[-\frac{Pr^4}{24I} + \tau_{r\theta} r^2 + k_{22} r_1^2 \left(\frac{r}{r_1}\right)^{-2} + k_{42} r_1^2 \right] \sin 2\theta + \left[-\frac{Pr^4}{48I} + k_{24} r_1^2 \left(\frac{r}{r_1}\right)^{-4} + k_{44} r_1^2 \left(\frac{r}{r_1}\right)^{-2} \right] \sin 4\theta \tag{29}$$

The stress function ψ for the ring will have the same general form as φ for the web but with possibly different constants:

$$\left.\begin{aligned}
\psi &= (a_{32} r^4 + a_{12} r^2 + a_{22} r^{-2} + a_{42}) \sin 2\theta + (a_{14} r^4 + a_{24} r^{-4} + a_{34} r^6 + a_{44} r^{-2}) \sin 4\theta \\
\sigma_r &= -2(a_{12} + 3a_{22} r^{-4} + 2a_{42} r^{-2}) \sin 2\theta - 2(6a_{14} r^2 + 10a_{24} r^{-6} + 5a_{34} r^4 + 9a_{44} r^{-4}) \sin 4\theta \\
\sigma_\theta &= 2(6a_{32} r^2 + a_{12} + 3a_{22} r^{-4}) \sin 2\theta + 2(6a_{14} r^2 + 10a_{24} r^{-6} + 15a_{34} r^4 + 3a_{44} r^{-4}) \sin 4\theta \\
\tau_{r\theta} &= -2(3a_{32} r^2 + a_{12} - 3a_{22} r^{-4} - a_{42} r^{-2}) \cos 2\theta - 4(3a_{14} r^2 - 5a_{24} r^{-6} + 5a_{34} r^4 - 3a_{44} r^{-4}) \cos 4\theta
\end{aligned}\right\} \tag{30}$$

From Boundary Condition (2): $(\sigma_r)_{r=r_2} = (\tau_{r\theta})_{r=r_2} = 0$

$$\left.\begin{aligned} d_{12} + 3d_{22} + 2d_{42} &= 0 \\ d_{12} - 3d_{22} + 3d_{32} - d_{42} &= 0 \\ 6d_{14} + 10d_{24} + 5d_{34} + 9d_{44} &= 0 \\ 3d_{14} - 5d_{24} + 5d_{34} - 3d_{44} &= 0 \end{aligned}\right\} \qquad (31)$$

where:

$$\left.\begin{aligned} d_{12} &= a_{12} & d_{14} &= a_{14}r_2^2 \\ d_{22} &= a_{22}r_2^{-4} & d_{24} &= a_{24}r_4^{-6} \\ d_{32} &= a_{32}r_2^2 & d_{34} &= a_{34}r_2^4 \\ d_{42} &= a_{42}r^{-2} & d_{44} &= a_{44}r_2^{-4} \end{aligned}\right\} \qquad (32)$$

From Boundary Condition (4): force equilibrium at $r = r_1$:

$$\left.\begin{aligned} f_2\lambda(d_{12} + 3d_{22}p^{-4} + 2d_{42}p^{-2}) &= \frac{\tau r}{2} + 3k_{22} + 2k_{42} \\ f_2\lambda(d_{12} - 3d_{22}p^{-4} + 3d_{32}p^2 - d_{42}p^{-2}) &= \frac{\tau r}{2} - 3k_{22} + 3K\frac{r_1}{L} - k_{42} \\ f_4\lambda(6d_{14}p^2 + 10d_{24}p^{-6} + 5d_{34}p^4 + 9d_{44}p^{-4}) &= 3K\frac{r_1}{L} + 10k_{24} + 9k_{44} \\ f_4\lambda(3d_{14}p^2 - 5d_{24}p^{-6} + 5d_{34}p^4 - 3d_{44}p^{-4}) &= \frac{3K}{2}\frac{r_1}{L} - 5k_{24} - 3k_{44} \end{aligned}\right\}$$

(33)

where:

$$\lambda = \frac{b^I}{tw}$$

$$p = r_1/r_2$$

f_2, f_4 = factors to allow for three-dimensional effect at junction of ring and web

$$K = -\frac{PLr_1}{24I}$$

From Equations (31) and (33):

$$d_{12} = \frac{\frac{\tau\Gamma}{2}(p^2+3p^{-2}-4p^{-4}) + \frac{6\kappa r_1}{L}(p^{-2}-p^{-4}) + 3k_{22}(p^2-p^{-2}) + 2k_{42}(p^2-p^{-4})}{f_2 \lambda D_2}$$

$$d_{22} = \frac{\frac{\tau\Gamma}{2}(p^2-p^{-2}) + \frac{2\kappa r_1}{L}(1-p^{-2}) + k_{22}(3p^2+p^{-2}-4) + 2k_{42}(p^2-1)}{f_2 \lambda D_2}$$

$$d_{32} = -\frac{\tau\Gamma(p^{-2}-p^{-4}) - \frac{\kappa r_1}{L}(1-4p^{-2}+3p^{-4}) + 2k_{22}(1-p^{-2}) + k_{42}(1-p^{-4})}{f_2 \lambda D_2}$$

$$d_{42} = -\frac{\tau\Gamma(p^2-p^{-4}) + \frac{3\kappa r_1}{L}(1-p^{-4}) + 6k_{22}(p^2-1) + k_{42}(4p^2-3p^{-4})}{f_2 \lambda D_2}$$

$$D_2 = p^2 - 4 + 6p^{-2} - 4p^{-4} + p^{-6}$$

$$d_{14} = \frac{\frac{\kappa r_1}{2L}(p^4+15p^{-4}-16p^{-6}) + 5k_{24}(p^4-p^{-4}) + 4k_{44}(p^4-p^{-6})}{f_4 \lambda D_4}$$

$$d_{24} = \frac{\frac{3\kappa r_1}{2L}(p^4-p^{-4}) + k_{24}(15p^4-16p^2+p^{-4}) + 12k_{44}(p^4-p^2)}{f_4 \lambda D_4}$$

$$d_{34} = -\frac{\frac{6\kappa r_1}{L}(p^{-4}-p^{-6}) + 4k_{24}(p^2-p^{-4}) + 3k_{44}(p^2-p^{-6})}{f_4 \lambda D_4}$$

$$d_{44} = -\frac{\frac{2\kappa r_1}{L}(p^4-p^{-6}) + 20k_{24}(p^4-p^2) + k_{44}(16p^4-15p^2-p^{-6})}{f_4 \lambda D_4}$$

$$D_4 = p^6 - 16 + 30p^{-2} - 16p^{-4} + p^{-10}$$

(34)

When $\lambda = 1$; i.e., no reinforcement for a hole whose radius = r_2,

$$\left.\begin{aligned} d_{12} + 3d_{22} + 6d_{32} &= 2\tau\Gamma + \frac{12Kr_1}{PL} \\ 6d_{14} + 10d_{24} + 15d_{34} + 3d_{44} &= \frac{12Kr_1}{PL} \end{aligned}\right\} \quad 23 \qquad (35)$$

Therefore:

$$\left.\begin{aligned} f_2 &= \frac{2\tau\Gamma(p^2 - 3p^{-2} + 2p^{-4}) + \frac{12Kr_1}{L}(1 - 2p^2 + p^{-4}) + 12(k_{22})_{\lambda=1}(p^2 - 2 + p^{-2}) + 4(k_{42})_{\lambda=1}(2p^2 - 3 + p^{-4})}{(2\tau\Gamma + \frac{12Kr_1}{pL})D_2} \\ f_4 &= \frac{\frac{3Kr_1}{L}(p^4 - 5p^{-4} + 4p^{-6}) + 10(k_{24})_{\lambda=1}(3p^4 - 4p^2 + p^{-4}) + 6(k_{44})_{\lambda=1}(4p^4 - 5p^2 + p^{-6})}{\frac{3Kr_1}{pL} D_4} \end{aligned}\right\} \qquad (35a)$$

And:

$$d_{12} = \frac{\tau\Gamma + \frac{6Kr_1}{pL}}{\lambda} \cdot \frac{\frac{\tau\Gamma}{2}(p^2 + 3p^{-2} - 4p^{-4}) + \frac{6Kr_1}{L}(p^{-2} - p^{-4}) + 3k_{22}(p^2 - p^{-2}) + 2k_{42}(p^2 - p^{-4})}{D_2'}$$

---

23. See Equation (18a).

$$d_{22} = \frac{\tau r + \frac{6Kr_1}{pL}}{\lambda} \cdot \frac{\frac{\tau r}{2}(p^2-p^{-2}) + \frac{2Kr_1}{L}(1-p^{-2}) + k_{22}(3p^2-4+p^{-2}) + 2k_{42}(p^2-1)}{D_2'}$$

$$d_{32} = \frac{\tau r + \frac{6Kr_1}{pL}}{\lambda} \cdot \frac{\tau r(p^{-2}-p^{-4}) - \frac{Kr_1}{L}(1-4p^{-2}+3p^{-4}) + 2k_{22}(1-p^{-2}) + k_{42}(1-p^{-4})}{D_2'}$$

$$d_{42} = \frac{\tau r + \frac{6Kr_1}{pL}}{\lambda} \cdot \frac{\tau r(p^2-p^{-4})\lambda \frac{3Kr_1}{L}(1-p^{-4}) + 6k_{22}(p^2-1) + k_{42}(4p^2-3-p^{-4})}{D_2'}$$

$$d_{14} = \frac{3Kr_1}{pL\lambda} \cdot \frac{\frac{Kr_1}{2L}(p^4 15p^{-4}-16p^{-6}) + 5k_{24}(p^4-p^{-4}) + 4k_{44}(p^4-p^{-6})}{D_4'}$$

$$d_{24} = \frac{3Kr_1}{pL\lambda} \cdot \frac{\frac{3Kr_1}{2L}(p^4-p^{-4}) + k_{24}(15p^4-16p^2+p^{-4}) + 12k_{44}(p^4-p^2)}{D_4'} \qquad (36)$$

$$d_{34} = -\frac{3Kr_1}{pL\lambda} \cdot \frac{\frac{6Kr_1}{L}(p^{-4}-p^{-6}) + 4k_{24}(p^2-p^{-4}) + 3k_{44}(p^2-p^{-6})}{D_4'}$$

$$d_{44} = -\frac{3Kr_1}{pL\lambda} \cdot \frac{\frac{2Kr_1}{L}(p^4-p^{-6}) + 20k_{24}(p^4-p^2) + k_{44}(16p^4-15p^2-p^{-6})}{D_4'}$$

$$D_2' = \tau r(p^2-3p^{-2}+2p^{-4}) + \frac{6Kr_1}{L}(1-2p^{-2}+p^{-4}) + 6(k_{22})_{\lambda=1}(p^2-2+p^{-2}) + 2(k_{42})_{\lambda=1}(2p^2-3+p^{-4})$$

$$D_4' = \frac{3Kr_1}{L}(p^4-5p^{-4}+4p^{-6}) + 10(k_{24})_{\lambda=1}(3p^4-4p^2+p^{-4}) + 6(k_{44})_{\lambda=1}(4p^4-5p^2+p^{-6})$$

It is interesting to note that as $p \rightarrow 1$ (i.e., no reinforcement for a hole of radius = r_1), $k_{22} \rightarrow \frac{2Kr_1}{L} + \frac{\tau r}{2}$; $k_{24} \rightarrow \frac{3Kr_1}{2L}$; $k_{44} \rightarrow -\frac{2Kr_1}{L}$; $k_{42} \rightarrow -\frac{3Kr_1}{L} - \tau r$ and

$$d_{12} = d_{22} = d_{32} = d_{42} = d_{14} = d_{24} = d_{34} = d_{44} \rightarrow 0. \qquad (36a)$$

which certainly agrees with the fact that with no reinforcement present there can be no stress in the reinforcement.

If Equations (32) and (36) are substituted into Equations (30) at $r = r_2$:

$$(\sigma_r)_{r=r_2} = 0$$

$$(\sigma_\theta)_{r=r_2} = \frac{4\tau r + \frac{24Kr_1}{pL}}{\lambda} \cdot$$

$$\frac{\tau r(p^2 - 3p^{-2} + 2p^{-4}) + \frac{6Kr_1}{L}(1 - 2p^{-2} + p^{-4}) + 6k_{22}(p^2 - 2 + p^{-2}) + 2k_{42}(2p^2 - 3 + p^{-4})}{\tau r(p^2 - 3p^{-2} + 2p^{-4}) + \frac{6Kr_1}{L}(1 - 2p^{-2} + p^{-4}) + 6(k_{22})_{\lambda=1}(p^2 - 2 + p^{-2}) \; 2(k_{42})_{\lambda=1}(2p^2 - 3 + p^{-4})} \sin 2\theta +$$

$$+ \frac{24Kr_1}{\lambda pL} \cdot \frac{\frac{3Kr_1}{L}(p^4 - 5p^{-4} + 4p^{-6}) + 10k_{24}(3p^4 - 4p^2 + p^{-4}) + 6k_{44}(4p^4 - 5p^2 + p^{-6})}{\frac{3Kr_1}{L}(p^4 - 5p^{-4} + 4p^{-6}) + 10(k_{24})_{\lambda=1}(3p^4 - 4p^2 + p^{-4}) + 6(k_{44})_{\lambda=1}(4p^4 - 5p^2 + p^{-6})} \sin 4\theta \qquad (37)$$

$$(\tau_{r\theta})_{r=r_2} = 0 .$$

Now the nominal bending stress at the extreme fiber located above the vertical diameter of the hole, $\sigma_L = \frac{PLh}{I}$, is introduced:

$$\frac{(\sigma_\theta)_{r=r_2}}{\sigma_L} = \frac{4\Gamma\frac{\tau}{\sigma} - \frac{r_1}{L}\cdot\frac{r_2}{h}}{\lambda} \cdot$$

$$\cdot \frac{\frac{\tau\Gamma}{K}(p^2-3p^{-2}+2p^{-4})+\frac{6r_1}{L}(1-2p^{-2}+p^{-4})+\frac{6k_{22}}{K}(p^2-2+p^{-2})+\frac{2k_{42}}{K}(2p^2-3+p^{-4})}{\frac{\tau\Gamma}{K}(p^2-3p^{-2}+2p^{-4})+\frac{6r_1}{L}(1-2p^{-2}+p^{-4})+6(\frac{k_{22}}{K})_{\lambda=1}(p^2-2+p^{-2})+2(\frac{k_{42}}{K})_{\lambda=1}(2p^2-3+p^{-4})}\sin 2\theta -$$

$$- \frac{\frac{r_1}{L}\cdot\frac{r_2}{h}}{\lambda} \cdot \frac{\frac{3r_1}{L}(p^4-5p^{-4}+4p^{-6})+10\frac{k_{24}}{K}(3p^4-4p^2+p^{-4})+\frac{6k_{44}}{K}(4p^4-5p^2+p^{-6})}{\frac{3r_1}{L}(p^4-5p^{-4}+4p^{-6})+10(\frac{k_{24}}{K})_{\lambda=1}(3p^4-4p^2+p^{-4})+6(\frac{k_{44}}{K})_{\lambda=1}(4p^4-5p^2+p^{-6})}\sin 4\theta$$

(37a)

If we now consider that throughout the analysis the hole has been considered quite small compared to the panel (accuracy for $0 < \frac{r_2}{h} < 0.25$), then:

$$\frac{r_1}{L} \approx 0$$

$$\frac{2k_{22}}{K} \approx -\frac{\tau\Gamma}{KD}[2-\alpha(1+4\delta)](1+\delta+.385\beta)+(1-\delta-.25\beta)\alpha(.462-6.154\delta)$$

$$\frac{2k_{42}}{K} \approx -\frac{\tau\Gamma}{KD}[2-\alpha(1+4\delta)](1+3+.25\beta)+(1-\delta-.25\beta)[2+\alpha(3-4\delta)]$$

$$\frac{k_{24}}{K} \approx 0$$

$$\left.\begin{aligned} \frac{k_{44}}{K} &\approx 0 \\ D &= [2+\alpha(3-4\delta)](1+\delta+.385\beta) - (1+3\delta+.25\beta)\alpha(.462-6.154\delta) \end{aligned}\right\} \quad (38)$$

Then:

$$\frac{(\sigma_\theta)_{r=r2}}{\sigma_L} = \frac{4r}{\lambda}\cdot\frac{\tau}{\sigma}\cdot\frac{(p^2-3p^{-2}+2p^{-4})+3(p^2-2+p^{-2})\frac{k'_{22}}{K}+(2p^2-3+p^{-4})\frac{k'_{42}}{K}}{(p^2-3p^{-2}+2p^{-4})+3(p^2-2+p^{-2})\left(\frac{k'_{22}}{K}\right)_{\lambda=1}+(2p^2-3+p^{-4})\left(\frac{k'_{42}}{K}\right)_{\lambda=1}}\sin 2\theta \quad (39)$$

where:

$$\frac{k'_{22}}{K} = \frac{[2-\alpha(1+4\delta)](1+\delta+.385\beta)+(1-\delta-.25\beta)\alpha(.462-6.154\delta)}{D}$$

$$\frac{k'_{42}}{K} = -\frac{[2-\alpha(1+4\delta)](1+3\delta+.25\beta)+(1-\delta-.25\beta)[2+\alpha(3-4\delta)]}{D} \quad (39a)$$

D as in Equation (38)

If Equations (28a) and (39) are combined, the resulting relation corresponds to the loading of Fig. XIV:

$$\frac{(\sigma_\theta)_{r=r2}}{\sigma_L} = \frac{r_2}{h}\cdot\frac{1}{\lambda}\left[\frac{3+\frac{k_{31}}{K}}{3+\left(\frac{k_{31}}{K}\right)_{\lambda=1}}\cos\theta + \frac{(p^3-4p^{-3}+3p^{-5})-(4p^3-6p+2p^{-3})\frac{k_{23}}{K}-(3p^3-4p+p^{-5})\frac{k_{43}}{K}}{(p^3-4p^{-3}+3p^{-5})-(4p^3-6p+2p^{-3})\left(\frac{k_{23}}{K}\right)_{\lambda=1}-(3p^3-4p+p^{-5})\left(\frac{k_{43}}{K}\right)}\cos 3\theta\right] +$$

$$+\frac{4r}{\lambda}\cdot\frac{\tau}{\sigma}\cdot\frac{(p^2-3p^{-2}+2p^{-4})+3(p^2-2+p^{-2})\frac{k_{22}}{K}+(2p^2-3+p^{-4})\frac{k_{42}}{K}}{(p^2-3p^{-2}+2p^{-4})+3(p^2-2+p^{-2})\left(\frac{k_{22}}{K}\right)_{\lambda=1}+(2p^2-3+p^{-4})\left(\frac{k_{42}}{K}\right)_{\lambda=1}}\sin 2\theta \qquad (40)$$

Figures XXXIV - XXXVIII show the constraint coefficient vs. α in contours of δ. These are the results of cross-fairing the calculated values of the rectangular type of reinforcement used in the experimental investigations, and, therefore, include a typical allowance of β for that type of reinforcement.

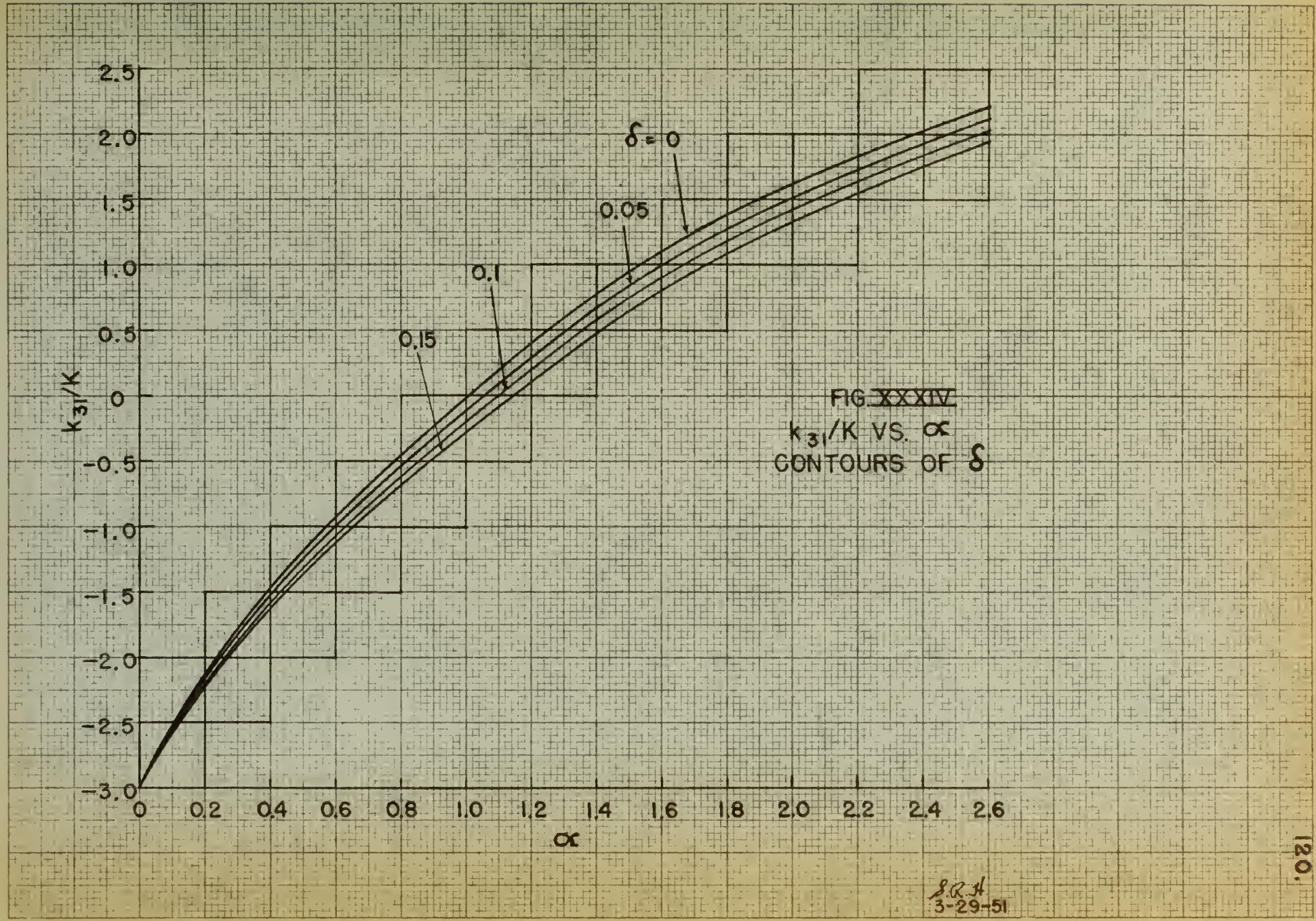

FIG. XXXIV
k_{31}/K VS. α
CONTOURS OF δ

S.R.H.
3-29-51

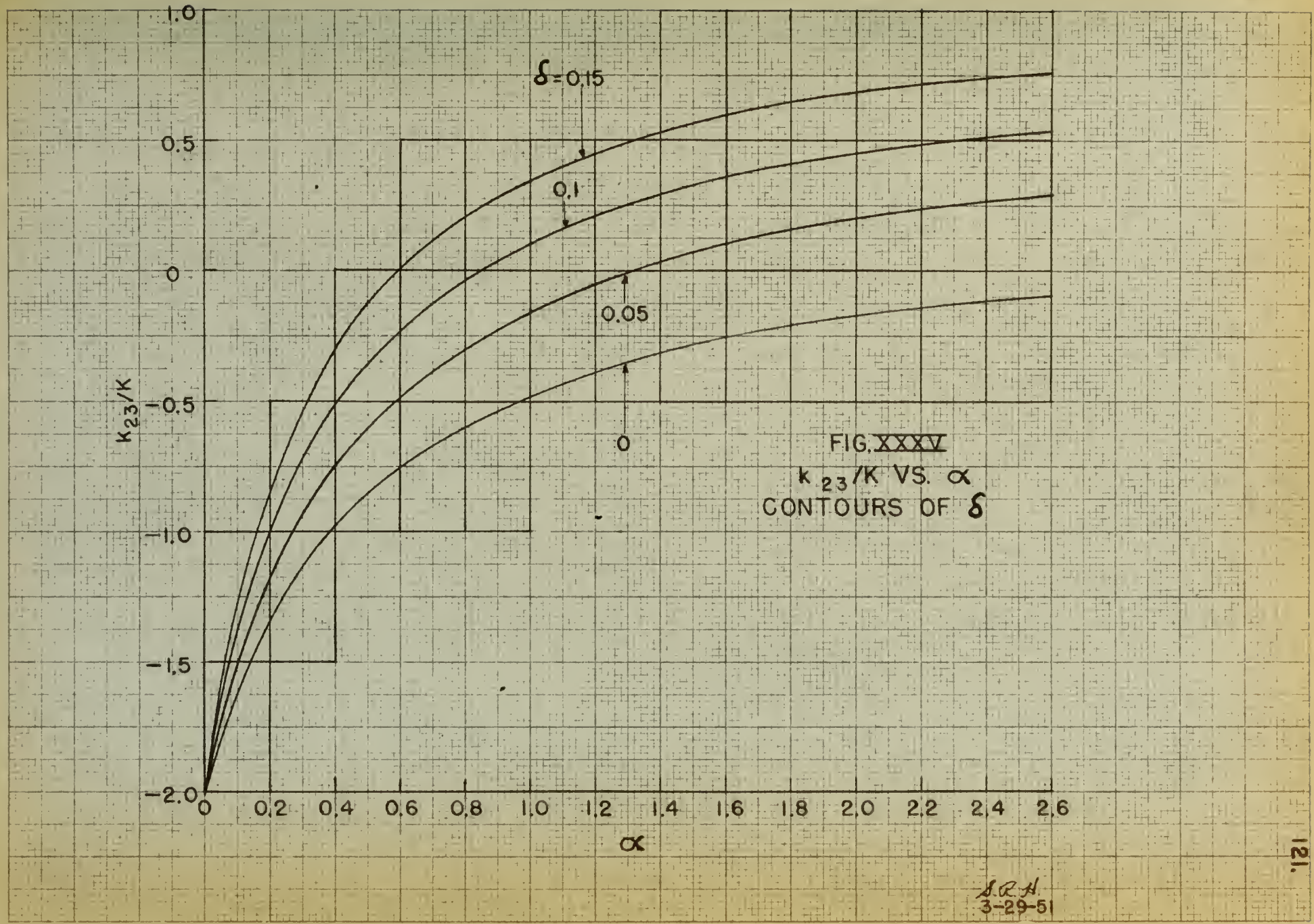

FIG. XXXV
k_{23}/K VS. α
CONTOURS OF δ

S.R.H.
3-29-51

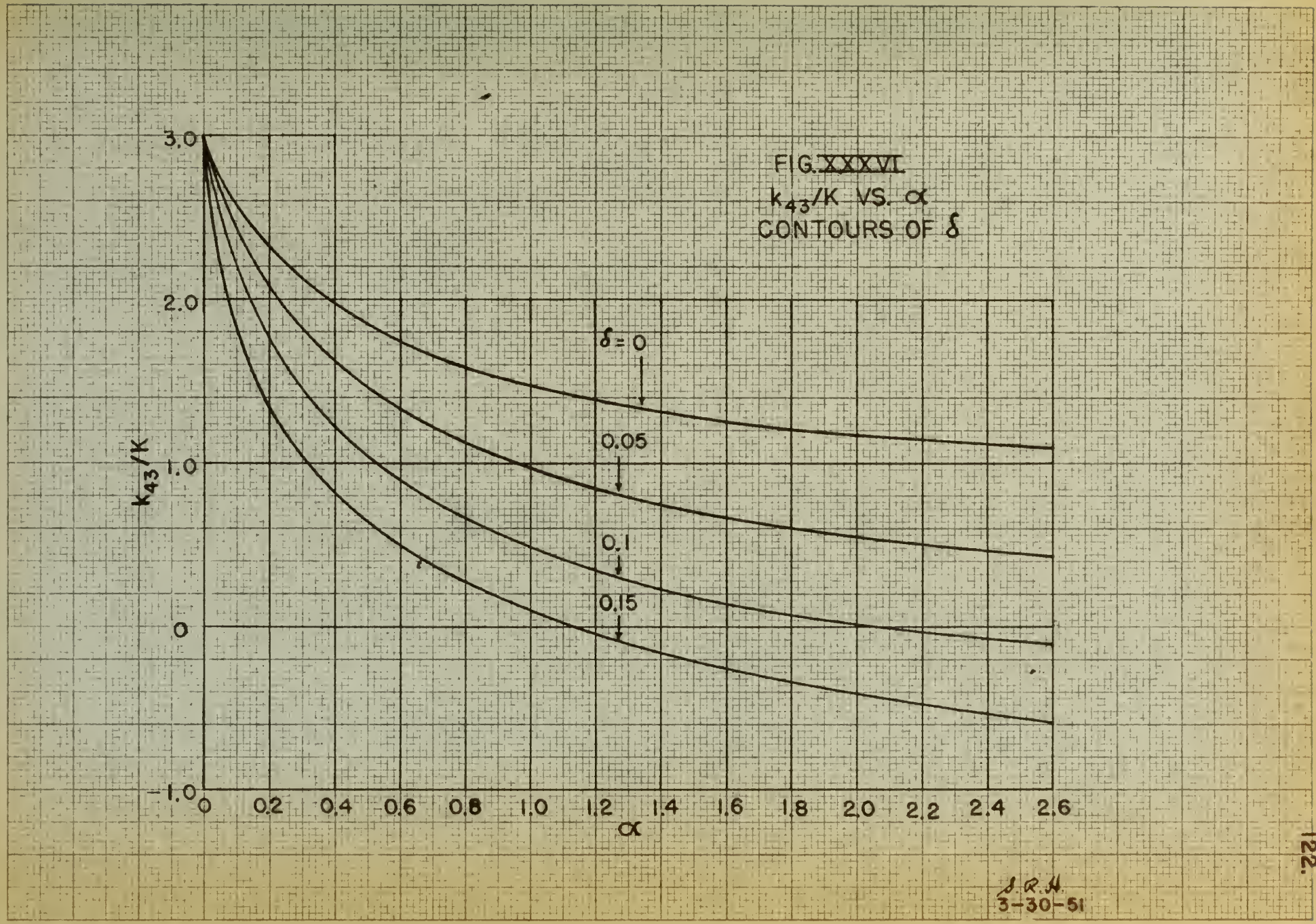
FIG. XXXVI
k_{43}/K VS. α
CONTOURS OF δ
3.0
2.0
1.0
0
-1.0
k_{43}/K
$\delta = 0$
0.05
0.1
0.15
0
0.2
0.4
0.6
0.8
1.0
1.2
1.4
1.6
1.8
2.0
2.2
2.4
2.6
α
J.R.M.
3-30-51

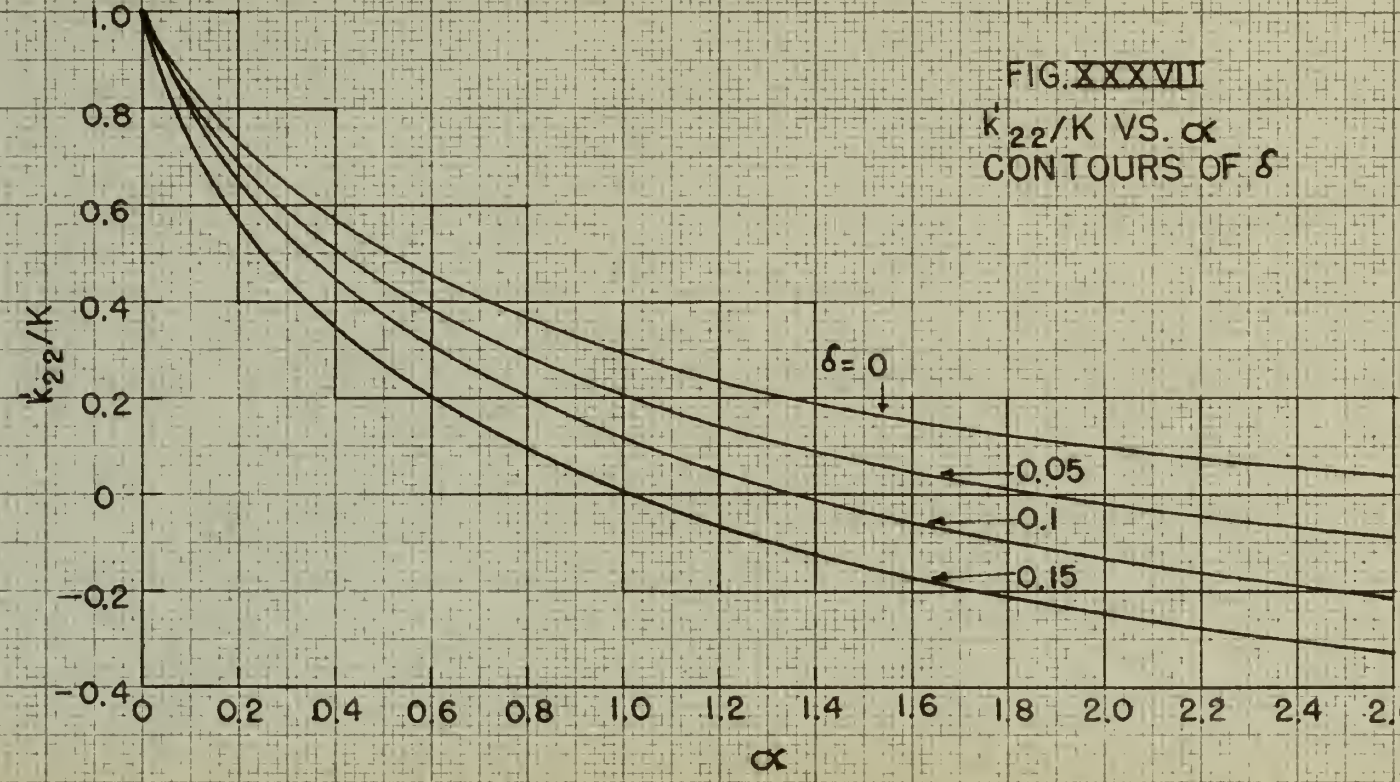

FIG. XXXVII

k'_{22}/K VS. α
CONTOURS OF δ

LRA
3-30-51

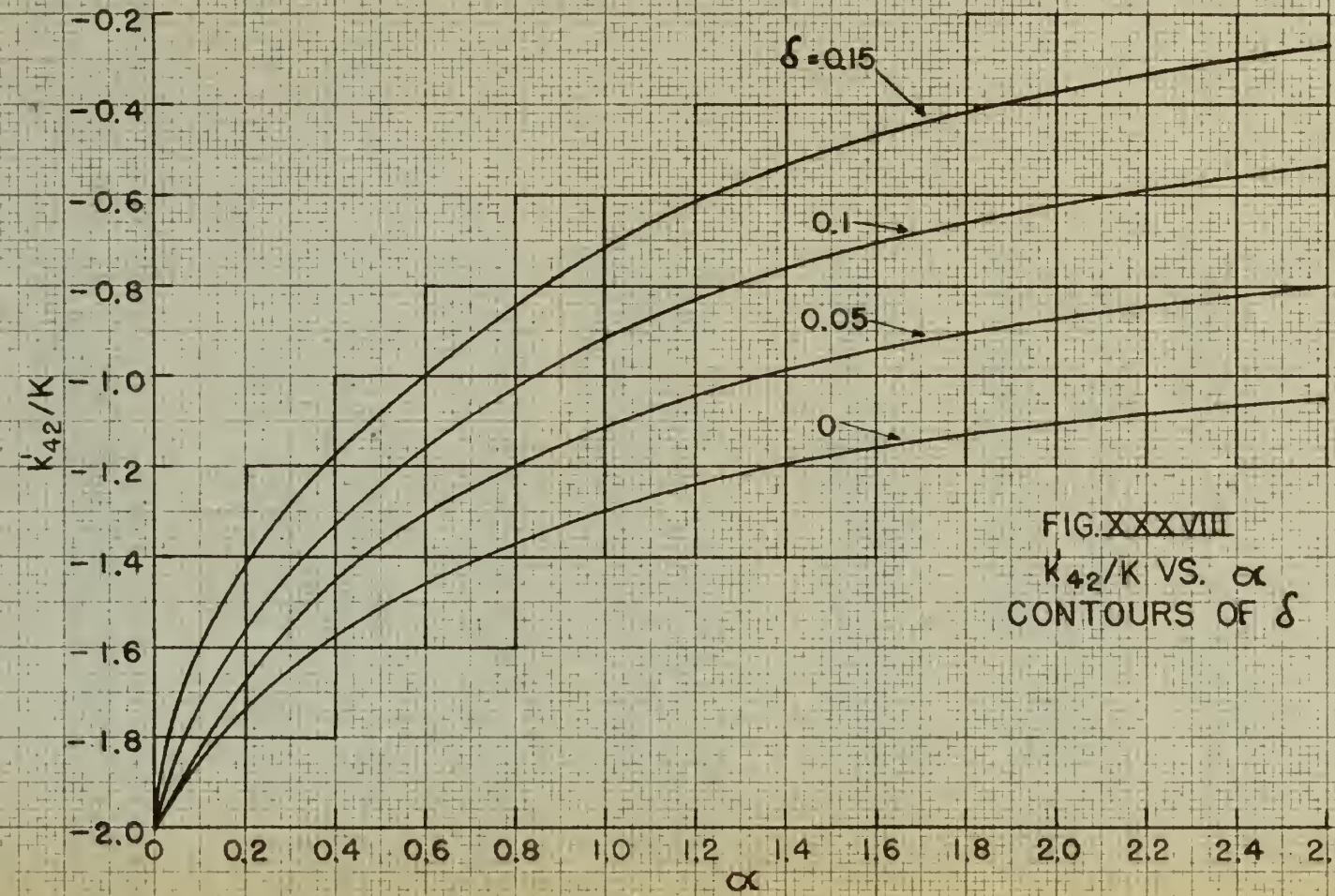

FIG. XXXVIII
k'_{42}/K VS. α
CONTOURS OF δ

S.R.M.
3-30-51

APPENDIX F

BIBLIOGRAPHY

I. Openings

Circle

[1] Kirsch, G.: "Die Theorie der Elastizitätund die Bedurfnisse der Festigkeitslehr," Zeitschrift des Vereines Deutscher Ingenieure, Vol. 42, 1898.

[2] Tuzi, Z.: "Effect of a Circular Hole on the Stress Distribution Under Uniform Bending Moment," Scientific Papers of the Tokyo Institute of Physical and Chemical Research, Vol.9, Aug. 20, 1928, pp. 65 - 89.

[3] Howland, R. C. J. and Stevenson, A. C.: "Biharmonic Analysis in a Perforated Strip," Philosophic Transactions of the Royal Society of London, Series A, Vol. 232, 1933, pp. 155 - 222.

Ellipse

[4] Inglis, C. E.: "Stresses in a Plate Due to the Presence of Cracks and Sharp Corners," Transactions of the Institution of Naval Architects, London, Vol. 55, 1913, pp. 219 - 242.

[5] Wolf, K.: "Beitrage zur ebenen Elastizitätstheorie," Zeitschrift fur technische Physik, Vol. 2, No. 8, 1921, p. 209, and Vol. 3, No. 5, 1922, pp. 160 - 166.

[6] Neuber, H.: "Theory of Notch Stresses," David Taylor Model Basin Translation No. 74, (Translated by F. A. Raven and J. S. Brook, Nov. 1945; Distributed by J. W. Edwards, Ann Arbor, Mich.) pp. 52 - 62.

Ovaloid

[7] Greenspan, M.: "Effect of a Small Hole on the Stresses in a Uniformly Loaded Plate," Quarterly Applied Mathematics, Vol. 2, 1944, pp. 60 - 71.

[8] Morkovin, V.: Discussion of "Effect of a Small Hole on the Stresses in a Uniformly Loaded Plate," Quarterly Applied Mathematics, Vol. 2, No. 4, 1944, pp. 350 - 352.

[9] Joseph, J. A. and Brock, J. S.: "The Stresses Around a Small Opening in a Beam Subjected to Pure Bending," Journal of Applied Mechanics, Vol. 17, No. 4, Dec. 1950.

[10] Heller, S. R.: "The Stresses Around a Small Opening in a Beam Subjected to Bending With Shear." Unpublished.

II. Reinforcement

Circle

[11] Timoshenko, S.: "On the Stresses in a Flat Plate with a Circular Hole," Journal of the Franklin Institute, Vol. 197, 1924.

[12] Sobrero, L.: "Sollecitazioni elastiche di un sistema piano con foro rinforzato," Memorie della Classe di Scienze Fiziche, Matematiche e Naturali, Vol. X, No. 4, 1939-XVII, Reale Accademia d'Italia, Rome. (Translation No. 103, David Taylor Model Basin, Translated by F. A. Raven and J.S. Brock.)

[13] Gurney, C.: "An Analysis of the Stresses in a Flat Plate with a Reinforced Circular Hole under Edge Forces," Aeronautical Research Committee, R & M No. 1834, 1938, London.

[14] Reissner, H. and Morduchow, M.: "Reinforced Circular Cutouts in Plane Sheets," National Advisory Committee for Aeronautics, Technical Note No. 1852, April, 1949, Washington.

[15] Sezawa, K. and Kubo, K.: "Stresses in Plate with Flanged Circular Hole," Tokyo Imperial University - Aeronautical Research Institute, Report V7, 1932.

[16] Crecca, J. D.: "Welded Floor Test," C & R Bulletin #6, 1932, Washington.

Ellipse

[17] Ffird, T. A. and Skinner, A. H.: "Determination of Effective Width of Stiffening Ring Installed Around Elliptical Access Hole in Beam Subjected to Shear and Bending," Nav. E. Thesis, M. I. T., 1950.

Ovaloid

[18] Ballinger, J. M. and Obermeyer, J. A.: "Investigation of the Tensile Stress Distribution Around an Access Hole," M.S. Thesis, M. I. T., 1941.

Various

[19] - - - - - - - - - - "The Effect of Openings on the Ultimate Tensile Strength of Flat Plates," U. S. Experimental Model Basin, Report No. 446, March, 1938, Washington.

III. General

[20] Timoshenko, S.: Strength of Materials, Part II - Advanced Theory and Problems, Second Edition, Aug., 1941, D. Van Nostrand Co., Inc., New York.

[21] Timoshenko, S.: Theory of Elasticity, First Edition, 1934, McGraw-Hill Book Co., Inc., New York.

[22] Hewson, T. A.: "A Nomographic Solution to the Strain Rosette Equations," Proceedings of the Society for Experimental Stress Analysis, Vol. IV, No 1, 1946, pp. 9 - 26.

AUG 31
BINDERY
DISPLAY

Thesis
H43
21000
Heller
Reinforced circular holes in bending with shear.

BINDERY
DISPLAY

Thesis
H43
21000
Heller
Reinforced circular holes in bending with shear.

Library
U. S. Naval Postgraduate School
Monterey, California

thesH43
Reinforced circular holes in bending wit
3 2768 001 91810 5
DUDLEY KNOX LIBRARY